Design, optimization and validation of a diagnostic panel comprised of ABCA4 pathogenic variants causing Stargardt disease in the Newfoundland and Labrador population

by © Hoda Rajabi

A Thesis submitted to the School of Graduate Studies in the partial fulfillment of the requirements for the degree of

Master of Science in Medicine (Human Genetics)

Faculty of Medicine, Discipline of Genetics

Memorial University of Newfoundland

October 2016

St. John's Newfoundland and Labrador

ABSTRACT

The objective of this translational research project was to develop, optimize and validate a diagnostic panel of the 20 pathogenic variants in the ABCA4 gene previously identified to cause Stargardt disease in the population of Newfoundland and Labrador (NL). Two different laboratory developed test (LDT) panels (1x20-plex & 2x20-plex) were designed and genotyping was performed on the Sequenom MassARRAY 4 system using genomic DNA from both Stargardt patients and population controls. A set of minimum criteria was established to accurately determine genotyping calls; 1x20-plex LDT panel was selected based on quality metrics. Assessment of the validation cohort including 78 previously tested genomic DNA samples, blind to the investigator, resulted in establishing analytical sensitivity (100%), specificity (100%), accuracy (100%), and reproducibility (100%). A total of 1039 control samples were assessed using the 1x20-plex LDT panel and the minor allele frequencies of 0% - 0.76% for NL, and 0% - 0.60% for non-NL samples were determined.

ACKNOWLEDGEMENTS

First and foremost, I would like to thank my lovely family, especially my husband. I spent much time and energy pursuing my goals that took me away from my family. Without my husband's support, encouragement and patients, I would not have been able to finish this challenging project.

I would like to express my deepest appreciation to my supervisor Dr. Darren O'Rielly. He consistently guided me in the right direction and consulted regarding the best solutions. The door to Darren's office was always open whenever I ran into a trouble or had a question about my research or writing.

I would like to thank my co-supervisor Dr. Jane Green and my supervisory committee members Drs. Terry-Lynn Young and Proton Rahman for their warmest support and constructive advice. It was a great honour to work with these respected and well-known Faculty members in the area of human genetics.

I would like to thank all my friends and staff in the Drs. Young, Rahman and O'Reilly laboratories. They were always there to train, help and guide me whenever needed.

Finally, I would like to acknowledge the funding agencies and all participants who donated samples to finish this project.

TABLE OF CONTENTS

LIST OF TABLES

LIST OF FIGURES

ABBREVIATIONS

Adeno-associated virus	(AAV)
ATP-binding cassette	(ABC)
ATP binding cassette transporter gene	(ABCA4)
Applied Biosystem instrument	(ABI)
Angiotensin-converting-enzyme	(ACE)
Allele height	(AH)
Age related macular dystrophy	(AMD)
Array primer extension	(APEX)
Adenosine triphosphate	(ATP)
Cone dystrophy	(CD)
Complementary deoxyribonucleic acid	(cDNA)
Comparative genomic hybridization	(CGH)
Copy number variants	(CNVs)
Cone-rod dystrophy	(CRD)
Denaturing high-performance liquid chromatography	(dHPLC)
Deoxyribonucleic acid	(DNA)
Electrooculogram	(EOG)
Electroretinogram	(ERG)
Ethanol	(EtOH)
Extension	(EXT)
Forward primer	(F)
Fluorescein Angiography	(FA)
Fundus Autofluorescence	(FAF)
Full-Field Electroretinogram	(FF ERG)
Fractional unextended primer	(F-UEP)
False hit	(H.False)
Null hit	(H.Null)
True hit	(H.True)
Highly deionized	(Hi-Di)
Indocyanine green angiography	(ICGA)
Knowledge translation	(KT)
Laboratory developed test	(LDT)
Minor allele frequencies	(MAF)
Matrix-assisted laser desorption/ionization time-of-flight	(MALDI-TOF)
Macular dystrophy	(MD)

Next-generation sequencing	(NGS)
Newfoundland and Labrador	(NL)
Nano-liter	(nl)
Non-viral DNA nanoparticles	(NPs)
N-retinylidene-Phosphatidylethanolamine	(N-ret-PE)
Non-template control	(NTC)
Optical Coherence Tomography	(OCT)
Polymerase chain reaction	(PCR)
Phosphatidylethanolamine	(PE)
Quality control	(QC)
Reverse primer	(R)
Relative centrifugal force	(rcf)
Retinal degeneration	(RD)
Research ethics board	(REB)
Retinitis pigmentosa	(RP)
Research advisory committee	(RPAC)
Retinal-pigment epithelium	(RPE)
Shrimp Alkaline Phosphatase	(SAP)
Single nucleotide polymorphism	(SNP)
Signal to noise ratio	(SNR)
Single nucleotide variant	(SNV)
Stargardt disease	(STGD)
Autosomal recessive Stargardt disease	(STGD1)
Tris Borate EDTA	(TBE)
Tris Ethylenediaminetetraacetic acid	(TE)
Time-of-flight mass spectrometer	(TOF-MS)
Unextended primers	(UEP)
Uracil-N-glycosylase	(UNG)
Used primer	(UP)
Ultraviolet	(UV)

Chapter 1

1.0 – INTRODUCTION

1.1 – EYE, STARGARDT DISEASE AND GENETICS

1.1.1 – Structure of the Retina

The eye is comprised of many different layers and specialized cell types. One of the most important sensory layers responsible for vision at the back of the eye is the retina (**Figure 1.1**). The major types of neural cells in the sensory layer of the retina are photoreceptors, bipolar cells, horizontal cells, amacrine cells and ganglion cells (including Mueller cells). Just outside the neurosensory retina there is a layer of pigmented cells known as the retinal-pigmented epithelium (RPE). These cells posterior to the photoreceptors provide several supportive functions for neural cells in the sensory layer of the retina. These supportive functions are: 1) phagocytosis of photoreceptor outer segments; 2) providing nutritive support in the form of various growth factors for photoreceptors; 3) synthesis of inter-photoreceptor matrix; 4) providing a selectively permeable barrier between the neurosensory retina and its posterior layers; 5) renewal of an integral part of the visual cycle; and 6) absorption and reduction of light within the eye (Sundaram 2014, Yu et al. 2010) (**Figure 1.1**).

Photoreceptors, comprised of rods and cones, are highly differentiated cells with regards to their structure and function. Cone photoreceptors function only in bright light, and are responsible for color vision and best visual acuity (**Figure 1.2A**). In contrast, rod photoreceptors are highly light sensitive, and

function in dim light conditions and also provide peripheral vision (**Figure 1.2B**). There are an estimated 60-125 million rods and 3.2-6.5 million cones cells that are unevenly distributed in the retina (Nentwich, Rudolph 2013). The macula is a region in the retina, which has the highest concentration of cone photoreceptors. Within the macula there is a densely packed cone region, providing high visual acuity, called the fovea. Rods are absent in the fovea region, but their numbers start to increase toward the peripheral retina (Nentwich, Rudolph 2013, Sundaram 2014, Yu et al. 2010).

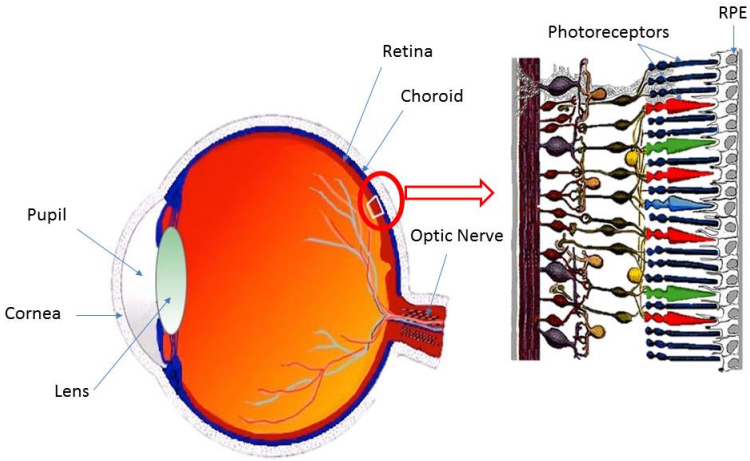

Figure 1.1. A schematic picture of the eye with different layers and an enlarged segment of the retina. Adapted from a website (http://webvision.med.utah.edu/book/part-i-foundations/simple-anatomy-of-the-retina/)); used under a creative commons attribution license.

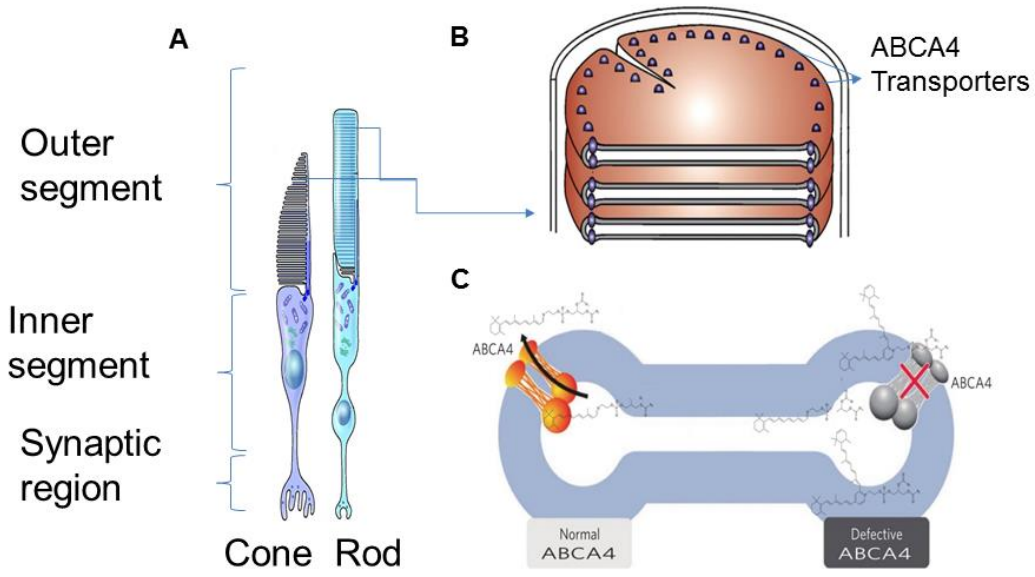

Figure 1.2. A) A schematic picture of cone and rod photoreceptors. Adapted from: (http://dmm.biologists.org/content/8/2/109); used under a creative commons attribution license. B) Magnified view of the outer segments of photoreceptors showing the disc rims and distribution of the ABCA4 channels **(Molday, Zhang 2010);** adapted by permission. C) Normal ABCA4 protein compared with defective ABCA4 **(Maeda et al. 2011);** adapted by permission**.**

1.1.2 – The visual cycle

Each photoreceptor consists of an outer segment, connecting cilium, inner segments, nuclear region and a synaptic region (**Figure 1.2**). Photoreceptor outer segments detect light and convert it into electrical signals where the signal passes through the inner segment and transmits to the secondary retinal neurons by the synapsis region. The phototransduction process depends on utilizing the unique properties of 11-cis retinal, a photosensitive derivative of vitamin A, which is covalently bound to an opsin signalling protein to form a visual pigment molecule. When a photon of light reaches rhodopsin (in the outer segment of photoreceptors), 11-cis retinal is isomerized to all-trans retinal and causes a

conformational change. All-trans retinal is reduced to all-trans retinol once it is released from rhodopsin due to photoexcitation. This molecule is transferred to the RPE cells and converted to retinyl esters before being isomerized to make all-trans retinol and oxidized to all-trans retinal and finally shuttled back to photoreceptors to finish the visual cycle (**Figure 1.3**). However, rhodopsin also releases a substantial fraction of all-trans retinal which reacts with phosphatidylethanolamine acid (PE) to form the Schiff base adduct N-retinylidene-Phosphatidylethanolamine (N-ret-PE) (Molday, Moritz 2015, Yu et al. 2010).

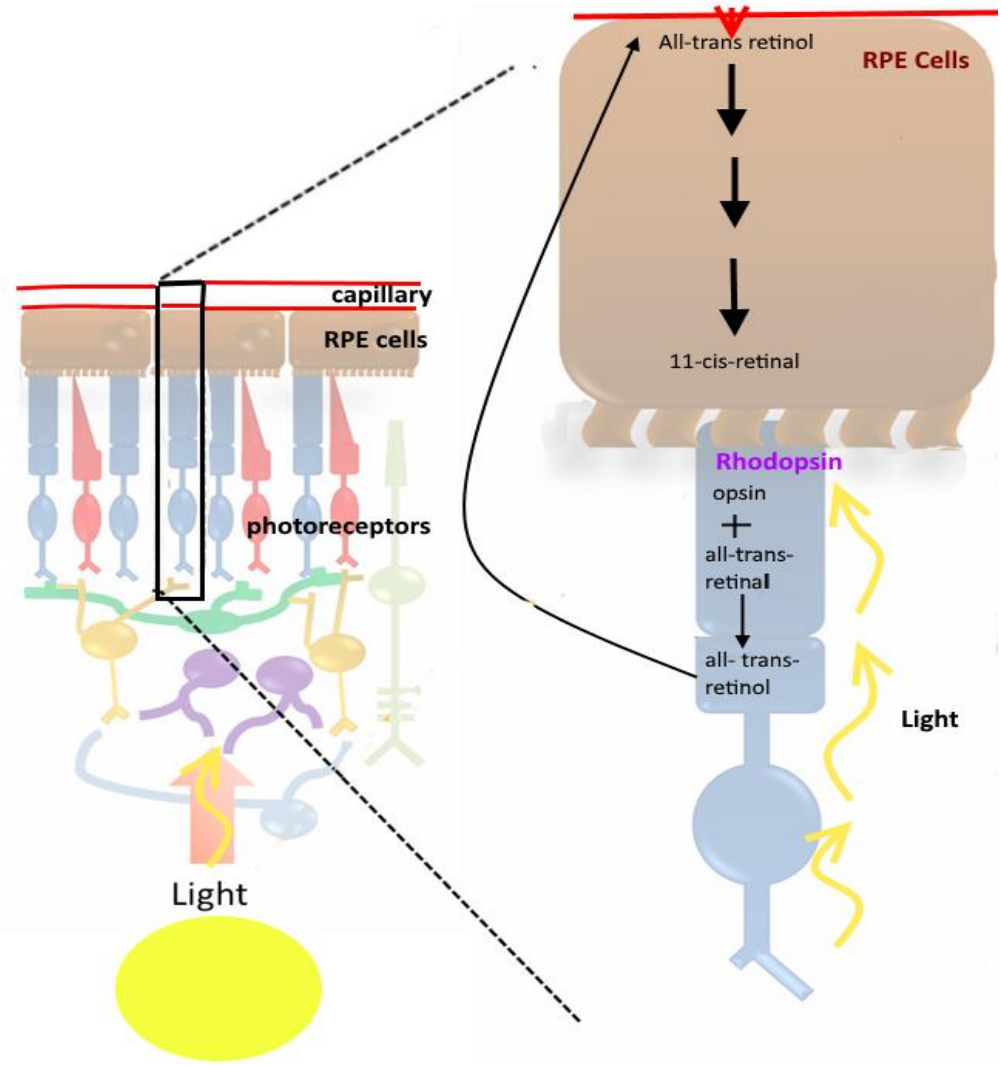

Figure 1.3. A schematic picture of light absorption by the retina, and the visual cycle. Adapted from: (http://www.d.umn.edu/~jfitzake/Lectures/DMED/Vision/Retina/VisualCycle.html), (http://www.mdpi.com/2072-6643/5/7/2646/htm)); used under a creative commons attribution license..

1.1.3 – Retinal degeneration disorders

Retinal degeneration (RD) disorders are one of the major causes of blindness (Molday, Zhang 2010). Classification of RD disorders is based on phenotypic

characteristics of the disease and the affected specialized cells. For example, retinitis pigmentosa (RP) and macular dystrophy (MD) disorders (two of the major categories in RD disease) affect photoreceptor cells (Rivolta et al. 2002). The main phenotypic characteristics of RP include night blindness and progressive peripheral vision loss, which eventually may lead to central vision loss and total blindness (Rivolta et al. 2002). This is due to the fact that RP mostly affects rod photoreceptors, and as mentioned earlier, rods are responsible for night and peripheral vision. In contrast to RP, MDs are characterized by central vision loss and usually by preservation of peripheral vision. As the name of the disease reveals, this type of disorder mostly affects the macula region of the eye with high concentration of cone photoreceptors (Rattner, Nathans 2006). MDs are further divided into juvenile and age-related macular disorders with similar clinical features (Quellec et al. 2011). Early onset or juvenile MD is a hereditary form caused by disruptions in visual cycle pathway proteins or deficiencies in eye structural proteins due to various pathogenic variants in related genes encoding these important proteins (Molday, Zhang 2010). The juvenile hereditary MD is further subdivided to other diseases, the most common of which are Stargardt disease (MIM # 601691) and Best disease (MIM # 153700. Age-related macular dystrophy (AMD), however, occurs at later ages. AMD is described as a complex disorder with both genetics and environmental factors playing a role in causing the disease (Montezuma, Sobrin & Seddon 2007, Jager, Mieler & Miller 2008).

1.1.4 – Stargardt disease

Among all hereditary juvenile MDs, Stargardt disease (STGD) is the most common and accounts for almost 7% of all retinal diseases (Heathfield et al. 2013). In 1909, Karl Stargardt, a 34-year-old German ophthalmologist, was the first person who comprehensively defined the nature and clinical features of STGD. He identified seven affected individuals from two families with the disease (Fishman 2010, Allikmets et al. 1997, Stargardt 1909); and described STGD as a bilateral progressive atrophic MD characterized by perimacular and peripheral yellowish flecks (Nentwich, Rudolph 2013, Haji Abdollahi, Hirose 2013). He concluded that STGD is a genetic, neuroepithelial disease that affects cone photoreceptors initially and RPE cells and choroid layer, subsequently (Fishman 2010). STGD is subdivided into autosomal recessive Stargardt (STGD1; MIM# 248200), caused by homozygous or compound heterozygous mutations in the Adenosine triphosphate (ATP) binding cassette transporter (ABCA4; MIM #601691) gene (Valverde et al. 2006, Allikmets et al. 1997); and Stargardt-like diseases (STGD3; MIM #600110 and STGD4; MIM# 603786), which are phenotypically similar but inherited in an autosomal dominant manner, and caused by mutations in the ELOVL4 (MIM #605512) (Zhang et al. 2001) and PROM1 (MIM #604365) (Miraglia et al. 1997) genes, respectively (Molday, Zhang 2010, Nentwich, Rudolph 2013, Miraglia et al. 1997).

1.1.5 – STGD1

Autosomal recessive STGD1 (MIM #248200), which is the focus of this thesis, is the most common form of the disease (Sohrab et al. 2010). It has a prevalence of 1 in 8,000-10,000 individuals in the United States (Haji Abdollahi, Hirose 2013) and a carrier frequency that is 1/20 or possibly higher (Burke, Tsang 2011, Molday, Zhang 2010). The clinical symptoms start in the first two decades of life; however, in some individuals' symptoms appear later in life. As expected in all MD disorders, the symptoms include progressive loss of central vision, while the peripheral visual field remains unaffected (Fishman et al. 1987). Some patients may also have photophobia and color vision loss (Aguirre-Lamban et al. 2009, Fishman, Farbman & Alexander 1991, Mantyjarvi, Tuppurainen 1992). The hallmark of the disease is the presence of yellow flecks surrounding the macula area (Birnbach et al. 1994). However, according to the literature these flecks may not appear in all STGD1 patients (Fishman, Sokol 2001).

1.1.6 – Fundus Flavimaculatus

A retinal disease called Fundus Flavimaculatus is a variant of STGD1 (Anderson et al. 1995) described by Franceschetti in the 1960's (CARR 1965). It is characterized by appearance of fundus flecks with no evidence of atrophy in macular lesions. Affected individuals with Fundus Flavimaculatus may also appear with flecks outside of macular region (Haji Abdollahi, Hirose 2013, Noble, Carr 1979). This condition has the same pattern of inheritance as STGD1 and is also caused by mutations in the ABCA4 gene (Noble, Carr 1979). Compared with

STGD1, it generally affects older people and represents a milder form of the disease (Weleber 1994, Westerfeld, Mukai 2008). However, it is important to know that a person who is diagnosed with Fundus Flavimaculatus might be in the earliest stages of classic STGD1, and typical STGD1 appearance might present as the disease progresses (Armstrong et al. 1998, Westerfeld, Mukai 2008).

1.1.7 – The ABCA4 gene and ABC transporters

Mutations in the ABCA4 gene, previously called the ABCR gene, are known to cause STGD1. The ABCA4 gene is a 150kb gene located on the short arm of chromosome 1 (1p22.1), which consists of 50 exons that can vary in size from 33bp to 266bp and produces a transcript of 7309bp (Aguirre-Lamban et al. 2009, Kaplan et al. 1993, Oldani et al. 2012). ATP-binding cassette (ABC) transporters are a large family of ATP binding transmembrane proteins, divided to seven subfamilies, responsible for transporting a variety of compounds across the cell membrane (Dean, Annilo 2005). ABCA1 (MIM #600046) (Luciani et al. 1994), ABCA3 (MIM #601615) (Klugbauer, Hofmann 1996), ABCA4 (MIM #601691) (Allikmets et al. 1997) and ABCA12 (MIM #607800) (Annilo et al. 2002) are associated with inherited diseases with deficiencies in transporting lipids (Kaminski, Piehler & Wenzel 2006). The presence of these transporters in all living organisms, including plants, animals and micro-organisms, is evidence for their important function. Research indicates that mutations causing deficiencies in the majority of the seven subfamilies of ABC transporters in the human genome are linked to severe genetic disorders. For example, mutations in the

ABCC7 (Cystic fibrosis transmembrane conductance regulator; MIM #602421) gene cause cystic fibrosis (MIM #219700) (Riordan et al. 1989). Mutations in the ABCB11 (Bile Salt Export Pump; MIM #603201) gene cause liver disease (Jansen et al. 1999). Defects in the ABCD1 (adrenoleukodystrophy; MIM #300371) gene cause adrenoleukoystrophy (MIM #300100) (Borst, Elferink 2002, Mosser et al. 1993). Allikmets and coworkers discovered the ABCA4 gene in 1997 when they were studying families with STGD1 (Allikmets et al. 1997). The ABCA4 gene is the only currently recognized gene associated with STGD1.. Despite the expression of the ABCA4 gene in many tissues of the human body, the only highly detectable expression of this protein is located in the retina (Allikmets et al. 1997). Within the retina, the ABCA4 gene has been localized to the photoreceptor's outer segment. Using immunofluorescent labeling and subcellular fractionation, ABCA4 was localized to the outer layer of membrane protein of light sensitive photoreceptors next to the RPE (Sun, Nathans 1997, Papermaster, Reilly & Schneider 1982).

1.1.8 – Variants in ABCA4 and genotype-phenotype correlations

In the outer segment of photoreceptors, an organized disc-like membrane exists (**Figure 1.2B**). The rim region of rod and cone outer segments is where ABCA4 membrane proteins are responsible for transporting all-trans retinal out of the cell (Klien, Krill 1967). When pathogenic variants occur in the ABCA4 gene, there is an accumulation of all-trans retinal and its derivatives (i.e., N-retinylidene-N-

retinylethanolamine or A2E) due to dysfunctional ABCA4 transporter protein (**Figure 1.2C**). This accumulation has a toxic effect on photoreceptors and RPE cells (Dorey et al. 1989). The derivatives appear as lipofusion vesicles scattered within the inner half of the pigment epithelial cell. This is a histopathology characteristic of STGD1 (Klien, Krill 1967, Birnbach et al. 1994).

Although pathogenic variants located in the ABCA4 gene were initially found in STGD1 patients, other retinal dystrophies may result from pathogenic variants located in the same gene. These retinal degenerations include cone dystrophy (CD), cone-rod dystrophy (CRD) and RP (Cremers et al. 1998, Maugeri et al. 2000, Shroyer et al. 2001). Genotype-phenotype correlations were proposed by Maugeri et al. for pathogenic variants located in the ABCA4 gene. This model proposes an inverse relationship between the residual activity of the ABCA4 gene and severity of retinal diseases. It classifies the ABCA4 pathogenic variants into three (3) groups of severe (null), moderate and mild. Based on this classification, the most severe phenotype is RP, which results from two null pathogenic variants. The moderate phenotype is CRD, which has partly retained protein activity and is caused by moderate and severe pathogenic variants. Finally, STGD is the result of a combination of mild and severe pathogenic variants or two moderate variants (Haji Abdollahi, Hirose 2013, Maugeri et al. 2000).

Regardless of other retinal degenerations caused by mutations in ABCA4, even Stargardt presents with various clinical symptoms and rate of progression

(Lambertus et al. 2015). A classification of the disease was proposed by Nobel and Carr, which is based on fundus appearance at the time of disease presentation: 1) MD without flecks; 2) MD with perifoveal flecks; 3) MD with diffuse flecks; and 4) diffuse flecks without a MD (Noble, Carr 1979). This classification may not be ideal, since the disease manifestation differs as it progresses (Haji Abdollahi, Hirose 2013). In the early stages of the disease when the flecks are not present, or in cases such as Fundus Flavimaculatus that flecks appear outside of the macula region of the eye, the diagnosis of STGD1 might be difficult; hence, in these situations visiting a retina specialist is necessary for patients (Haji Abdollahi, Hirose 2013).

1.1.9 – Clinical examinations and diagnostic tools

Given that clinical phenotype can be variable in patients with ABCA4 pathogenic variants, based on the variant type and stage of disease, ophthalmologists and retina specialists use different examination methods to diagnosis the disease and determine the disease progression. One of the first useful markers to check for progression of disease is the visual acuity follow-up (Burke, Tsang 2011). The progression rate of the STGD1 can be predicted based on the age they were first diagnosed with the disease. Usually, patients who present with symptoms after 20 years of age are more likely to maintain a better visual acuity compared with those presenting with symptoms before 20 years of age (Lambertus et al. 2015, Burke, Tsang 2011).

Fundus photography is the most common retinal screening application for investigation of retinal disorders such as STGD1 (Abràmoff, Garvin & Sonka 2010). Fundus pictures provide images of the retina that document most abnormalities in the retina such as presence of flecks. Due to the relatively low cost, safety and user friendliness of the cameras in imaging the retina, Fundus pictures are one of primary methods used to investigate STGD1 (Abràmoff, Garvin & Sonka 2010, Burke, Tsang 2011).

Visual field measurement is another useful method in demonstrating defects of central visual field in patients with STGD1 (Burke, Tsang 2011). Defects in central vision can be detected at early stages of STGD1 and defects in peripheral vision can be detected as disease progresses and starts to affect rod photoreceptors. **Table 1.1** lists methods used to investigate STGD1 after visual acuity, Fundus photos and visual field testing. These methods are listed in the table base on their efficiency. Other diagnostic modalities such as Optical Coherence Tomography (OCT), Indocyanine green angiography (ICGA), electrooculogram (EOG) are also listed in the literature (Burke, Tsang 2011).

Table 1.1. The most common methods used to investigate STGD1

Methods name	Abbreviation	Description	Efficiency/practicality
Fluorescein Angiography	FA	Imaging that demonstrates RPE atrophy or advanced choroidal degeneration. When subretinal lipofuscin blocks the blue light from reaching to choroid, a “Dark choroid” appears which can be a characteristic of STGD.	A useful and commonly used method to diagnose patients with STGD1(Abràmoff, Garvin & Sonka 2010, Burke, Tsang 2011, Fishman et al. 1987). The only downfall to this method is that the light can be a progression cofactor, also cannot be performed in young children.
Fundus Autofluorescence	FAF	Visualize the build-up and distribution of lipofuscin in the RPE. This assessment can help to evaluate the disease stages and monitor the progression of disease by showing the increase in accumulation of lipofuscin over time (Boon et al. 2008).	A common and useful method to diagnose patients with STGD1.
Electroretinogram/Full-Field Electroretinogram	ERG/ FF ERG	Record of the photoreceptors performance. In STGD1 (FF ERG) is frequently normal until late stages of the disease. Abnormal FF ERG is reported in more advanced stages of the disease.	This method is not usually altered at young ages and may never be altered in some patients(Lois et al. 2001).

1.1.10 – STGD1 pathogenic variants

Currently, approximately 1,000 disease causing pathogenic variants have been identified in the ABCA4 gene, although this is increasing (Sangermano et al. 2016). The most frequent of these variants contribute to STGD1 in ~10% of cases (Burke, Tsang 2011, Sangermano et al. 2016, Burke et al. 2012). Most STGD1 causing pathogenic variants in the ABCA4 gene are "ethnic-group-specific", meaning that the pathogenic variants most frequent in a specific geographic area but less frequent in a different population (Zernant et al. 2014b, Burke, Tsang 2011). Some of the known ethnic group specific pathogenic variant are: 1) the c.2588G>C (p.[G863A; G863del]) founder pathogenic variant in Northern European patients (Maugeri et al. 1999); 2) the c.[1622T>C; 3113C>T] (p.[L541P; A1038V]) complex allele in patients of mostly German origin (Maugeri et al. 2000); 3) the c.3386G>T (p.R1129L) founder pathogenic variant in Spain (Valverde et al. 2006); 4) the c.2894A>G (p.N965S) variant in the Danish population (Rosenberg et al. 2007); and 5) the c.5318 (p.A1773V) variant in Mexico (Chacon-Camacho et al. 2013).

1.1.11 – Phenotypic variations in STGD1

Diagnosis of STGD1 with standard and typical clinical symptoms such as appearance of fundus flecks and progression rate of visual loss can be easy for retina specialists. However, STGD1 cases may present with variable progression rate, and even variability in fleck sizes, numbers and appearance, which makes the diagnosis much more difficult (Haji Abdollahi, Hirose 2013). This variability in

manifestation of the disease can be due to different parameters, the most important of which are the different pathogenic variants (i.e., ~1,000) in the ABCA4 gene of an affected individual and the stage of disease at the time of diagnosis (Itabashi et al. 1993). This variability could be also due to interaction of other genes or the possibility of environmental modifiers (including light exposure, smoking, and diet) for STGD1 patients (Ryan et al. 2013).

1.1.12 – Animal models and potential therapy

Despite the ongoing research in various fields including genetics, disease mechanism, gene therapy and cell replacement, there is currently no available treatment for STGD1 patients (Haji Abdollahi, Hirose 2013). However, advances in therapeutic applications for ABCA4-associated pathology may show promising results for STGD1 treatment in the near future (Auricchio, Trapani & Allikmets 2015). Genetically engineered mice that lack the ABCA4 gene exhibit many features similar to STGD1 patients, even though mice lack a macula. These symptoms include delayed dark adaptation in ERG, increased all trans-retinaldehyde in light exposure and accumulation of A2E in the RPE. Yellow-white flecks and atrophy are also present in fundus of older ABCA4-/- mice (Weng et al. 1999). Research showed that less exposure to the light or treatment with isotretinoin (a medicine to treat severe acne) might be beneficial for these mice (Radu et al. 2003); however, long-term isotretinoin usage might be harmful (Han, Conley & Naash 2014). Finally, in order to decrease the potential formation of bisretinoids (i.e., N-retinylidene-N-retinylethanolamine or A2E) in the retina, it

is recommended to avoid high-dose of vitamin A supplements for STGD1 patients (Haji Abdollahi, Hirose 2013).

Current success of viral-mediated gene delivery has made gene replacement a reasonable option to treat STGD1 patients, however, the size of the ABCA4 complementary deoxyribonucleic acid (cDNA) is 6.8kb, which is too large to be delivered by an adeno-associated virus (AAV) (Han, Conley & Naash 2014, Trapani et al. 2014). To overcome this issue, research groups successfully exploited the ability of AAV genomes to concatemerize (i.e., packaging of a long continuous DNA molecules with the similar series of the sequences of DNA) via intermolecular recombination, and used dual AVV vectors to transfer the large ABCA4 cDNA. Although using dual AVV vectors showed improvement in phenotype of STGD mouse and pig models, it resulted in expressing lower levels of transgene compared with a single AAV or truncated proteins (Trapani et al. 2014, Colella et al. 2014). Due to larger carrying capacity compared with AAV, Lentiviruses were successful in delivering the gene, but the progress of this method to treat STGD1 has been slowed due to random integration of the gene throughout the genome (Thomas, Ehrhardt & Kay 2003). Non-viral DNA nanoparticles (NPs) have been shown to be an effective gene delivery method for ABCA4-deficient mice, which recovered anatomically and functionally, and showed reduced lipofuscin granules and significant correction in dark adaption by ERG (Han et al. 2012). Although further studies are necessary to determine the efficiency of NP in improving the phenotypic characteristics and immune

responses of STGD1 mice, currently this approach has proved to have the least systemic toxicity (Han, Conley & Naash 2014).

Cell therapy using human embryonic stem cells derived from RPE to transplant sub-retinally is another potential approach to cure STGD1 (Schwartz et al. 2012). The first attempt to do this type of therapy, as a 4-year assessment, was successful (Schwartz et al. 2016). This research demonstrated more than half of treated patients had improvement in visual acuity. Also, no adverse cell therapy related events such as tumorogenicity, hyperproliferation, or ectopic tissue formation or rejection were reported in the cases with STGD. Although the rate of success in this study has opened a new door to advance therapies for macular degeneration disorders, further research in this field is essential due to the lack of a large sample cohort, long follow-up duration, formal control group, plus poor initial visual acuity of patients in this study (Schwartz et al. 2016).

Another option to treat STGD1 with medicines such as dobesilate and angiotensin-converting-enzyme (ACE) inhibitor treatment has been performed by small research groups. Dobesilate is a synthetic fibroblast growth factor inhibitor that was injected intravitreously and resulted in some improvement in the visual acuity of a STGD1 patient after four weeks (Cuevas et al. 2012). Improvement in visual acuity in a group of patients treated with the ACE inhibitor (Ramipril 2%) was reported by another research group after a three-month period follow-up (Rekik, Charfeddine 2012).

1.2 – NEWFOUNDLAND AND LABRADOR POPULATION AND STARGARDT DISEASE

1.2.1 – History of Newfoundland and Labrador

The population of Newfoundland and Labrador (NL) located on the eastern part of Canada is evidenced to be genetically isolated. In 1497, John Cabot discovered Newfoundland. In 1610, the first seasonal colonies of English fishermen became established (Mannion 1977) in the current Conception Bay area (Handcock 2000). In the late 1700s and early 1800s, Protestant settlers from the south-west of England and Roman Catholic settlers from the south of Ireland comprised the main population of immigrants. Natural expansion then resulted in population growth, but still 98% of the NL population are of English or Irish decent (Mannion 1977). Several studies showed the persistent geographic isolation and homogeneity in isolated areas in NL using the data from three representative outport communities (Bear et al. 1988). Although genetic isolation has been confirmed some heterogeneity has been identified in the overall population (Martin et al. 2000). Genetic consequences of such a small and isolated population of Newfoundland settlers are genetic drift, founder effect and inbreeding (Pope et al. 2011).

1.2.2 – Genetic drift, founder effect and the NL population

The process of random alteration in allele frequency over generations is genetic drift. Bottleneck and founder effect are two of the most common consequences of genetic drift. Bottleneck occurs when there is a sudden reduction in the population size, which decreases allelic heterogeneity. The newly generated

population is left with fewer allelic variations creating a founder population (ArcosBurgos, Muenke 2002). The founder population of NL was created by a bottleneck effect due to immigration of English and Irish settlers, resulting in genetic drift and subsequently lower genetic heterogeneity. Therefore, a lower or higher prevalence of some disorders might occure. Examples of higher prevalence for monogenic disorders is Bardet-Biedel syndrome (i.e., 1/17,500 in NL compared with 1/160,000 in more admixed Caucasian populations of northern European ancestry) (Green et al. 1989, Karvonen et al. 2000), likewise some complex diseases such as juvenile type 1 diabetes mellitus have increased incidence in NL (Rahman et al. 2003). Also, founder pathogenic variants identified to increase risk of developing diseases such as cancer (e.g., the exon 8 deletion and an intron 5 splice site mutation (c.942+3A>T) in MSH2 for colorectal cancer) can be one of the major reasons of having a higher incidence rate for colorectal cancer in NL (Woods et al. 2005). It is worth noting that inbreeding (i.e., the tendency of mating with distance relatives or within the community and avoiding others) in NL has been shown to have a higher average value compared to other larger and isolated areas (Bear et al. 1988).

1.2.3 – Hereditary eye diseases in NL

It has been established that NL has a genetically unique structure, large family pedigrees and available clinical information have created an ideal population to study various monogenic diseases including hereditary eye disease (Green, Bear

& Johnson 1986, Doucette et al. 2013). The hereditary eye diseases (caused by mutations in a single-gene) accounted for 33% of all individuals registered blind in 1983, which was previously statistically underestimated in the records from the Canadian National Institute for the Blind (Green, Johnson 1983). Among all single-gene diseases, the frequency of specific recessive disorders was higher due to inbreeding and a founder effect in the NL population (Green, Bear & Johnson 1986).

1.3 – MOLECULAR DETECTION OF STGD1

Clinically, among all currently available genotyping technologies, Sanger sequencing and microarray chips are two of the commonly used methods to genotype individuals with clinical features of STGD1 (Burke, Tsang 2011, Aguirre-Lamban et al. 2009, Zernant et al. 2014a). Utilization of these two techniques in the clinical setting aids in the detection of pathogenic variants in affected individuals or reveals the genotyping status of carriers and unaffected persons.

1.3.1 – Sequencing technology

Determining the order of nucleotides or decoding the chemical building blocks (i.e., bases) of the deoxyribonucleic acid (DNA) molecules is called DNA sequencing. Identification of genetic variation may result in detecting the cause of the various diseases. DNA sequencing can be performed using various techniques, the most common of which was Sanger sequencing. Sanger sequencing is based on incorporation and detection of a fluorescent labeled

terminal nucleotide in the DNA amplified by polymerase chain reaction (PCR) (Sanger, Nicklen & Coulson 1977). Thus, with this method a particular part of the genome is amplified and then sequenced.

After the Human Genome project was completed in 2003, technical improvement and automation with the aim of higher speed and lower cost was achieved. The development of next-generation sequencing (NGS) technologies with the ability to generate a sequence of the whole-genome or whole-exome had a major impact on DNA sequencing approaches (de Magalhaes, Finch & Janssens 2010). NGS can be more targeted utilizing approaches such as whole-exome sequencing which targets protein-coding regions of the human genome. Utilization of whole-genome/exome sequencing has resulted in identifying new variations in the human genome at higher resolution and greater sensitivity than previously possible (Mardis 2008).

1.3.2 – Genotyping using microarray technology

Microarray is a tool to detect particular variants in different segments of DNA. Microarray is a chip-based technology, which requires DNA fragments to be labeled (for example by fluorescent dye). Comparative genomic hybridization (CGH) and single nucleotide polymorphism (SNP) array are two important applications to microarray technology. The microarray application used to detect ABCA4 disease associated pathogenic variants is called the ABCR400 chip. In this microarray application, SNP array genotyping is coupled with array primer extension (APEX) technology to detect the pathogenic variants causing STGD1

in the ABCA4 gene (Jaakson et al. 2003). Although both techniques are based on fluorescent dyes, unlike Sanger sequencing, which genotypes the amplified segment of DNA, microarray probes target specific genetic mutation. Due to the low cost compared with Sanger sequencing, microarray is still used as a clinical test for Stargardt disease.

According to Burke and Tsang, microarray is a common method to detect many variants in the ABCA4 gene that are known as disease causing. The microarray chip is being updated as new variants have been added to the pathogenic list. Based on the Burke and Tsang study, this genotyping method is reported to detect ~65% to 75% of all disease-associated alleles in Stargardt patients, ~30% to 65% of all alleles causing autosomal recessive CRD and finally ~16% of disease associated alleles in autosomal recessive RP patients (Burke, Tsang 2011). However, in a study by Aguirre-lamban et al., the ABCR400 microarray yielded a variant detection rate of 43.5% for STGD1 patients, 4.8% for arCRD patients and 4.8% for arRP patients (Aguirre-Lamban et al. 2009). In this study, authors also reported 1.6% of false positives and 1.6% of false negatives for the ABCR400 microarray. Thus, they attempted to combine the microarray with other high-throughput approaches such as denaturing high-performance liquid chromatography (dHPLC) scanning to achieve a higher mutation detection rate. Using microarray and dHPLC in that study increased the detection frequency of mutated allele to 64.8% for STGD1 patients and 6.4% for autosomal recessive CD patients, but no changes were seen for autosomal recessive RP

detection rate (Aguirre-Lamban et al. 2009). The efficiency of direct Sanger sequencing of coding regions and intronic-exonic boundaries is estimated to be 80% for STGD1 patients (Zernant et al. 2014b). In general, around 25% to 30% of patients were found with just one pathogenic variant, and approximately 15% of them remain without any identified pathogenic variant even after complete sequencing of the ABCA4 gene. Three possible reasons for not finding any pathogenic mutations included: 1) the disease-causing variant is located in a non-coding region of ABCA4 gene; 2) phenocopies (i.e., similar phenotype but not same underlying genetic etiology); 3) Locus Heterogeneity; and 4) the lack of testing for copy number variants (CNVs) which were shown to be rare (~1% of all patients) in the ABCA4 locus (Zernant et al. 2011).

1.3.3 – Previous studies on Stargardt in NL

Families with STGD1 have been identified since 1978 through the ocular genetics clinic and medical record, family history and geographic origin were collected (J. Green, 2013, personal communication). In a study cohort of 46 STGD1 patients from 29 families utilizing targeted Sanger sequencing and haplotype analysis resulted in the identification of 63 variants in the ABCA4 gene. Of these 63 variants, 14 were known pathogenic missense variants, 2 others were mild pathogenic variants that were disease causing where present with a severe mutation in trans and 1 was a novel pathogenic variant found in a family from NL (T.L. Young and J. Green, 2013, personal communication).

The most common mutation seen among ~50% of families was the c.5714+5G>A (splice site) pathogenic single nucleotide variant (SNV). This SNV, which is also common among Northern European populations, was either homozygous or compound heterozygous in patients. The second most common pathogenic variant in patients was the c.5461-10T>C (splice site) SNV, which is another known variant associated with the Stargardt disease (Klevering et al. 2005, Azarian et al. 1998, Roberts et al. 2012). This mutation was seen in 12 patients and has a higher frequency in people from Conception Bay, NL. The following pathogenic variants were seen with a lower frequency: c.2564G>A (p.W855X); c.3322C>T (p.R1108C); c.4139C>T (p.P1380L); c.4163T>C (p.L1388P); c.4469G>A (p.C1490Y); c.4577C>T (p.T1526M) mutations were found in 2-4 families. However, the c.634C>T (p.R212C); c.1522C>T (p.R508C); c.3323G>A (p.R1108H); c.4537delC (p.Q1513fs); c.6089G>A (p.R2030Q); c.6449G>A (p.C2150Y) pathogenic SNVs were only identified in one family each. The 2 milder pathogenic SNVs mentioned above were: c.455G>A (p.R152Q) and c.2588G>C (p.G863A). Each of these mutations was repeatedly seen in cis with another mutation such as: c.455G>A (p.R152Q) and c.4163T>C (p.L1388P) or c.2588G>C (p.G863A) and c.5714+5G>A (splice site) making a complex allele. A novel pathogenic SNV, c.67-1delG (splice site), was found in the affected members of one family in NL (T.L. Young and J. Green, 2013, personal communication).

Recent research on 2 other STGD1 patients from NL using Sanger sequencing indicated three other causal SNVs: c.3064G>A (p.E1022K) c.4222T>C (p.W1408R) and c.4918C>T (p.R1640W). Based on family studies and literature review, c.4222T>C (p.W1408R) and c.4918C>T (p.R1640W). SNVs are in cis and form a complex allele (Valverde et al. 2006).

1.3.4 – Genotyping using Sequenom MassARRAY technology

Genotyping with this technology is based on the weight of final molecular products. Genotyping using iPLEX chemistry on the Sequenom MassARRAY has two levels of specificity. This first is the PCR, in which the locus specific PCR primers bind to the sequences of target DNA and amplify the region of interest. The second level of specificity is when the extension (EXT) reaction occurs. In this step, another locus specific oligonucleotide primer anneals next to the polymorphic (or variant) site to genotype. The EXT primer has an indicated mass and immediately binds to the locus where the variant is located and adds a single complementary mass-modified base. Using matrix-assisted laser desorption/ionization time-of-flight (MALDI-TOF) mass spectrometry, the mass of the extended primer based on the alternative alleles present at the polymorphic site of interest, is determined (Gabriel, Ziaugra & Tabbaa 2009). According to Meyer et al, in the process of allele detection by MALDI mass spectrometry, the laser beam serves as desorption and ionization source, and the matrix absorbs the laser light energy and causes part of the illuminated substrate to vaporize. The process occurs as a rapidly expanding matrix plume carries some of the

analyte into the vacuum with it and assists the sample to ionize. The majority of the laser's energy is absorbed by the matrix molecules. Once the sample molecules are vaporized and ionized, they are transferred electrostatically into a time-of-flight mass spectrometer (TOF-MS), where they are separated from the matrix ions, independently detected based on their mass-to-charge ratios. The Typer software (provided by the company) automatically translated the detected mass of primers to a genotype call for each reaction (Meyer, Ueland 2011, Gabriel, Ziaugra & Tabbaa 2009).

1.4 – KNOWLEDGE TRANSLATION

Knowledge translation (KT) is the ability to transfer or translate the knowledge acquired by a research group to another part of society. The knowledge and/or experience gained by the first group is beneficial to the second group (Argote, Ingram 2000). KT encompasses a wide range of activities; among these activities translation of genetic innovations into a better healthcare system is highly important. In order to improve the healthcare system, it is critical to conduct research both on KT strategies and the technology transfer process (Kristoffersson, Schmidtke & Cassiman 2010). At Memorial University, collaboration between research and clinic has already benefited society. This KT project will translate known genetic findings into a clinically useful diagnostic test. The aim of this KT project is to enhance the healthcare by offering a cost-effective, easy to use molecular diagnostic test.

1.5 – ANALYTIC VALIDITY, CLINICAL VALIDITY, AND CLINICAL UTILITY

The evaluation of a genetic test is based on three criteria that were proposed by the National Institutes of Health–Department of Energy Task Force in 1997. These criteria include analytic validity, clinical validity, and clinical utility(National Human Genome Research Insititue 03/2012).

Analytical validity includes accuracy (concordance of the results) based on analytical sensitivity (measuring the rate of true positives), and analytical specificity (measuring the rate of true negatives); precision (reproducibility of the results); reportable range (the possible outcome of the results); reference range (Wild Type sequence). They all measure the performance characteristics of a lab developed test.

Clinical validity refers to preciseness of results produced by a test in relation to presence or absence of a pathogenic variant.

Clinical utility is the “the balance of benefits to risks” which refers to the ability of a diagnostic test in recognizing the disease, preventing adverse health care practices and aiding in possible treatments(Grosse, Khoury 2006, Burd 2010) .

The objectives of this study are to: 1) design, optimize and validate a genetic test to facilitate the accurate diagnosis of (already known pathogenic variants causing) Stargardt disorder in the NL population; 2) determine the allele

frequency of known and recurrent pathogenic variants causing Stargardt disorder in the NL population; and 3) compare the allele frequency of known and recurrwent pathogenic variants causing Stargardt disorder in the NL population with non-NL populations.

Chapter 2

2.0 – MATERIALS & METHODS

2.1 – STUDY COHORT AND ETHICS

Affected and unaffected family members with STGD1 disease were previously recruited and informed consent was obtained from all participants in the study (T.L. Young and J. Green, 2013, personal communication). The project was approved by the Human Investigation Committee, now known as the research ethics board (REB) of the Faculty of Medicine, Memorial University of Newfoundland (HIC No. 02.116) and the research advisory committee (RPAC) of Eastern Health, St. John's, NL. In the previous study, all extended family histories, geographic origin and consanguinity were recorded. Clinical investigations such as visual acuity, central and full visual field, fundus photos (i.e., retinal photographs), fluorescein angiography, ERG, EOG and OCT were performed on affected individuals if possible. All blood samples were collected and genomic DNA was extracted from peripheral leukocytes as previously described (Miller, Dykes & Polesky 1988).

In this study, the DNA samples and clinical information of participants in the former study were used for the optimization and validation cohorts. The optimization cohort was comprised of 14 samples covering all the 20 known pathogenic variants causing STGD1 in the NL population (**Table 2.1**). The validation cohort was comprised of 78 samples from individuals suspected to

have a clinical diagnosis of STGD1 or parents/siblings/relatives of affected individuals diagnosed with STGD1, with known genetic status, that were blinded to me, the investigator.

Regarding control samples, 536 de-identified genomic DNA samples from disease or control populations used in other research studies [such as ankylosing spondylitis (n=170), hereditary hearing loss (n=187), cardiomyopathy (n=94) and colorectal cancer (n=85)] were used to determine the allele frequency of pathogenic variants in the ABCA4 gene in the NL population. DNA samples used for the non-NL populations included samples from United Kingdom population (n=191) and de-identified samples from the Alberta (n=187) and Ontario (n=125) population controls, totalling 503 samples. No clinical vision information was available for population controls as they were originally participants of other studies.

To assess the clinical validity in this study, a small cohort (n=15) of genomic DNA samples with unknown mutational status was assessed using the custom genotyping panel.

Table 2.1. The 20 pathogenic variants identified in NL causing STGD1 disease

Nucleotide change	Amino acid change	Number of alleles	Exon
c.67-1delG	splice site	3	2

c.455G>A	p.R152Q	3/11	5
c.634C>T	p.R212C	1	6
c.1522C>T	p.R508C	2	11
c.2564G>A	p.W855X	5	16
c.2588G>C	p.G863A	2/4	17
c.3064G>A	p.E1022K	1	21
c.3322C>T	p.R1108C	3	22
c.3323G>A	p.R1108H	1	22
c.4139C>T	p.P1380L	4	28
c.4163T>C	p.L1388P	8	28
c.4222T>C	p.W1408R	1	28
c.4469G>A	p.C1490Y	2	30
c.4537delC	p.Q1513fs	1	30
c.4577C>T	p.T1526M	3	31
c.4918C>T	p.R1640W	1	35
c.5461-10T>C (IVS38)	splice site?	12	38
c.5714+5G>A (IVS40)	splice site	31	40
c.6089G>A	p.R2030Q	1	44
c.6449G>A	p.C2150Y	1	47

2.2 – IN-SILICO DESIGN OF MULTIPLEX PANEL

To multiplex using the Sequenom MassArray technology, I used two different programs (i.e., Assay Design Suite and Typer4) to design polymerase chain reaction (PCR) and extension (EXT) primers for each of SNVs to be included in the multiplex laboratory developed test (LDT) panel. Five different automatic steps were used in the Assay Design Suite software (Agena Bioscience, San Diego, Ca, USA) in designing a multiplex panel, which included: 1) retrieve and format sequences; 2) find proximal single nucleotide polymorphisms (SNPs); 3)

identify optimal primer areas; 4) attempt to design panel; and 5) validate panel design.

The processes of designing primers in the Design Assay Suite software through the five steps is briefly described below. In the first step (i.e., retrieve and format sequences), the retrieved sequences were reformatted into a SNV group file format, and then the target sequence was generated based on the selected flank size. In the second step (i.e., find proximal SNPs), the SNV sequence was aligned to the human genome to determine if there was a registered SNP within the proximal area of the selected assay, which could prevent design of primers. In the third step (i.e., identify optimal primer areas), the PCR primers were designed. Then the human genome was scanned to determine if there were any other similar amplification products that could be used by the specific extend primer, which could prevent multiple targets being produced for the EXT primers. In the fourth step (i.e., attempt to design panel), the EXT primers were designed for different alleles with a specific weight to be sorted by mass. Then, the multiplex panel was generated including the sequence of PCR and EXT primers, which was used to order the primers or to import the design into MassARRAY Typer software. The design summary also created in step 4 provided information regarding the number of SNVs that multiplex together, the number of wells in the design and the weight of the EXT primers. In the fifth step (i.e., validate panel design), the amplification products were validated to prevent, or at least, mitigate unintentional false positives in the mass spectra analysis.

The Design Assay Suite software estimated in a validation report (which was assessed when step 5 of the program was complete) the number of locations that the designed primers could have a potential homology with, in the desired part of genome. These locations or hits were divided into three (3) categories. The true hit (i.e., H.True) value represented the number of possible PCR amplicons produced by the designed PCR primer pair that contained a valid target for the subsequent EXT primer. In contrast, the false hit (i.e., H.False) value represented the number of possible amplicons generated by the designed PCR pair that contained an invalid target for the following EXT primer. The null hit (i.e., H.Null) value represented the number of possible amplicons created by the designed PCR pair that did not contain a valid target for the related EXT primer. Also, the frequency that forward or reverse PCR primers were independently matched with the genome was reported for each “rs” number.

2.2.1 – In-silico design of 20 pathogenic variants causing Stargardt disease

In-silico design in Assay Design Suite software was accomplished by importing sequences in FASTA format (i.e., a text-based format using single letter codes showing nucleotide sequences) or SNP “rs” identification numbers to the software for all 20 pathogenic variants, determined using Alamut software (Interactive Biosoftware, France) and dbSNP (

Table 0.1). SNV “rs” numbers were used for the majority of pathogenic variants (i.e., 18/20), whereas FASTA sequences (1,035 base pairs) were used for the

two deletions (i.e., c.67-1delG and c.4537delC) lacking “rs” identification numbers. Desired organism type, chemistry, genomic database and multiplex level of assay were also selected for the design (**Table 2.2**).

If any of the design steps failed due to issues in the sequence that interfered with effective primer binding, the software showed a reject for that step. Each reject generated a code and a brief description of the reason or potential for the rejection. For example, the potential for false-priming, hairpin formation and primer-dimer formation was described in scales of high, moderate and weak. When there was a high potential of an issue for a given SNP, it was rejected and consequently excluded from the multiplex primer design. To incorporate the rejects, the “advanced settings” option in the software was used to modify the default settings for each of the 5 steps involved in the assay design, which can raise or lower the stringency of each option.

I used a trial-and-error approach with respect to parameters within “advanced settings” in order to incorporate all the SNVs into one well. In each version of the design, one or two options were altered and the results of those changes were reviewed. Further changes to other options were applied based on results from previous alterations.

Table 2.2. Options selected for the multiplex LDT design using Assay Design Suite software.

Organism	Human
Database	Feb.2009(GRCh37/hg19)
Chemistry	iPLEX

Multiplex Level	20

2.3 – PRIMER MIXTURES AND ADJUSTMENTS

I prepared a pool containing all forward (F) and reverse (R) primers with the final concentration of 0.5uM for each primer. The original PCR primers were ordered at 100uM concentration and a calculated amount of each primer was added to each tube based on the final volume of the reaction mixture. UltraPure distilled water was then added to dilute and bring the final volume to 1,000ul. When a PCR primer was shared for multiple SNVs, that primer was added to the mix only once. For example, in the 1x20-plex LDT panel, rs61750130, rs61750131 and rs61750135 had shared PCR primers and only one unit of primer (i.e., F and R) was added the PCR primer mix.

The EXT primers for the iPLEX reaction were adjusted by concentration prior to genotyping by one of our laboratory assistants. Three-tier method in the protocol provided by manufacturer was selected for adjusting the primers. Briefly, the method included dividing the mass into three groups: low mass (LM), medium mass (MM) and high mass (HM). A 5µL for each LM primer, 10µL for each MM primer and 15µL for each HM primer were added to make the EXT primer cocktail. UltraPure distilled water (49µL) and EXT primer mix (1µL) was added to the wells in a PCR plate and run in triplicate. The plate was vortexed, centrifuged and placed in the plate holder of the Sequenom Nano-dispenser.

The assays transferred to the Typer4 software generated two types of reports that were used for EXT primer adjustment. The first report was an excel

sheet comprised of all the assays, their masses, signal to noise ratio (SNR) and the percent that was needed to be added for each assay based on the average over three wells (these numbers are based on the assay that has the maximum SNR). The second report was comprised of three histograms, which represented the SNR for each assay.

The quality control (QC) step simply measured the peak for each EXT primer in water rather than with a sample present. The report from the Typer4 software identified the ratio of each primer that should be added to the iPLEX primer cocktail in order to achieve the best peak. Given that we had three replicates for each SNV, the average percent to add for each primer for each assay was calculated. If the average volume to add was above 50% for any of the assays, I added a calculated amount of the extend primer to the EXT primer cocktail based on the mass of that EXT primer. Once the required amount was added to the mixture again, the resulting cocktail was spotted on the chip and transferred to the MassARRAY analyzer to determine if the SNR for each SNV increased compared with the initial SNR assessment. The result was analysed once again and the previous steps were repeated if more adjustments were required.

2.4 – SEQUENOM MASSARRAY AND IPLEX CHEMISTRY

The general procedure for iPLEX genotyping included the following steps: 1) normalize DNA concentration; 2) DNA amplification (PCR); 3) neutralize

unincorporated dNTPs (Shrimp Alkaline Phosphatase (SAP) reaction); 4) iPLEX extension reaction; 5) condition the iPLEX reaction products; and 6) dispense onto SpectroCHIP Arrays.

2.4.1 – Preparation of samples

A range of 5-10ng/µl concentrations for DNA was required for genotyping with Sequenom MassARRAY. I prepared a master plate of genomic DNA samples with concentration of 5ng/µl. All the DNA samples were first diluted to 100ng/µl in Tris Ethylenediaminetetraacetic acid (TE) buffer, further diluted in TE buffer to 10ng/µl and finally diluted to 5ng/µl in UltraPure distilled water.

2.4.2 – DNA amplification

The setting for the same multiplexed assays for all wells with different DNA samples, from the protocol provided by the manufacturer was selected. PCR cocktail was made following the protocol (**Table 2.3**) using a microtube. After a quick vortex and centrifuge of the microtube containing PCR cocktail, 3µL of the solution in the tube was aliquoted into the wells of PCR-96-LP-FLT-C PCR Microplate (AXYGEN, CA, USA). 2µL of DNA (5ng/µl) was then added to each well. The plate was gently vortexed and centrifuged at 290 relative centrifugal force (rcf) for 30 seconds, and then transferred to a Veriti® 96-Well Fast Thermal Cycler (Applied Biosystems, Life Technologies, CA, USA) and run under conditions stated in the **Table 2.4**.

2.4.3 – Neutralize unincorporated dNTPs (SAP reaction)

Shrimp Alkaline Phosphatase (SAP) enzyme solution was prepared in a microtube following the manufacturer's protocol (**Table 2.3**). The microtube was gently vortexed and spun. Then, 2µL of the SAP solution was dispensed to each of the wells in the plate containing the amplified PCR products. The plate was again gently mixed by vortexing and centrifuged at 290 rcf for 30 seconds and transferred to the thermal cycle with conditions that are indicated in **Table 2.4**.

Table 2.3. Master mix compositions in preparing an iPLEX reaction for the LDT panel, for different steps (i.e., PCR, SAP, Extension) included.

PCR MasterMix (µl)	**1x**
HPLC grade water	0.80
10X PCR Buffer	0.50
25 mM MgCl2	0.40
25 mM dNTP	0.10
5 u/µl Sequenom PCR Enzyme	0.20
PCR Primer (0.5uM)	1.00
Total volume-DNA per well	3.00
DNA	2.00
Total per well	5.00
Dispense 3µl of PCR mix to each well	
Dispense 2µl of DNA into each well	
SAP MasterMix (µl)	**1x**
HPLC grade water	1.53
SAP Buffer	0.17
SAP Enzyme	0.30
Total per well	2.00
Dispense 2µl of SAP mix into each well	
Extend MasterMix (µl)	**1x**
HPLC grade water	0.755

iPLEX-PRO Buffer	0.200
iPLEX Termination Mix	0.200
iPLEX PRO Enzyme	0.041
Extend Primer	0.804
Total per well	2.000
Dispense 2µl of Extend mix into each well	

Table 2.4. Thermal cycling parameters in preparing an iPLEX reaction for the LDT panel for the different steps (i.e., PCR, SAP, Extension) included.

Temp ˚C	Time	Cycles	
PCR			
95	2 min		
95	30 sec	45 cycles	
56	30 sec		
72	1 min		
72	5 min		
4	∞		
SAP			
37	40 min		
85	5 min		
4	∞		
Extension iPLEX			
94	30 sec		
94	5 sec		40 cycles
52	5 sec	5 cycles	
80	5 sec		
72	180 sec		
4	∞		

2.4.4 – iPLEX extension reaction

The same multiplexed assays for all wells with different DNA in each well, from the protocol provided by the manufacturer was selected. Extension cocktail was

made following the manufacturer's protocol (**Table 2.3**) in a microtube. After quickly vortexing and a quick spin, 2µL of the extension mix was added to each well of the plate containing PCR and SAP products. The plate was then gently mixed by vortexing and centrifuged at 290 rcf for 30 seconds and transferred to the thermal cycler with conditions that are indicated in **Table 2.4**.

2.4.5 – Condition the iPLEX reaction products

Briefly, resin was carefully added to the required wells of the dimple plate using a scraper. It was then left to dry for 10 minutes. While the resin was drying, 41µL of UltraPure distilled water was added to each well of the plate and centrifuged at 290 rcf for 1 minute. In order to add the dried resin into the wells of the plate, I gently turned the plate upside down so that the resin fell out of the dimple plate into the wells. Then, the sample plate containing the resin was rotated for 30 minutes on a rotator with the lowest speed at room temperature and centrifuged for 5 minutes at 805 rcf to be prepared for dispensing into a chip.

2.4.6 – Dispense onto SpectroCHIP arrays and defining assays and plates

Following the manufacturer's protocol, the 6-pin option for 96 well plate format was selected to transfer samples onto the chip in the Nanodispenser machine. The order of spotting (i.e., for which sample from which wells in the sample plate, to which region on the chip) was given under Mapping section (i.e., Software option) of the Nanodispenser machine (Agena Bioscience, San Diego, Ca, USA)

and saved with a specific name. Also, under Mapping section (i.e., Software option) systematic options of analyte or auto-Tuning could be selected. The spotting settings under Method section (i.e., Software option) include 3 different icons, which included setup, cleaning and aspirate/dispense. In setup, after selecting the correct mapped file, a target volume of 14nl; a lower limit of 8nl; and an upper limit of 18nl were selected. Cleaning settings were as default, and under aspirate/dispense settings included in **Table 0.2** were selected. In case of using a new chip, the calibrant was first dispensed to the chip by Nano-dispenser machine, and analyte + calibrant (i.e., Software option) option was selected under the Method section (i.e., Software option). Finally, the proper method file was selected under Transfer section (i.e., Software option), and the chip spotting was started. When dispensing by the Nanodispenser machine was completed, the chip was carefully transferred to the MassARRAY system. To link the chip and samples with the designed assays, the following file inputs were created and uploaded to the MassARRAY Typer4 software: 1) a special file input (.txt) with the name of samples in the order of how they are located in the actual plate was created, which was then transferred to the MassARRAY Typer4 software under Plate Editor (i.e., Software option) and saved as a new sample group with a given group ID; and 2) the excel design output file including the information about the designed assays was uploaded under Assay Editor (i.e., Software option) of MassARRAY Typer4 software. Then, create plate (i.e., Software option) under Plate Editor (i.e., Software option) was selected and the assays were applied to

the plate and sample groups that were created. In the MassARRAY database, the assays and order of samples in the spotted plate were setup. The plate in the MassARRAY database was connected to the dispensed samples on the chip with a program called “chiplinker” before the MassARRAY analyzer started shooting lasers and ionizing the reaction products on the chip. The acquired spectra and data generated by Typer4 software were then analysed in detail.

2.5 – ASSESSMENT AND SELECTION OF BEST PERFORMING LDT PANEL

The raw data generated by the MassARRAY using Typer4 software (Agena Bioscience, San Diego, Ca, USA) was analyzed separately for every run. A cohort of 14 samples (i.e., optimization cohort), which were positive for at least one of the SNVs, was assessed in duplicate on both LDT panels (i.e., 2x10-plex and 1x20-plex). The first step in the analysis was to inspect the automated genotype call followed by manually visualizing all genotype calls to ensure accuracy. The second step was to devise a calling algorithm for a more stringent method of accepting calls rather than visually inspecting the data or relying solely on the automated genotype call. The threshold for two (2) specific parameters were chosen based on two (2) runs for each LDT panel and was applied for each subsequent run. The initial candidate parameters included: fractional unextended primer (F-UEP) or yield (1 - F-UEP) and allele height (AH). Minimum and average values for yield and AH were calculated for every SNV in each run in order to set a threshold. Non-template control (NTC) wells, which contain all

reagents of a regular well but no test samples, were assessed on each run and the percentage of assays containing automatic genotype calls was documented.

To determine if the quality metrics were improved by replacing iPLEX Gold with iPLEX Pro chemistry, the optimization cohort along with two NTC wells were assessed in duplicate for both the 1x20-plex and 2x10-plex LDT panels. To determine the differences between the 2x10-plex vs 1x20-plex LDT panels, the optimization samples were assessed on each LDT in triplicate using iPlex Pro chemistry.

2.6 – CONFIRMATION OF GENOTYPES BY SANGER SEQUENCING

2.6.1 – Designing PCR primers

Specific F and R primers were designed to amplify the regions of interest. In the previous study (T.L. Young and J. Green, 2013, personal communication), thirty-two (32) F and R primers were extracted or redesigned in the ABCA4 gene based on the paper by Ariazan et al. (Azarian et al. 1998). These primers were used to amplify 16 exons and introns (depending on where the mutation of interest occurs) in the ABCA4 gene to find causal variants for STGD1 in the NL population. The same primers in addition to six more primers (i.e., including F and R strands) that we designed for exon 5, 22 and 39 were used in my study. The primers for exon 5, 22 and 39 were redesigned in order to achieve a bigger amplicon size and expand the sequenced region. All primers (i.e., both F and R strands) were designed using primer 3 software (http://bioinfo.ut.ee/primer3-0.4.0/).

2.6.2 – Preparing the DNA samples at the required concentration

A master plate of 5ng/µl was prepared for all samples in the optimization cohort. All the DNA samples were first diluted to 100ng/µl in TE buffer, then diluted in TE buffer once more to 10ng/µl and finally diluted to 5ng/µl in UltraPure distilled water. For patient samples with unknown status, 10ng/µl DNA was prepared in microtubes by diluting the prepared 100ng/µl in TE Buffer first and then diluting further in UltraPure distilled water to 10ng/µl.

2.6.3 – PCR procedure, examining the amplification on the gel electrophoresis, and purifying the products using Sephacryl

Following the standard protocol for PCR, a mixture containing 2µL of 10X PCR Buffer (containing MgCl2), 5µL of Betain (3.75µ), 0.4µL of dNTPs (10 mM), 0.08 µL of KapaTaq DNA Polymerase (5 U/µL) (Kapa Biosystems, Boston, MA), 8.92 µL of distilled dH20, 0.8 µL of F primer (10 µM) and 0.8 µL of R primer (10 µM) was made. 18µL of the mixture was then aliquoted into the 96-well PCR plate followed by 2µL of 5 ng/µl of each DNA sample. The plate was then sealed, centrifuged and transferred to the GeneAmp PCR System 9700 Thermal Cycler (Applied Biosystems, Foster City, CA) with a program setting described in **Table 2.5**. The amplified PCR products were examined on gel electrophoresis using a 1% agarose gel consisting of 1.5g of agarose, 100 mL of Tris Borate EDTA (TBE) and 3.5µL of SyberSafe. The PCR products and ladder (100 bp) were loaded into the gel and the gel was then transferred to the electrophoresis

system. The electrophoresed gel containing PCR amplicons was then observed under Ultraviolet (UV) light from a Kodiak GEL LOGIC 100 Molecular Imaging System (Rochester, Y, Version 4.01, 2005). Successfully amplified PCR products, which were observed with a correct band size under the imaging system, were required to be purified before the cycle sequencing reaction. The purification step was done using Sephacryl S-300HR. Re-suspended Sephacryl (300µL) was aliquoted to the wells on a Millipore Multi-screen plate, which was placed on top of a corresponding 96-well waste plate to catch flow-through. They were then balanced and centrifuged for 5 minutes at 1811 rcf. The solutions in the catch plate were discarded. The PCR products were added to the Millipore Multi-screen plate, which was aligned and positioned over a clean PCR plate. As described above, the plates were balanced and centrifuged for 5 minutes at 1811 rcf. The collected flow-through in the PCR plate contained the purified PCR products.

Table 2.5. Thermal cycling parameters for the touch-down PCR step of Sanger sequencing.

Temp ˚C	Time	Cycles
PCR		
94	5 min	
94	30 sec	5 cycles
64	30 sec	
72	30 sec	
94	30 sec	30 cycles
54	30 sec	
72	30 sec	
72	7 min	
4	∞	

2.6.4 – Cycle sequencing, ethanol precipitation and sample setup on the ABI 3130 or 3730 XL DNA Analyser

A reaction mixture consisting of 0.5µL of Sequencing Enzyme Big Dye Terminator V. 3.1, 2µL of 5X sequencing buffer (Applied Biosystem, Carlsbad, CA, USA), 0.32µL of primer (10 µM) and 15.18µL of dH2O was made and aliquoted to an optical 96-well reaction plate (Applied Biosystem, Carlsbad, CA, USA). Note that the same mixture was made twice, once with the F primer and the other with the R primer. Purified PCR products (2µL) were then added to each well. The plate was covered with a silicon mat, quickly spun down on a centrifuge and then loaded to the thermal cycler with the program settings shown in **Table 2.6.**

Table 2.6. Thermal cycler settings for the cycle sequencing reaction.

Temp ˚C	Time	Cycles
ABI CYCIE SEQ		
96	1 min	24 cycles
96	10 sec	
50	5 sec	
60	4 min	
4	∞	

For the Ethanol precipitation step, I added 5µL of 125mM EDTA followed by 65µL of 95% Ethanol (EtOH) to each reaction well. The plate was then covered with a silicon mat, it was then briefly vortexed, centrifuged and incubated at ambient temperature in the dark for 15 minutes. After incubation, the plate was centrifuged for 30 minutes at 1811 rcf, and then inverted to discard the

supernatant. The inverted plate covered with paper towels underneath, was then centrifuged briefly at 18 rcf. Then, 150µL of 70% EtOH was added to each sample on the plate and centrifuged for 15 min at 1811 rcf. The supernatant was again discarded by inverting the plate, and in the same manner as the previous step, the inverted plate covered with folded paper towels was centrifuged at 18 rcf. The plate was then left in the dark to air dry at room temperature for 15 minutes. Highly deionized (Hi-Di) formamide (15µL) was subsequently aliquoted to each well and covered with a septa mat. The plate was briefly vortexed, centrifuged and loaded into Thermal Cycler for denaturation at 95˚C for 2 minutes. The plate was centrifuged briefly and loaded either into the Applied Biosystem instrument (ABI) 3130 or 3730 XL DNA analyser (Applied Biosystem, Carlsbad, CA, USA), depending on which was available at the time.

2.6.5 – Analyzing Sanger sequencing data

Data collected from the ABI DNA analyser instrument was first analyzed by the sequencing analysis software (version 5.4, Applied Biosystem, Carlsbad, CA, USA) to see the raw data. The high quality sequences were then transferred to Mutation Surveyor (Version 3.0, Softgenetics, State College, PA) to identify DNA sequence variants by comparison with the reference genome.

2.7 – OPTIMIZATION OF THE 1X20-PLEX LDT PANEL

2.7.1 – Adjustments to eliminate automated genotype calls in NTC wells

To determine if increasing the annealing temperature (from 56 to 57˚C) in the PCR thermal cycling program (**Table 2.4**) resulted in elimination of automated

genotype calls in the NTC wells, I assessed the optimization cohort including 2 NTC wells on the selected LDT panel. To determine if an interaction between PCR or EXT primers might cause automated genotype calls in the NTC wells, the optimization cohort including two regular NTC wells (with both PCR and EXT primers) in addition to four NTC wells that had all required reagents except for PCR primers (i.e., ultrapure water replaced PCR primers) was assessed on the 1x20-plex LDT panel. To determine if using Uracil-N-glycosylase (UNG) enzyme results in elimination of automated genotype calls in the NTC wells, the optimization cohort including two NTC wells using the UNG kit was assessed using the 1x20-plex LDT in triplicate. The percentage of automated SNV calls run in triplicate was calculated. Preparation of the PCR mix, which is the only step that differed using UNG kit is summarized in **Table 2.7** and **Table 2.8**. The master mix composition and thermal cycling program for PCR using UNG kit are displayed in **Table 2.7** and **Table 2.8**, respectively.

Table 2.7. Master mix compositions for PCR step using UNG kit.

PCR MasterMix (µl)	**1x**
UNG Enzyme	0.05
HPLC grade water	0.75
10X PCR Buffer	0.50
25 mM MgCl2	0.40
25 mM dNTP/dUTP	0.10
5 u/µl Sequenom PCR Enzyme	0.20
PCR Primer (0.5uM)	1.00
Total volume-DNA per well	3.00
DNA	2.00
Total per well	5.00

Dispense 3µl of PCR mix to each well	
Dispense 2µl of DNA into each well	

Table 2.8. Thermal cycling parameters for the PCR step using UNG kit.

Temp ˚C	Time	Cycles
PCR		
30	10 min	
95	2 min	
95	30 sec	45 cycles
56	30 sec	
72	1 min	
72	5 min	
4	∞	

2.7.2 – Adjustments to increase allele height

2.7.2.1 – Nanodispenser adjustments

To determine if auto-tuning results in consistently higher volumes compared with manual spotting, 64 samples were spotted with and without the auto-tuning function enabled. To determine if the viscosity of the multiplex LDT affects the volume spotted, 64 samples were spotted with and without the detergent Tween 20. To determine if a correlation exists between the spotted volume and the peak height, a range of 355-365 samples (i.e., samples used in 2.7.2.3) were selected. For each SNV, the peak height of homozygous alleles was divided into two groups based on their spotted volumes of nano-liter (nl) (i.e., <14nl and >14nl). The number of samples with a peak height below threshold of seven intensity units was recorded for each group.

2.7.2.2 – Adjustment of PCR/extension primer pool based on optimization cohort

To determine the amount of primer used for each SNV in each run, a formula was devised to calculate the percentage of used primer: allele height/ (allele height + primer height) x 100. The minimum and average numbers for percentage of used primer (UP) was calculated for each SNV in 3 runs that was assessed using the optimization cohort and the 1x20-plex LDT.

To determine if the new extension mix resulted in higher quality performance of the SNVs, the optimization cohort was assessed using the 1x20-plex LDT panel with the old EXT primer cocktail and with the newly made EXT primer cocktail. Then, for the specific SNVs that had higher amount of EXT primers in the cocktail, the minimum and average values for yield, AH and UP were compared between runs.

To determine if having unsatisfactory AH for specific SNVs is due to low amount of PCR products (i.e., as a result of low PCR primers in the mix). As before, the minimum and average numbers for percentage of used primer (UP) was calculated for each SNV in 3 random runs that was assessed on the optimization cohort on 1x20-plex. Then, a new PCR primer cocktail with double the amount of primers for SNVs that had unsatisfactory height of allele, and also minimum value of less than 80% UP, was made. The optimization cohort was assessed on the 1x20-plex LDT panel once with the old PCR primer cocktail and then with the newly made PCR primer cocktail. Then, for the specific SNVs that

had higher amount of EXT primers in the cocktail, the minimum and average values for yield, AH and UP were compared between the two runs.

2.7.2.3 – Allele frequency determination

The 1x20-plex LDT panel was used to determine the allele frequency of the 20 pathogenic variants in the general population (NL and non-NL). A total number of 1039 control samples compromised of 536 individuals from NL and 503 from non-NL (more detail information of these samples in the 2.1 **–** Study cohort) were tested on 1x20-plex LDT panel. All the automated genotype calls were inspected manually by visualizing and the accuracy of calls was confirmed. I excluded all inconclusive genotypes from downstream calculations for the allele frequency data, and minor allele frequencies (MAF) for each assay were calculated based on the total number of accepted genotype calls. In addition, the MAF of all the 20 SNVs for European non-Finnish population from EXAC browser was extracted and compared with the obtained data.

2.7.2.4 – Final optimization of the 1x20-plex LDT panel

Poor performing SNVs were selected, using the data generated for AHs of 400 samples from the NL control population. For each SNV, the percentage of samples that generated AHs greater than 10 intensity units for homozygous calls, and greater than 5 intensity units for heterozygous calls, was calculated. SNVs with a percentage of less than 95 were considered as low quality performers.

Another EXT primer cocktail (containing previous adjustments) with double the amount of primers for selected SNVs was made. To determine if the

AH improves using the new EXT primer cocktail, the optimization cohort was assessed on 1x20-plex once using new EXT primer cocktail and once with old extension primer cocktail. Same as above, I calculated the minimum and average values for AH and compared them.

2.7.3 – Final calling algorithm parameters

As mentioned previously in order to have a more stringent method of accepting calls rather than visually inspecting the data or relying solely on the automated genotype call, a calling algorithm was devised. All parameters and the cut-off values were developed based on the data collected from multiple runs performed using the 1x20-plex LDT panel. A separate algorithm for NTCs and samples was created.

2.8 – ANALYTICAL VALIDATION

During the analytical validation study, the following attributes were calculated: analytical sensitivity, specificity, accuracy, precision, reference range, and reportable range. The validation cohort that included 78 samples with known genotype status but blinded to the investigator was assessed on the optimized 1x20-plex LDT panel. The raw data generated by the MassARRAY in the Typer4 software was carefully analyzed for each SNV for every sample. All genotype calls were first manually visualized and then the calling algorithm was applied to ensure the accuracy and sensitivity of the LDT panel. Samples were reassessed on the 1x20-plex LDT panel if they failed to meet the quality metrics (i.e., calling algorithm) for any of the SNVs. To determine if the data is reproducible (i.e.,

precision) the optimization cohort was assessed on the 1x20-plex LDT panel three (3) times and the calling algorithm was applied to the runs. The formulas used to calculate, sensitivity, specificity and accuracy are displayed below:

$$\text{Sensitivity} = \frac{\text{True Positive}}{\text{True Positive+False Negative}} \times 100$$

$$\text{Specificity} = \frac{\text{True Negative}}{\text{True Negative+False Positive}} \times 100$$

$$\text{Accuracy} = \frac{\text{True positive+True Negative}}{\text{True Positive+False Positive+True Negative+False negative}} \times 100$$

2.9 – CLINICAL VALIDITY OF THE 1X20-PLEX LDT PANEL

The cohort of 15 genomic DNA samples from patients or family members of the patients with unknown genetic status was assessed using the optimized 1x20-plex LDT panel and the calling algorithm was applied to determine the genotype of each sample.

2.10 – STATISTICAL ANALYSIS

After assessing each run on any LDT panel, I stratified and categorized the data for each of the 20 SNVs. The calculation of minimum and average for the candidate parameters for each SNV in the group of homozygous and heterozygous calls was performed. Also, with regard to NTC wells, the percentage of SNVs that generated an automated genotype call in the NTC well was calculated by dividing the number of observed genotype calls by the total number of SNVs.

A paired t-test and Fisher exact test were the two analysing methods to achieve p-values and determine the significant difference. I used a paired t-test to compare auto-tuning function and using Tween 20 detergent between both LDT panels, and a Fisher exact test to compare the differences and correlation of peak height and spotted volume, also to compare the difference between the NL and non-NL control populations. The calculation to determine the MAF was based on the total number of accepted genotype calls.

Chapter 3

3.0 – RESULTS

3.1 – STUDY COHORT

Individuals in optimization and validation cohorts were selected to be genotyped for the most common mutations causing STGD1 in the NL population, if they were diagnosed with STGD1 through clinical features of the disease, family members of an affected member or suspected to have STGD1 by clinical features. **Table 3.1** displays the clinical methods used to support a diagnosis of STGD1 for the 14 affected members (previously tested) comprising the optimization cohort.

Table 3.1. Clinical methods used to diagnose STGD1 in the optimization cohort.

Sample #	Visual acuity	Visual field	Fundus photos	Fluorescein Angiography	ERG	Others
1	✓	✓	✓		✓	
2	✓	✓	✓	✓	✓	
3	✓	✓	✓	✓	✓	
4	✓	✓	✓		✓	EOG
5	✓	✓	✓	✓		OCT
6	✓	✓	✓	✓		
7	✓	✓	✓		✓	
8	✓	✓	✓	✓	✓	EOG
9	✓	✓	✓			
10	✓	✓	✓		✓	
11	✓	✓	✓	✓	✓	
12	✓					
13	✓	✓	✓	✓	✓	OCT
14	✓	✓	✓	✓	✓	

A representative visual acuity report (**Figure 3.1A**), visual field (**Figure 3.1B**), Fundus photograph (**Figure 3.1C**) and fluorescein angiography (**Figure 3.1D**) for both eyes of an individual in the optimization cohort (sample #13) is shown. Sample #13 had a normal ERG, so the data for ERG is not displayed.

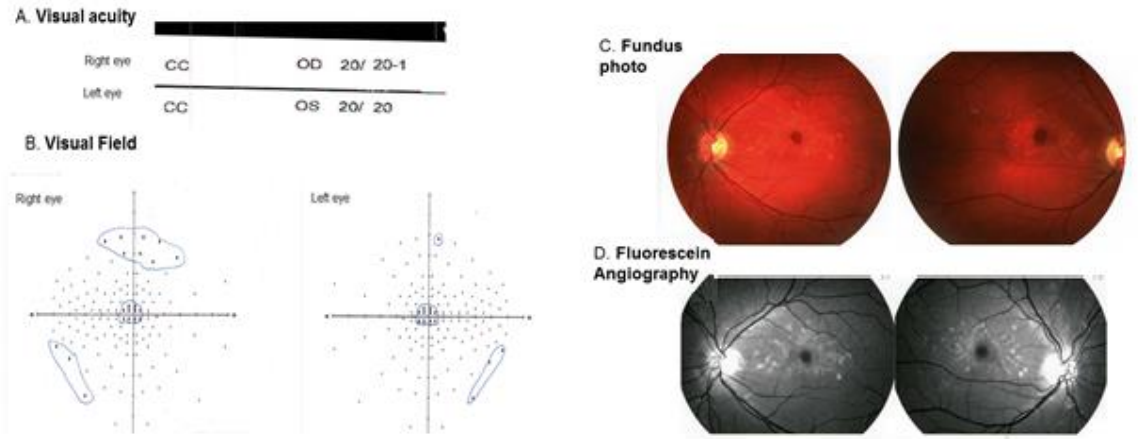

Figure 3.1. A representative diagram of the clinical methods used for diagnosis of STGD1. A representative visual acuity report. (A), visual field (B), Fundus photograph (C) and fluorescein angiography (D) for both eyes of an individual in the optimization cohort (sample #13).

3.2 – PRIMARY ATTEMPT AT IN-SILICO DESIGN OF A MULTIPLEX PANEL COMPRISING 20 PATHOGENIC VARIANTS CAUSING STGD1

All of the pathogenic variants included in the LDT panel (i.e., 20/20) successfully passed steps 1 to 3 in the Assay Design Suite software (refer to 2.2). Initially, 85% (i.e., 17/20) of the assays designed successfully without rejects in step 4 (i.e., attempting to design panel). The list of rejected SNVs (i.e., rs61749459, ABCA4_4537delC and rs138157885) along with the reason for rejection (**Table 0.4. SNVs** rejected and the reason for the rejection.) and details of design settings (**Table 0.5**) are provided.

Rejected SNVs were excluded from the design, to remove the rejects and incorporate the SNVs into my design, the following criteria were specifically changed: 1) the amplicon length control changed from minimum (80bp), optimum (100bp), and maximum (120bp) to minimum (80bp), optimum (100bp), and maximum (700bp); and 2) the stringency of the false priming, dimer potential, hair pin potential, number of sequential G's and overall cut-off for extension primers, and the number of sequential G's for PCR primers were changed (**Table 0.5 &**

Table 0.6). The design settings used to remove rejects is also provided (

Table 0.6).

Once the reject issues were solved, step 4 (i.e., attempting to design panel) and step 5 (i.e., validating panel design) were successfully completed for all 20/20 (100%) SNVs. However, the successful LDT design had SNVs distributed into a 3-well design (**Table 3.2**) due to multiplexing issues arising from the stringency settings for each SNV. With respect to the 3-well design, well#1 was a 15-plex design including: rs61750130, rs61751402, rs76157638, rs61751404, ABCA4_67-1delG, rs61752406, rs61750200, rs61751407, rs61750641, rs61751384, rs61750120, rs61749459, rs1800728, rs61750152 and rs138157885 (multiplex SNP capture confidence score of: 60.8). Well#2 was a 4-plex design including: ABCA4_4537delC, rs61750121, rs61750131 and rs62646862 (multiplex SNP capture confidence score of: 88.4). Finally, well#3

was a 1-plex design including rs61750135 (multiplex SNP capture confidence score of: 100).

Table 3.2. Initial design of the multiplex panel generating a 3-well design.

Well#1	Well#2	Well#3
rs61750130	ABCA4_4537delC	rs61750135
rs61751402	rs61750121	
rs76157638	rs61750131	
rs61751404	rs62646862	
ABCA4_67-1delG		
rs61752406		
rs61750200		
rs61751407		
rs61750641		
rs61751384		
rs61750120		
rs61749459		
rs1800728		
rs61750152		
rs138157885		

3.3 – SECONDARY ATTEMPT AT IN-SILICO DESIGN OF A MULTIPLEX PANEL COMPRISING 20 PATHOGENIC VARIANTS CAUSING STGD1

A trial-and-error approach was used to change design settings in order to relax the stringency of various design parameters used in the 3-well design, thereby reducing the overall number of wells. Given the inherent difficulties with multiplexing in general, we decided to design two different LDT multiplexes (i.e., 2x10-plex and 1x20-plex) the performance of which would be compared and the best performing LDT panel would be selected for subsequent optimization and validation.

3.3.1 – Designing the 2x10-plex LDT (2-well design)

The 20 SNVs were divided into two groups of 10 – each group in one well. The first alteration to achieve this goal was to change the multiplex level to 10. Additional variables were changed in “advanced settings” using a trial-and-error approach to incorporate the 20 SNVs into two different wells (i.e., 2x10-plex LDT panel). A summary of the final changes made in the settings to integrate each group of 10 SNVs into one well is provided (**Table 0.7**).

The SNVs included in the first well were: rs61751404, rs76157638, ABCA4_671delG, rs61750120, rs1800728, rs61751407, rs138157885, rs61751402, rs62646862 and rs61751384 (multiplex SNP capture confidence score 99.1%) (**Table 0.8**). The other 10 SNVs in the second well were: rs61750135, rs61749459, rs61750130, rs61750131, rs61750200, ABCA4_4537delC, rs61750152, rs61750641, rs61752406 and rs61750121 (multiplex SNP capture confidence score: 98.3%) (**Table 0.9**). The direction and sequence of the unextended primers (UEP), their alternative alleles that could be added, and the uniplex confidence score for well#1 (**Table 0.10**) and well#2 (**Table 0.11**) of the 2x10-plex is provided. Warnings and validation hits for both wells are indicated in **Table 0.12** and **Table 0.13**, respectively.

3.3.2 – Designing the 1x20-plex LDT (1-well design)

Using the more robust Typer4 software, 95% (i.e., 19/20) of the “rs” numbers were designed in one well (multiplex SNP capture confidence score: 98.6). The other SNV, rs61749459, was designed separately as a uniplex (SNP capture

confidence score: 100). This SNV was then manually added to the 1-well, 19-plex design creating a 1-well, 20-plex design. Design settings and warnings for the 1-well design using Typer4 are indicated in

Table 0.14 and **Table 0.16**, respectively. PCR primers (both F and R) and the corresponding confidence score for each assay including those with shared primers are provided (**Table 0.15**). The direction, sequence, alternative allele and the uniplex confidence score for the extension reaction is provided (**Table 0.17**).

3.4 – PRIMER MIXTURES AND ADJUSTMENTS

The QC assessment was performed in triplicate as described in the Materials and Methods section. A representative histogram for the 1x20-plex LDT panel and the 2x10-plex LDT panel is shown in **Figure 3.2** and **Figure 3.3**, respectively.

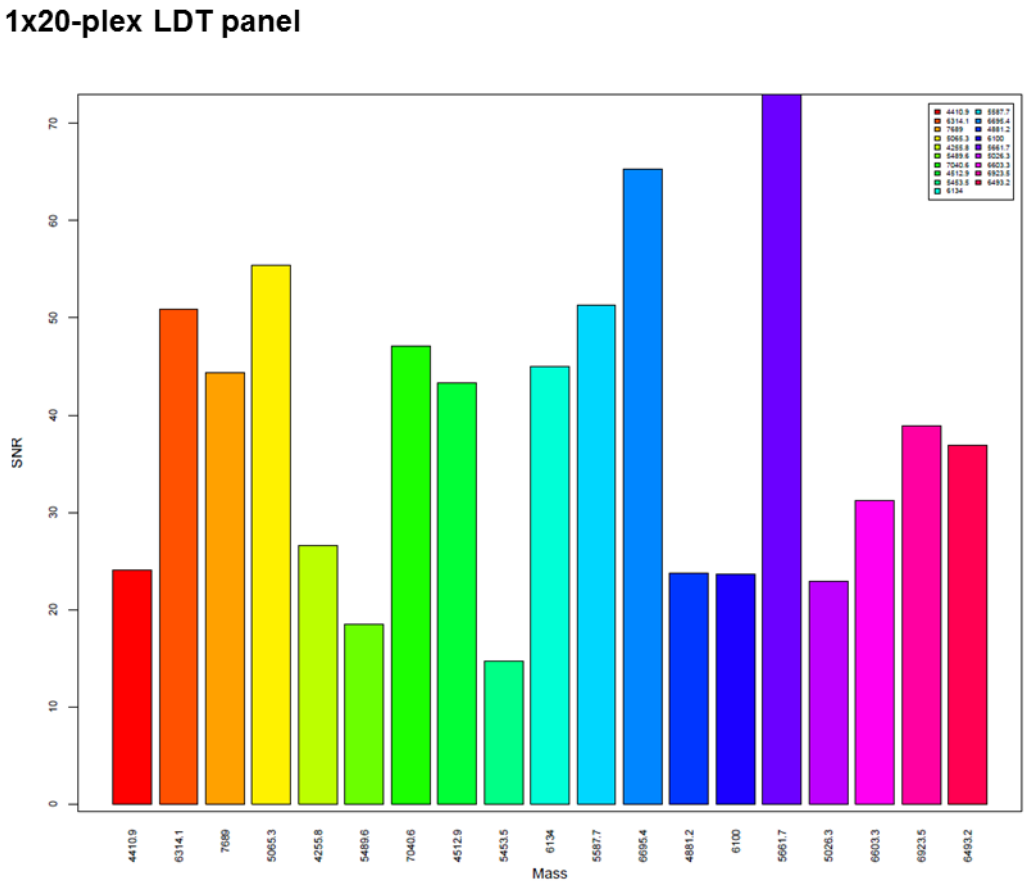

Figure 3.2. A representative graph of the first quality control assessment of the 1x20-plex LDT panel. All 20 SNVs (i.e., included in the 1x20-plex LDT panel) are displayed with different colour bars. For each SNV, the X axis represents the mass and Y axis represents the signal-to-noise ratio for that SNV in the quality control assessment. The more equal the bars on the Y axis (i.e., SNR), the better the quality of the primers.

2x10-plex LDT panel
Well #1

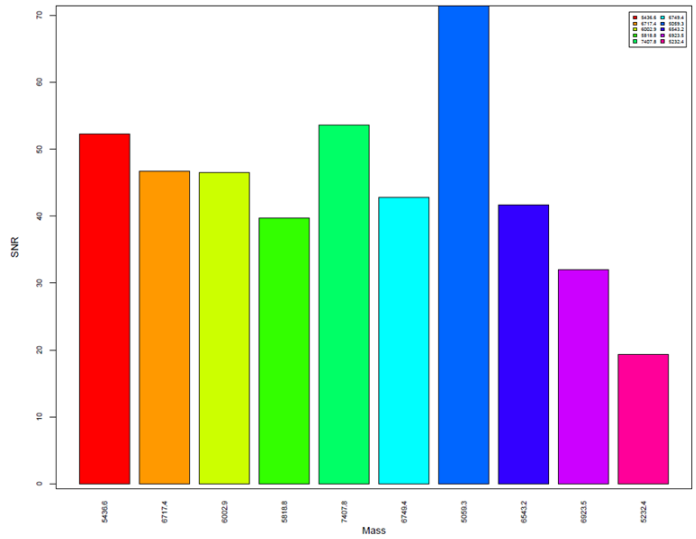

2x10-plex LDT panel
Well #2

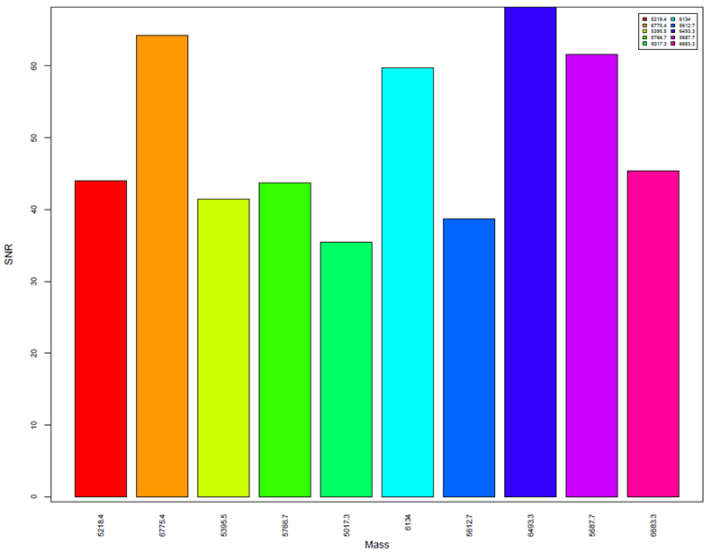

Figure 3.3. Representative pictures of the first quality control assessment for both wells of the 2x10-plex LDT panel. There are two wells each containing 10 SNVs. SNVs in each well are displayed with different colour bars. For each SNV, the X axis represents the mass and Y axis represents the signal-to-noise ratio for that SNV in the quality control assessment. In each well of the 2x10-plex LDT panel, the more equal the bars on the Y axis (i.e., SNR), the better the quality of the primers**.**

3.5 – ASSESSMENT AND SELECTION OF BEST PERFORMING LDT PANEL

The genotype call made by the Typer4 software was accurate (based on visual analysis) for all the 20 SNVs in each of the 14 samples across both LDT panels. All SNVs in both the 1x20-plex and 2x10-plex LDT panels produced a yield >50%. However, comparison of homozygous allele heights, including WT and MUT, for each SNV between the 1x20-plex and 2x10-plex LDT panels was performed (**Table 3.3**). The average peak height for all SNVs grouped together (i.e., irrespective of the SNV) was higher for the 2x10-plex LDT, which was 10.7 intensity units, compared with the 1x20-plex LDT, which was 6.7 intensity units (**Table 3.3**). Also, only 1 SNV (i.e., rs61751407) generated greater average allele heights for the 1x20-plex LDT panel compared with the 2x10-plex LDT panel. Moreover, 5 SNVs (i.e., ABCA4_67-1delG, rs61750120, rs61750200, rs61751402, rs76157638) generated almost the same (i.e., >0.9) average allele height in the 1x20-plex LDT panel compared with 2x10-plex LDT panel (**Table 3.3**). A comparison of heterozygous allele heights for each SNV between the 1x20-plex and 2x10-plex LDT panels was performed (**Table 3.4**). However, in the optimization cohort there was just one heterozygous call for most SNVs. Multiple calls appeared in the NTC wells for both the 1x20-plex and 2x10-plex LDT panels. An average of 11% (i.e., 9/80) of SNVs produced calls in the NTC wells for both the 1x20-plex and 2x10-plex LDT panels. In the 1x20-plex LDT panel, more than half (i.e., 56%) of the SNVs that were automatically called in the NTC wells were random (i.e., not consistently automatically called across runs).

However, in the 2x10-plex LDT panel, only 34% of the SNVs were automatically called as random.

But, the quality performance metrics for both assays (i.e., 1x20-plex and 2x10-plex) was unsatisfactory.

Table 3.3. Comparison of homozygous allele heights, including WT and MUT, for each SNV between 1x20-plex and 2x10-plex LDT panels.

SNV ID	Homozygous Allele Height	1x20-plex LDT	2x10-plex LDT
ABCA4_4537delC	Minimum	3.6	6.7
	Average	11.7	14.9
ABCA4_67-1delG	Minimum	3.8	2.5
	Average	8.3	8.0
rs138157885	Minimum	1.5	3.6
	Average	3.6	10.4
rs1800728	Minimum	2.8	4.8
	Average	5.8	10.4
rs61749459	Minimum	2.3	5.2
	Average	4.9	11.2
rs61750120	Minimum	2.9	3.9
	Average	9.2	9.0
rs61750121	Minimum	2.2	4.3
	Average	6.9	12.6
rs61750130	Minimum	2.3	6.0
	Average	6.5	21.9
rs61750131	Minimum	0.9	2.9
	Average	3.4	7.3
rs61750135	Minimum	2.3	5.3
	Average	7.2	13.6
rs61750152	Minimum	3.4	4.9
	Average	6.7	13.2
rs61750200	Minimum	3.1	2.7
	Average	6.9	6.9
rs61750641	Minimum	3.9	6.1

	Average	7.8	16.2
rs61751384	Minimum	2.2	3.5
	Average	6.0	8.0
rs61751402	Minimum	2.6	1.7
	Average	6.0	6.3
rs61751404	Minimum	6.9	5.6
	Average	12.3	15.7
rs61751407	Minimum	2.9	1.1
	Average	5.2	2.5
rs61752406	Minimum	2.0	3.0
	Average	4.4	8.3
rs62646862	Minimum	2.4	7.6
	Average	6.6	12.6
rs76157638	Minimum	2.5	1.7
	Average	5.1	4.7
All 20 variants	**Average**	**6.7**	**10.7**

Green colour represents almost the same average allele height in both 1x20-plex and 2x10-plex LDTs. Yellow colour represents a greater average allele height for the 1x20-plex vs 2x10-plex LDT.

Table 3.4. Comparison of the averages for heterozygous allele heights, for each SNV between 1x20-plex and 2x10-plex designs.

SNV ID	Heterozygous Allele Height	1x20-plex LDT		2x10-plex LDT	
		Alternative Alleles		Alternative Alleles	
ABCA4_4537delC	Average	8.7	3.8	10.7	5.6
ABCA4_67-1delG	Average	4.7	3.8	4.3	2.9
rs138157885	Average	2.0	2.0	5.3	5.9
rs1800728	Average	4.9	3.4	6.9	4.8
rs61749459	Average	2.2	1.8	2.1	1.9
rs61750120	Average	4.6	4.6	3.1	2.8
rs61750121	Average	2.8	2.6	4.2	3.3
rs61750130	Average	3.6	3.0	6.7	5.0
rs61750131	Average	1.4	1.8	3.7	3.7
rs61750135	Average	5.5	4.3	7.2	5.7
rs61750152	Average	3.4	2.2	4.9	4.4
rs61750200	Average	3.1	2.4	4.2	3.6

rs61750641	Average	3.8	3.6	8.7	8.9
rs61751384	Average	6.3	3.0	4.9	3.7
rs61751402	Average	2.4	2.5	2.6	3.3
rs61751404	Average	8.7	4.0	9.8	4.3
rs61751407	Average	2.2	1.9	1.4	1.5
rs61752406	Average	4.1	3.0	4.8	3.0
rs62646862	Average	3.2	2.1	7.4	5.2
rs76157638	Average	2.6	2.4	2.3	2.4

Due to having lower number of samples in the category of heterozygous calls, comparison was not valid, statistically.

3.5.1 – Comparison of iPLEX Gold vs iPLEX Pro

To determine if the quality metrics were improved by replacing iPLEX Gold with iPLEX Pro chemistry, the optimization cohort along with two NTC wells was assessed in duplicate for both the 1x20-plex and 2x10-plex LDT panels. To assess the overall performance of the LDT panels from a peak height perspective between iPLEX Gold and iPLEX Pro chemistry, the overall average of the homozygous allele heights for all SNVs grouped together were compared between the 1x20-plex and the 2x10-plex LDT panels. The overall average of the homozygous allele heights for all SNVs grouped together in the 1x20-plex LDT panel was 6.7 and 12 intensity units using iPLEX Gold and iPLEX Pro chemistry, respectively.

The number and percentage of samples with allele heights above and below the threshold of 6.7 intensity units was recorded for each group (i.e., iPLEX Gold vs iPLEX Pro). **Table 3.5** displays the frequency and percentage of samples from the optimization cohort in duplicate with allele height higher or lower than 6.7 intensity units between iPLEX Gold and iPLEX Pro chemistries for

the 1x20-plex LDT panel. The number of samples that had allele heights greater than 6.7 intensity units was greater using the iPLEX Pro compared with iPLEX Gold chemistry for all SNVs except rs61751404 for the 1x20-plx LDT panel. There was a significant difference between the results produced using iPLEX Pro compared with iPLEX Gold chemistry for all SNVs except rs61751404 (**Table 3.5**). With respect to automated genotype calls in the NTC wells, the performance of the iPLEX Pro chemistry considerably reduced the total number of incorrect automated genotype calls (<1%) and all SNVs that were called were random with the 1x20-plex LDT panel.

Table 3.5. The frequency and percentage of samples for homozygous alleles in 1x20-plex LDT panel that were above the average (AH>6.7) using Gold vs Pro iPlex chemistry in duplicate.

SNV ID	Homozygous Allele height	iPLEX Chemistry*		P-value
		Gold	Pro	
ABCA4_4537delC	**AH>6.7**	68% (17/25)	96% (25/26)	0.0109
	AH<6.7	32% (8/25)	4% (1/26)	
ABCA4_67-1delG	**AH>6.7**	71% 17/24	92% 22/24	<0.0001
	AH<6.7	29% 7/24	8% 2/24	
rs138157885	**AH>6.7**	0% 0/25	58% 15/26	<0.0001
	AH<6.7	100% 25/25	42% 11/26	
rs1800728	**AH>6.7**	32% 8/25	69% 18/26	0.0118
	AH<6.7	68% 17/25	31% 8/26	

rs61749459	**AH>6.7**	4% 1/25	73% 19/26	<0.0001
	AH<6.7	96% 24/25	27% 7/26	
rs61750120	**AH>6.7**	48% 12/25	100% 26/26	<0.0001
	AH<6.7	52% 13/25	0% 0/26	
rs61750121	**AH>6.7**	40% 10/25	100% 26/26	<0.0001
	AH<6.7	60% 15/25	0% 0/26	
rs61750130	**AH>6.7**	40% 10/25	75% 18/24	0.0209
	AH<6.7	60% 15/25	25% 6/24	
rs61750131	**AH>6.7**	0% 0/25	48% 12/25	<0.0001
	AH<6.7	100% 25/25	52% 13/25	
rs61750135	**AH>6.7**	44% 11/25	96% 23/24	0.0001
	AH<6.7	56% 14/25	4% 1/24	
rs61750152	**AH>6.7**	44% 11/25	88% 23/26	0.001
	AH<6.7	56% 14/25	12% 3/26	
rs61750200	**AH>6.7**	36% 9/25	100% 25/25	<0.0001
	AH<6.7	64% 16/25	0% 0/25	
rs61750641	**AH>6.7**	48% 12/25	100% 26/26	<0.0001
	AH<6.7	52% 13/25	0% 0/26	
rs61751384	**AH>6.7**	31% 8/26	96% 25/26	<0.0001
	AH<6.7	69% 18/26	4% 1/26	
rs61751402	**AH>6.7**	32% 8/25	96% 25/26	<0.0001
	AH<6.7	68% 17/25	4% 1/26	

rs61751404	**AH>6.7**	96% 24/25	100% 26/26	0.4902
	AH<6.7	4% 1/25	0% 0/26	
rs61751407	**AH>6.7**	0% 0/19	90% 18/20	<0.0001
	AH<6.7	100% 19/19	10% 2/20	
rs61752406	**AH>6.7**	9% 2/23	92% 22/24	< 0.0001
	AH<6.7	91% 21/23	8% 2/24	
rs62646862	**AH>6.7**	32% 7/22	96% 23/24	< 0.0001
	AH<6.7	68% 15/22	4% 1/24	
rs76157638	**AH>6.7**	11% 2/19	83% 15/18	< 0.0001
	AH<6.7	89% 17/19	17% 3/18	

*Some samples failed to yield a genotype for certain variants in the multiplex assay.

The optimization cohort samples were assessed in duplicate using the 2x10-plex LDT with the iPLEX Gold and the iPLEX Pro. The average of homozygous allele heights with iPLEX Gold chemistry for all the 20 SNVs was calculated at 10.7 units. The number of samples with peak heights above and below threshold of 10.7 was recorded for each group (i.e., iPLEX Gold vs iPLEX Pro). **Table 3.6** displays the number of times the 14 samples produced a peak height higher and lower than 10.7 using Gold vs Pro chemistry. In the 2x10-plex LDT panel, 40% (i.e., 8/20) of SNVs failed to show a significant difference using the two different chemistries. Ten out of 20 SNVs (i.e., 50%) performed better using iPLEX Pro chemistry while only 2 out of 20 SNVs (i.e., 10%) performed better using the iPLEX Gold chemistry. With respect to automated genotype calls

in the NTC wells, the performance of the iPLEX Pro chemistry considerably reduced the total number of genotype calls (1.25%) and 50% of all SNVs that were called were random with the 2x10-plex LDT panel (**Table 3.7**).

Table 3.6. The number and percentage of samples for the homozygous allele in the 2x10-plex LDT panel that were above the average allele height (AH>10.7) using iPLEX Gold vs iPLEX Pro chemistry in duplicate.

SNV ID	**Homozygous Allele height**	**iPLEX Chemistry***		P-value
		Gold	Pro	
ABCA4_4537delC	AH>10.7	62% 16/26	85% 22/26	0.1164
	AH<10.7	38% 10/26	15% 4/26	
ABCA4_67-1delG	AH>10.7	12% 3/26	0% 0/25	0.2353
	AH<10.7	88% 23/26	100% 25/25	
rs138157885	AH>10.7	52% 13/25	100% 26/26	<0.0001
	AH<10.7	48% 12/25	0% 0/26	
rs1800728	AH>10.7	38% 10/26	8% 2/26	0.0188
	AH<10.7	62% 16/26	92% 24/26	
rs61749459	AH>10.7	46% 12/26	73% 19/26	0.0889
	AH<10.7	54% 14/26	27% 7/26	
rs61750120	AH>10.7	23% 6/26	73% 19/26	0.0007
	AH<10.7	77% 20/26	27% 7/26	
rs61750121	AH>10.7	52% 13/25	96% 25/26	0.0003
	AH<10.7	48% 12/25	4% 1/26	
rs61750130	AH>10.7	88% 23/26	73% 19/26	0.2913
	AH<10.7	12% 3/26	27% 7/26	

rs61750131	AH>10.7	31% 8/26	46% 12/26	0.3929
	AH<10.7	69% 18/26	54% 14/26	
rs61750135	AH>10.7	50% 13/26	96% 25/26	0.0003
	AH<10.7	50% 13/26	4% 1/26	
rs61750152	AH>10.7	58% 15/26	92% 24/26	0.0087
	AH<10.7	42% 11/26	8% 2/26	
rs61750200	AH>10.7	23% 6/26	27% 7/26	1
	AH<10.7	77% 20/26	73% 19/26	
rs61750641	AH>10.7	69% 18/26	100% 26/26	<0.0042
	AH<10.7	31% 8/26	0% 0/26	
rs61751384	AH>10.7	23% 6/26	69% 18/26	<0.019
	AH<10.7	77% 20/26	31% 8/26	
rs61751402	AH>10.7	5% 1/20	58% 15/26	< 0.0002
	AH<10.7	95% 19/20	42% 11/26	
rs61751404	AH>10.7	88% 23/26	85% 22/26	1
	AH<10.7	12% 3/26	15% 4/26	
rs61751407	AH>10.7	11% 2/19	10% 2/20	1
	AH<10.7	89% 17/19	90% 18/20	
rs61752406	AH>10.7	33% 8/24	96% 23/24	< 0.0001
	AH<10.7	67% 16/24	4% 1/24	
rs62646862	AH>10.7	63% 15/24	92% 22/24	0.0363
	AH<10.7	38% 9/24	8% 2/24	
rs76157638	AH>10.7	0% 0/20	89% 17/19	< 0.0001

	AH<10.7	100% 20/20	11% 2/19	

*Some samples failed to yield a genotype for certain variants in the multiplex assay.

Table 3.7. The percentage of calls and reproducibility of calls for the NTC in the 1x20-plex and 2x10-plex LDT panel using different iPLEX chemistries.

1x20-plex		**2x10-plex**	
Gold chemistry	**Pro chemistry***	**Gold chemistry**	**Pro chemistry***
11% (9/80)	0.94% (3/320)	11% (9/80)	1.25% (4/320)
44% non-random calls	0% non-random calls	66% non-random calls	50% non-random calls

*More than two NTC wells per run.

3.5.2 – Comparison of 2x10-plex vs 1x20-plex LDT (iPLEX Pro ONLY)

To determine the differences between the 2x10-plex and the 1x20-plex LDT panels, the optimization samples were assessed for each panel in triplicate using iPlex Pro chemistry. If a sample failed to yield a genotype for a certain SNV in one of the triplicate runs, it was confirmed that the same sample produced the correct genotype call for that SNV in the other replicate runs. We used the same experimental conditions (i.e., same PCR primer mix, extension primer mix and thermal cycling parameters) to select the best LDT panel based on: 1) no genotype calls in the NTC wells; and 2) the quality performance (i.e., allele height and yield) of the SNVs for each sample. The average and minimum yield values for all SNVs in all 3 runs of the 1x20-plex and the 2x10-plex LDT panels were higher than the 50% threshold. **Table 3.8** shows the comparison of the average and minimum value of homozygous allele heights for all samples based on 3

different runs of the 1x20-plex and the 2x10-plex LDT panels for each of the 20 SNVs. Four out of 20 SNVs (i.e., 20%) had a minimal difference (i.e., <1.0 intensity unit) in allele height for homozygous calls in both LDT panels. Five out of 20 SNVs (i.e., 25%) had a higher average allele height for homozygous calls in the 1x20-plex LDT panel compared with the 2x10-plex LDT panel. Eleven out of 20 SNVs (i.e., 55%) had a higher average allele height for homozygous calls in the 2x10-plex LDT compared with the 1x20-plex LDT panel (**Table 3.8**). The comparison of the average values of heterozygous allele heights is displayed in **Table 3.9**. Two out of 20 SNVs (i.e., 10%) had a minimal difference (i.e., <0.5 intensity unit) in allele height for heterozygous calls in both LDT panels. Eight out of 20 SNVs (i.e., 40%) had a higher average allele height for heterozygous calls in the 1x20-plex LDT panel compared with the 2x10-plex LDT panel. Ten out of 20 SNVs (i.e., 50%) had a higher average allele height for heterozygous calls in the 2x10-plex LDT panel compared with the 1x20-plex LDT panel (**Table 3.9**). No automated genotype calls (i.e., 0/120) were observed in the NTC wells of the 1x20-plex LDT panel; however, an average of 2.5% (i.e., 3/120) of SNVs produced genotype calls in the NTC wells for the 2x10-plex LDT panel. Noteworthy, 2/3 of the automated genotype calls in the NTC wells in the 2x10-plex LDT panel occurred with the same SNV.

Table 3.8. The average and minimum value of homozygous allele heights for all samples based on 3 different runs of the 1x20-plex vs 2x10-plex LDT panels for each of the 20 SNVs**.**

SNV ID	Homozygous Allele Height	1x20-plex LDT	2x10-plex LDT
ABCA4_4537delC	Minimum	4.0	6.3
	Average	9.8	19.1
ABCA4_67-1delG	Minimum	9.0	3.7
	Average	16.4	8.1
rs138157885	Minimum	5.0	9.8
	Average	8.2	21.0
rs1800728	Minimum	4.5	4.2
	Average	9.3	8.6
rs61749459	Minimum	4.5	4.8
	Average	8.2	14.3
rs61750120	Minimum	8.2	6.4
	Average	13.8	14.5
rs61750121	Minimum	5.6	10.8
	Average	10.2	20.1
rs61750130	Minimum	2.9	5.0
	Average	6.6	15.4
rs61750131	Minimum	3.6	3.0
	Average	7.1	10.7
rs61750135	Minimum	5.6	6.2
	Average	11.2	21.0
rs61750152	Minimum	6.0	8.3
	Average	10.7	21.1
rs61750200	Minimum	7.6	4.2
	Average	13.0	11.1
rs61750641	Minimum	8.0	10.2
	Average	13.7	25.8
rs61751384	Minimum	4.6	6.3
	Average	9.1	14.0
rs61751402	Minimum	7.9	5.9
	Average	13.5	12.5
rs61751404	Minimum	9.7	7.3

	Average	19.6	18.3
rs61751407	Minimum	5.2	1.5
	Average	7.7	3.8
rs61752406	Minimum	10.8	5.9
	Average	17.5	17.4
rs62646862	Minimum	7.4	8.7
	Average	13.1	19.9
rs76157638	Minimum	9.8	11.9
	Average	16.6	16.7

Green colour represents a similar yield regarding average allele height in both 1x20-plex and 2x10-plex LDT panels. Yellow colour represents a greater yield regarding the average allele height for the 1x20-plex compared with the 2x10-plex LDT panel. Red colour represents a greater yield regarding average allele height for the 2x10-plex compared with the 1x20-plex LDT panel.

Table 3.9. The average and minimum value of heterozygous allele heights for all samples based on 3 different runs of the 1x20-plex vs 2x10-plex LDTs for each of the 20 SNVs.

SNV ID	Heterozygous Allele Height	1x20-plex LDT		2x10-plex LDT	
ABCA4_4537delC	Minimum	3.5	3.2	6.1	5.3
	Average	5.7	4.7	7.7	6.8
ABCA4_67-1delG	Minimum	1.2	1.6	1.9	2.5
	Average	3.7	5.3	2.9	3.4
rs138157885	Minimum	3.8	4.9	4.4	5.3
	Average	4.4	5.5	6.4	8.3
rs1800728	Minimum	5.1	5.4	2.8	2.7
	Average	5.4	5.5	3.1	3.1
rs61749459	Minimum	3.2	2.8	3.9	4.3
	Average	3.8	3.2	4.0	4.5
rs61750120	Minimum	3.8	4.0	3.4	4.0
	Average	4.8	5.7	4.4	5.4
rs61750121	Minimum	3.1	3.0	5.1	5.4
	Average	3.8	3.4	8.1	7.3

rs61750130	Minimum	2.8	2.6	4.5	4.7
	Average	4.1	3.8	5.0	5.0
rs61750131	Minimum	2.5	3.3	3.3	3.4
	Average	2.8	3.5	5.3	5.4
rs61750135	Minimum	5.8	5.4	6.6	7.5
	Average	7.4	7.1	8.2	8.8
rs61750152	Minimum	3.1	3.9	5.0	6.1
	Average	5.0	4.9	8.8	10.2
rs61750200	Minimum	6.3	4.3	5.9	3.2
	Average	8.1	5.4	7.2	4.8
rs61750641	Minimum	5.3	5.2	8.1	9.8
	Average	6.7	6.3	8.9	10.5
rs61751384	Minimum	3.5	3.6	3.4	3.4
	Average	3.8	3.8	6.1	5.9
rs61751402	Minimum	4.4	5.6	3.3	3.6
	Average	5.4	6.6	4.8	5.3
rs61751404	Minimum	9.8	7.4	5.1	3.2
	Average	12.5	8.1	9.6	5.9
rs61751407	Minimum	3.3	3.2	1.8	1.6
	Average	4.3	4.1	2.2	2.3
rs61752406	Minimum	6.5	4.5	7.2	5.9
	Average	11.4	8.3	8.1	6.8
rs62646862	Minimum	5.1	3.2	4.8	5.6
	Average	5.5	4.2	7.3	8.6
rs76157638	Minimum	2.4	3.1	3.0	4.7
	Average	4.9	6.0	4.0	5.9

Green colour represents a similar yield regarding average allele height in both 1x20-plex and 2x10-plex LDT panels. Yellow colour represents a greater yield regarding the average allele height for the 1x20-plex compared with the 2x10-plex LDT panel. Red colour represents a greater yield regarding average allele height for the 2x10-plex compared with the 1x20-plex LDT panel.

3.6 – CONFIRMATION OF GENOTYPES BY SANGER SEQUENCING

Sanger sequencing was performed on all samples in the optimization cohort to confirm the result from the LDT panels. Three (3) amplicons covering exons 5, 22

and 39 were redesigned as the results from using the initially designed primers were unsatisfactory (data not shown). The pathogenic variants detected in the optimization cohort using the 1x20-plex LDT panel were confirmed using Sanger sequencing (**Table 3.10**). A representative electropherogram displaying each of the 20 pathogenic variants in the optimization cohort is displayed in **Figure 3.4.** The electropherogram for the individual who was homozygous for the c.5714+5G>A SNV is also displayed in **Fig 3.4C**.

Table 3.10. The pathogenic variants detected in the optimization cohort using the 1x20-plex LDT panel and Sanger sequencing.

DNA #	Pathogenic Variants	Detected by both LDTs	Bidirectional Sanger Sequencing
1	c.[2588G>C; 5714+5G>A];[5714+5G>A]	Yes	Yes
2	c.[2588G>C];[4537delC]	Yes	Yes
3	c.[2588G>C];[6449G>A]	Yes	Yes
4	c.[67-1delG];[5714+5G>A]	Yes	Yes
5	c.[634C>T];[5714+5G>A]	Yes	Yes
6	c. [2588G>C;5714+5G>A]; [5461-10T>C]	Yes	Yes
7	c.[3322C>T];[3323G>A]	Yes	Yes (only F strand)
8	c. [455G>A; 5714+5G>A]; [4163T>C]	Yes	Yes
9	c.[4469G>A];[6089G>A]	Yes	Yes
10	c.[2564G>A];[4139C>T]	Yes	Yes
11	c.[1522C>T];[2564G>A]	Yes	Yes
12	c. [455G>A];[4577C>T]	Yes	Yes
13	c.[4222T>C; 4918C>T]; ?	Yes	Yes
14	c.[3064G>A];?	Yes	Yes

A

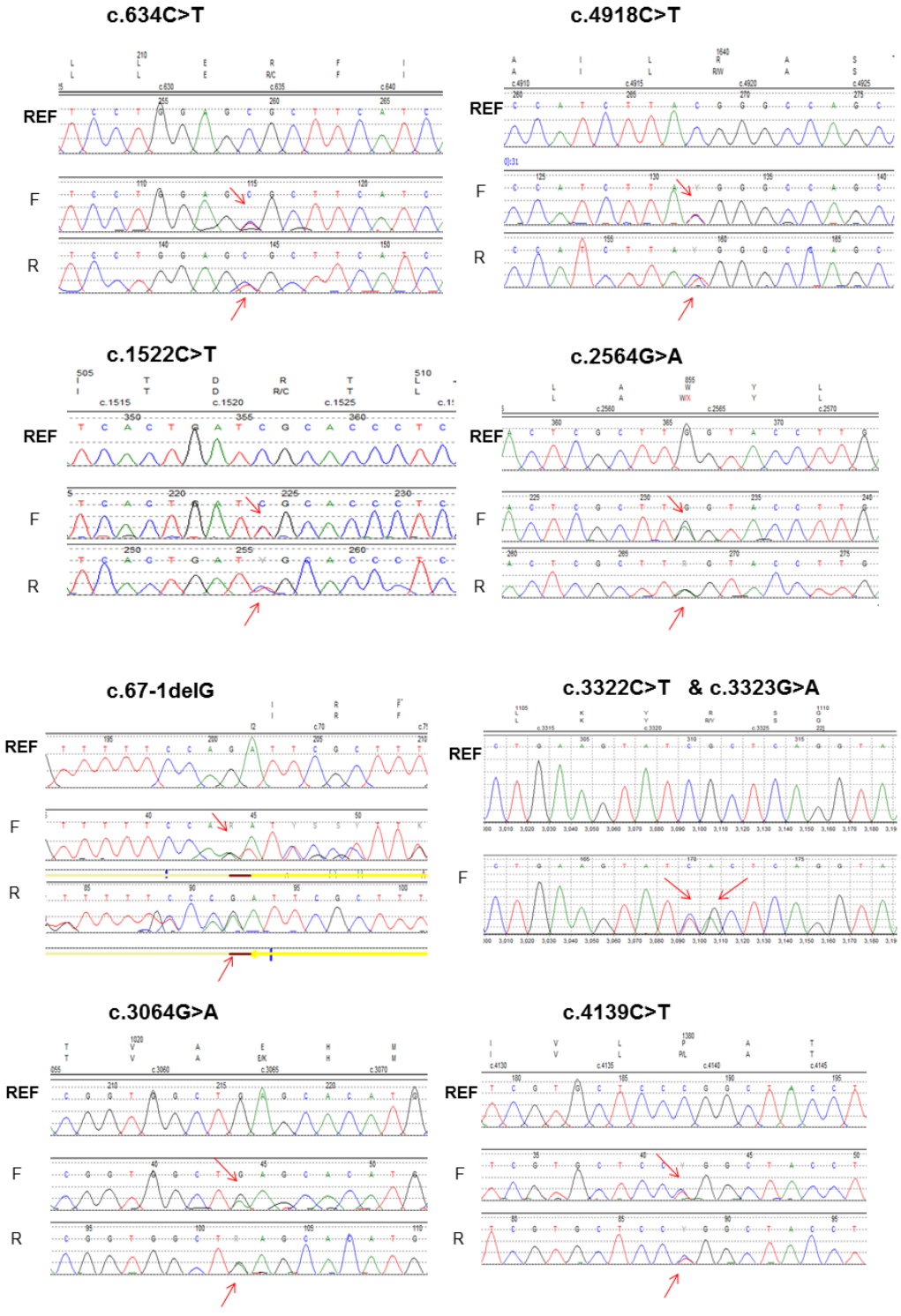
c.634C>T
c.4918C>T
c.1522C>T
c.2564G>A
c.67-1delG
c.3322C>T & c.3323G>A
c.3064G>A
c.4139C>T
REF
F
R

B

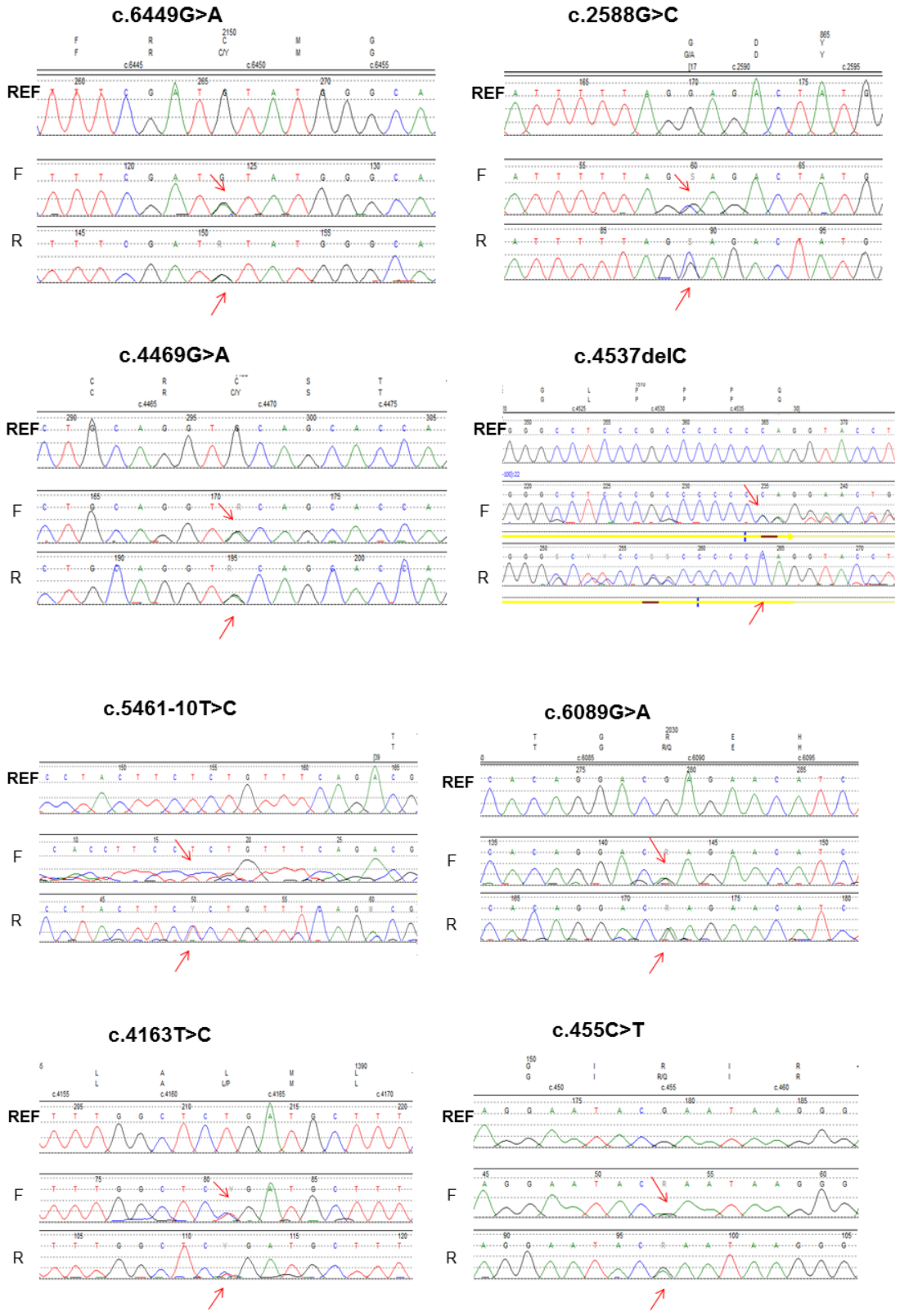
c.6449G>A
REF
F
R
c.2588G>C
REF
F
R
c.4469G>A
REF
F
R
c.4537delC
REF
F
R
c.5461-10T>C
REF
F
R
c.6089G>A
REF
F
R
c.4163T>C
REF
F
R
c.455C>T
REF
F
R

C

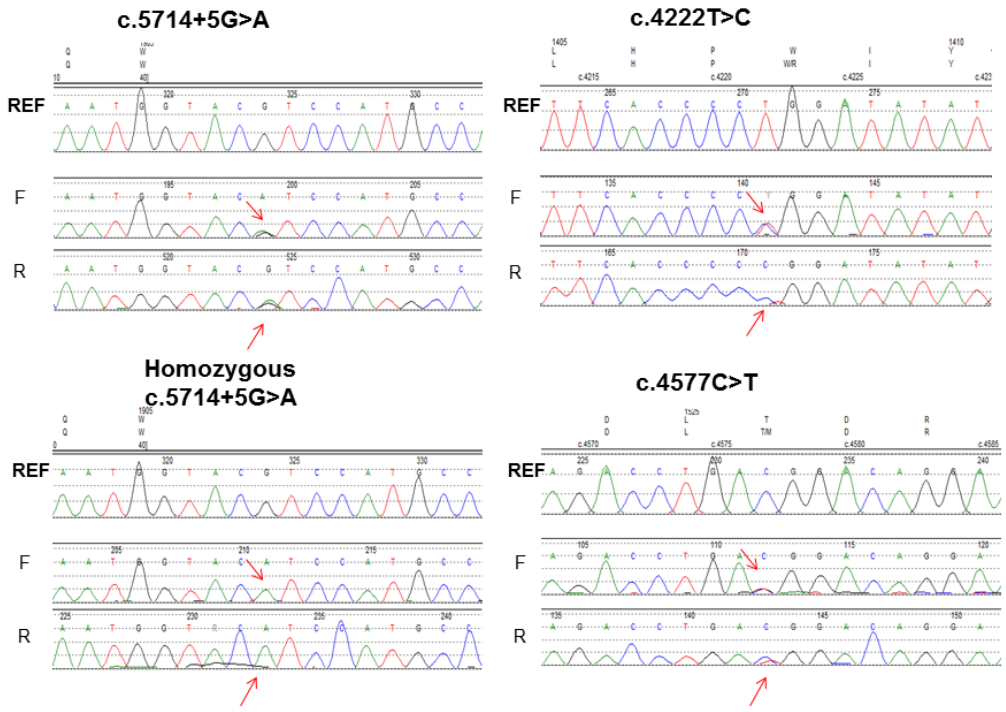

Figure 3.4. Representative electropherograms (A-C) of the 20 pathogenic variants included in the optimization cohort using Sanger sequencing. All 20 SNVs included in the LDT panels are displayed in heterozygous status. Figure 3.4C includes a representative electropherogram of the only individual who was homozygous for the C.5714+5 G>A SNV in the optimization cohort.

3.7 – OPTIMIZATION OF THE 1X20-PLEX LDT PANEL

3.7.1 – Adjustments to eliminate automated genotype calls in NTC wells

To determine if increasing the annealing temperature resulted in elimination of automated genotype calls in the NTC wells, the optimization cohort including 2 NTC wells was assessed using the 1x20-plex LDT panel. The increase in annealing temperature did not eliminate automated genotype calls in the NTC wells, as 1.25% (i.e., 1/80) of SNVs were still called in the NTC wells. However,

we noticed that changing the annealing temperature contributed to a significant decrease in the yield and allele heights of all the optimization cohort samples for all SNVs.

To determine if an interaction between PCR or EXT primers might cause automated genotype calls in the NTC wells, the optimization cohort including two regular NTC wells in addition to four NTC wells that had all required reagents except for PCR primers was assessed on the 1x20-plex LDT panel. In the four NTC wells without any PCR primers, there were no automated genotype calls. However, for the NTC wells that contained both PCR and EXT primers, 1.25% (i.e., 1/80) of SNVs still produced automated genotype calls.

To determine if using UNG enzyme results in elimination of automated genotype calls in the NTC wells, the optimization cohort including two NTC wells using the UNG kit was assessed using the 1x20-plex LDT in triplicate. The UNG enzyme failed to completely eliminate the automated genotype calls in the NTC wells across three runs. The percentage of SNVs that generated automated genotype calls in NTC wells for each run was as follows: 1st run (3.75% or 3/80 SNVs); 2nd run (1.25% or 1/80 SNVs); and 3rd run (5% or 4/80 SNVs). Also, all SNVs that produced a call in the NTC wells were random.

3.7.2 – Adjustments to increase allele height

3.7.2.1 – Nanodispenser adjustments

To determine if there was a correlation between the spotted volume and the peak height, a range of 355-365 samples (i.e., samples used in 2.6.2.3) were selected. There was no significant difference (p=0.6090) when samples were spotted with or without the auto-tuning function enabled (**Table 0.18**). However, with auto-tuning enabled, the spotted volumes were closer to the target volume, which was set to 14nl of volume (**Table 0.18**).

To determine if the viscosity of the multiplex assay affects the volume spotted, 64 samples were spotted with and without the detergent Tween 20. There was no significant difference (p=0.4316) when samples were spotted with and without Tween 20 (**Table 0.19**). However, with Tween 20 the spotted volumes were closer to the target volume, which was set to 14nl of volume (**Table 0.19**).

To determine if there was a correlation between the spotted volume and the peak height, a range of 355-365 samples (i.e., samples used in 2.7.2.3) were selected. Interestingly, there was no significant difference between the two groups that were spotted using a predetermined cut-off (i.e., <14nl and >14nl) for the SNVs (**Table 0.20**). However, the rs61750152 SNV showed a significant difference (p=0.0346) between the two groups.

3.7.2.2 – Adjustment of PCR/extension primer pool based on optimization cohort

To determine if the new extension mix resulted in higher quality performance of the SNVs (i.e., specifically achieving higher AH), the optimization cohort was assessed using the 1x20-plex LDT panel with the old EXT primer cocktail and with the newly made EXT primer cocktail. The average allele height for three (3) SNVs (i.e., ABCA4_4537delC, rs61750131 and rs61751407) was lower compared with the rest of the tested SNVs. The average value of the unexpended primer for those same SNVs was above 80%. Increasing the amount (i.e., by double) of the extension primers for those three (3) variants failed to improve the average values for yield and unextended primer. Table 0.21 represents the homozygous and heterozygous AHs for the ABCA4_4537delC, rs61750131 and rs61751407 SNVs with the old and new extension primers. For the ABCA4_4537delC and rs61750131 SNVs, the AH for both homozygous and heterozygous calls was improved using the new EXT primer mix.

To determine if having unsatisfactory AHs for specific SNVs is due to a low amount of PCR product (i.e., as a result of low PCR primers in the mix), the percentage of used primer (UP) was calculated for each SNV run in triplicate. The SNVs, rs138157885, rs1800728 and rs61749459, produced an unsatisfactory minimum allele height and had a UP under 80%. Comparing the data using old PCR mix and new PCR mix failed to improve the average values for yield and unextended primer. Table 0.22 represents the homozygous and heterozygous AH for rs138157885, rs1800728 and rs61749459 with the old and

new extension primers. Using new PCR mix did not result in an improvement of AH for homozygous calls compared with using the new extension mix. Interestingly, the average and minimum values for AH homozygous calls for the rs1800728 SNV decreased, but the AH homozygous call increased.

3.7.2.3 – Allele frequency determination

A total number of 1039 control samples were tested for the 20 most common ABCA4 mutations causing STGD1 in the NL population. In the multiplex panel of 1039 individuals, a range of 987-1024 control samples was successful in generating a genotype call. The MAF of the 20 mutations within populations of European descent, ranged from 0% to 0.50% (i.e., NL and non-NL controls combined). This data was compared with the MAF of all 20 SNVs for European non-Finnish population using EXAC browser (**Table 3.11**).

The MAF of the 20 mutations in the NL population ranged from 0% to 0.76 % (**Table 3.12**). Five SNVs had a higher MAF in the NL population including rs61752406, rs76157638, rs61750130, rs1800728 and rs61751407 (pathogenic variants c.2564G>A, c.2588G>C, c.4139C>T, c.5461-10T>C, and c.5714+5G>A, respectively). The c.5714+5G>A SNV MAF was significantly increased in the NL population compared with the non-NL populations (p-value = 0.0078).

The MAF of the 20 mutations in the non-NL population ranged from 0% to 0.60% (**Table 3.12**). The MAF for the rs61750120 SNV and the rs62646862 SNV (i.e., c.3322C>T and c.455G>A mutations, respectively) were higher in the non-

NL population compared with the NL population controls, but this was not statistically significant (p-value=0.4858). Interestingly, the rs61750120 SNV (i.e., c.3322C>T) was homozygous in a single non-NL individual, which was not reported in the EXAC browser and also was not detected in the NL population. Another non-NL sample was a heterozygous for the c.67-1delG mutation, which is a novel mutation found in just one family from NL.

Table 3.11. Comparison of the MAF of the 20 mutations within populations of European descent and European non-Finish from ExAC browser**.**

Mutations	c.67-1delG	c.455G>A	c.634C>T	c.1522C>T	c.2564G>A	c.2588G>C	c.3064G>A	c.3322C>T	c.3323G>A	c.4139C>T
RS#	ABCA4_67-1delG	rs62646862	rs61750200	rs138157885	rs61752406	rs76157638	rs61749459	rs61750120	rs61750121#2	rs61750130
Allele Frequency combined (In NL + non-NL)										
Total number of Allele	2044	1974	2038	2048	2042	2024	2042	2046	2046	2034
Allele Frequency combined (In NL+non-NL)(%)	0.0489%	0.5066%	0.0000%	0.0000%	0.2449%	0.3458%	0.0000%	0.0978%	0.0000%	0.0492%
Allele Frequency from ExAC browser										
European Non-Finnish (%)	unknown	0.3087%	0.0121%	0.0270%	0.0060%	0.8096%	0.0000%	0.0180%	0.0030%	0.0349%
Total number of Allele	unknown	66412	66028	66594	66720	65218	66602	66662	66664	65842
Total number of Homo	unknown					2				

Mutations	c.4163T>C	c.4222T>C	c.4469G>A	c.4537delC	c.4577C>T	c.4918C>T	c.5461-10T>C	c.5714+5G>A	c.6089G>A	c.6449G>A
RS#	rs61750131	rs61750135	rs61751402	ABCA4_4537delC	rs61750152	rs61751404	rs1800728	rs61751407	rs61750641	rs61751384
Allele Frequency combined (in NL + non-NL)										
Total number of Allele	2034	2036	2040	2036	2044	2044	2030	2038	2038	2042
Allele Frequency combined (in NL+non-NL)(%)	0.0000%	0.0000%	0.0000%	0.0000%	0.0000%	0.0000%	0.0493%	0.3925%	0.0000%	0.0000%
Allele Frequency from ExAC browser										
European Non-Finnish (%)	0.0015%	0.0015%	0.0384%	unknown	0.0030%	0.0015%	0.0391%	0.0616%	0.0554%	0.0045%
Total number of Allele	66158	66536	31222	unknown	66736	66728	66486	66522	66736	66734
Total number of Homo				unknown						

Table 3.12. Carrier frequency and MAF in NL and non-NL

Mutations	c.67-1delG	c.455G>A	c.634C>T	c.1522C>T	c.2564G>A	c.2588G>C	c.3064G>A	c.3322C>T	c.3323G>A	c.4139C>T
RS#	ABCA4_67-1delG	rs62646862	rs61750200	rs138157885	rs61752406	rs76157638	rs61749459	rs61750120	rs61750121#2	rs61750130
Newfoundland and Labrador Population										
Total number of Samples	527	493	525	526	525	521	526	526	526	523
Total number of WT	527	489	525	526	521	517	526	526	526	522
Total number of Het	0	4	0	0	4	4	0	0	0	1
Total number of Homo (mut)	0	0	0	0	0	0	0	0	0	0
Carrier Frequency in NL										
WT (%)	100.00%	99.19%	100.00%	100.00%	99.24%	99.23%	100.00%	100.00%	100.00%	99.81%
Het (%)	0.00%	0.81%	0.00%	0.00%	0.76%	0.77%	0.00%	0.00%	0.00%	0.19%
Homo (mut) (%)	0.00%	0.00%	0.00%	0.00%	0.00%	0.00%	0.00%	0.00%	0.00%	0.00%
Allele Frequency in NL										
Total number of Alleles	1054	986	1050	1052	1050	1042	1052	1052	1052	1046
Allele Frequency in NL (%)	0.0000%	0.4057%	0.0000%	0.0000%	0.3810%	0.3839%	0.0000%	0.0000%	0.0000%	0.0956%

Mutations	c.4163T>C	c.4222T>C	c.4469G>A	c.4537delC	c.4577C>T	c.4918C>T	c.5461-10T>C	c.5714+5G>A	c.6089G>A	c.6449G>A
RS#	rs61750131	rs61750135	rs61751402	ABCA4_4537delC	rs61750152	rs61751404	rs1800728	rs61751407	rs61750641	rs61751384
Newfoundland and Labrador Population										
Total number of Samples	523	524	525	524	526	528	523	524	524	524
Total number of WT	523	524	525	524	526	528	522	516	524	524
Total number of Het	0	0	0	0	0	0	1	8	0	0
Total number of Homo (mut)	0	0	0	0	0	0	0	0	0	0
Carrier Frequency in NL										
WT (%)	100.00%	100.00%	100.00%	100.00%	100.00%	100.00%	99.81%	98.47%	100.00%	100.00%
Het (%)	0.00%	0.00%	0.00%	0.00%	0.00%	0.00%	0.19%	1.53%	0.00%	0.00%
Homo (mut) (%)	0.00%	0.00%	0.00%	0.00%	0.00%	0.00%	0.00%	0.00%	0.00%	0.00%
Allele Frequency in NL										
Total number of Alleles	1046	1048	1050	1048	1052	1056	1046	1048	1048	1048
Allele Frequency in NL (%)	0.0000%	0.0000%	0.0000%	0.0000%	0.0000%	0.0000%	0.0956%	0.7634%	0.0000%	0.0000%

Mutations	c.67-1delG	c.455G>A	c.634C>T	c.1522C>T	c.2564G>A	c.2588G>C	c.3064G>A	c.3322C>T	c.3323G>A	c.4139C>T
RS#	ABCA4_67-1delG	rs62646862	rs61750200	rs138157885	rs61752406	rs76157638	rs61749459	rs61750120	rs61750121#2	rs61750130
non-Newfoundland and Labrador Population										
Total number of Samples	495	494	494	498	496	491	495	497	497	494
Total number of WT	494	488	494	498	495	488	495	496	497	494
Total number of Het	1	6	0	0	1	3	0	0	0	0
Total number of Homo (mut)	0	0	0	0	0	0	0	1	0	0
Carrier Frequency in non-NL										
WT (%)	99.80%	98.79%	100.00%	100.00%	99.80%	99.39%	100.00%	99.80%	100.00%	100.00%
Het (%)	0.20%	1.21%	0.00%	0.00%	0.20%	0.61%	0.00%	0.00%	0.00%	0.00%
Homo (mut) (%)	0.00%	0.00%	0.00%	0.00%	0.00%	0.00%	0.00%	0.20%	0.00%	0.00%
Allele Frequency in non-NL										
Total number of Alleles	990	988	988	996	992	982	990	994	994	988
Allele Frequency in non-NL (%)	0.1010%	0.6073%	0.0000%	0.0000%	0.1008%	0.3055%	0.0000%	0.2012%	0.0000%	0.0000%

Mutations	c.4163T>C	c.4222T>C	c.4469G>A	c.4537delC	c.4577C>T	c.4918C>T	c.5461-10T>C	c.5714+5G>A	c.6089G>A	c.6449G>A
RS#	rs61750131	rs61750135	rs61751402	ABCA4_4537delC	rs61750152	rs61751404	rs1800728	rs61751407	rs61750641	rs61751384
non-Newfoundland and Labrador Population										
Total number of Samples	494	494	495	494	496	494	492	495	495	497
Total number of WT	494	494	495	494	496	494	492	495	495	497
Total number of Het	0	0	0	0	0	0	0	0	0	0
Total number of Homo (mut)	0	0	0	0	0	0	0	0	0	0
Carrier Frequency in non-NL										
WT (%)	100.00%	100.00%	100.00%	100.00%	100.00%	100.00%	100.00%	100.00%	100.00%	100.00%
Het (%)	0.00%	0.00%	0.00%	0.00%	0.00%	0.00%	0.00%	0.00%	0.00%	0.00%
Homo (mut) (%)	0.00%	0.00%	0.00%	0.00%	0.00%	0.00%	0.00%	0.00%	0.00%	0.00%
Allele Frequency in non-NL										
Total number of Alleles	988	988	990	988	992	988	984	990	990	994
Allele Frequency in non-NL (%)	0.0000%	0.0000%	0.0000%	0.0000%	0.0000%	0.0000%	0.0000%	0.0000%	0.0000%	0.0000%

3.7.2.4 – Final optimization of the 1x20-plex LDT panel

SNVs with lower quality performance were selected based on the data generated for AH of 400 samples from the NL control samples. All of the SNVs, with the exception of the list below, had more than 95% of homozygous calls above 10 intensity units and heterozygous calls above 5 intensity units. The rs138157885 SNV had 82% of homozygous AH>10 intensity units, rs1800728 had 94% of homozygous AH>10 intensity unit, and rs61749459 had 88% of homozygous AH>10 intensity units. Thus, a new EXT primer cocktail with increased amount of extension primers was made for three (3) SNV (i.e., rs138157885, rs1800728 and rs61749459) and used to check if it improved quality performance. **Table 0.23** represents the homozygous and heterozygous AHs for the rs138157885, rs1800728 and rs61749459 SNVs with the new and the old extension primers. The AHs clearly improved after using the new EXT primer cocktail after adjustment.

A

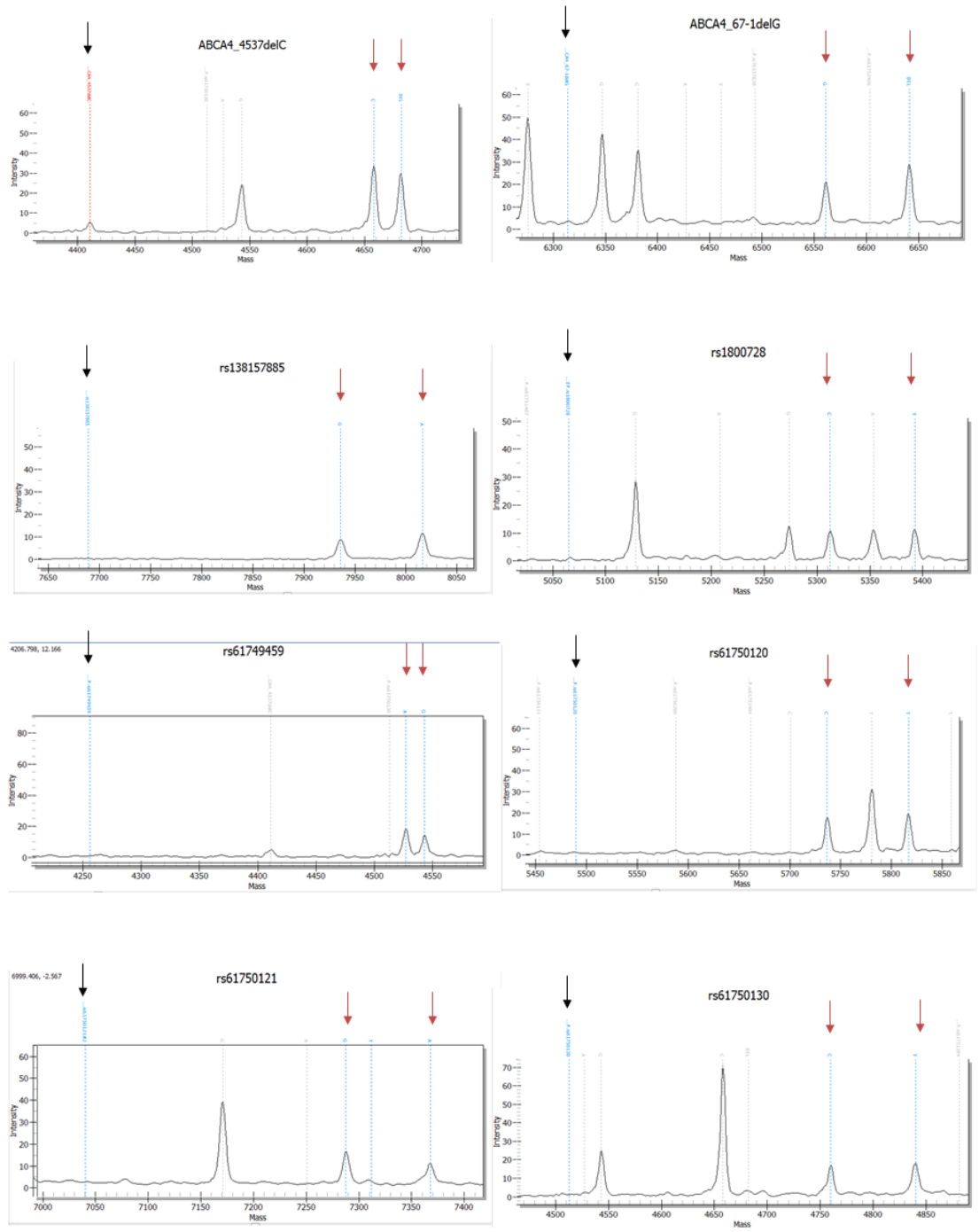
ABCA4_4537delC
ABCA4_67-1delG
rs138157885
rs1800728
rs61749459
rs61750120
rs61750121
rs61750130
Intensity
Mass

B

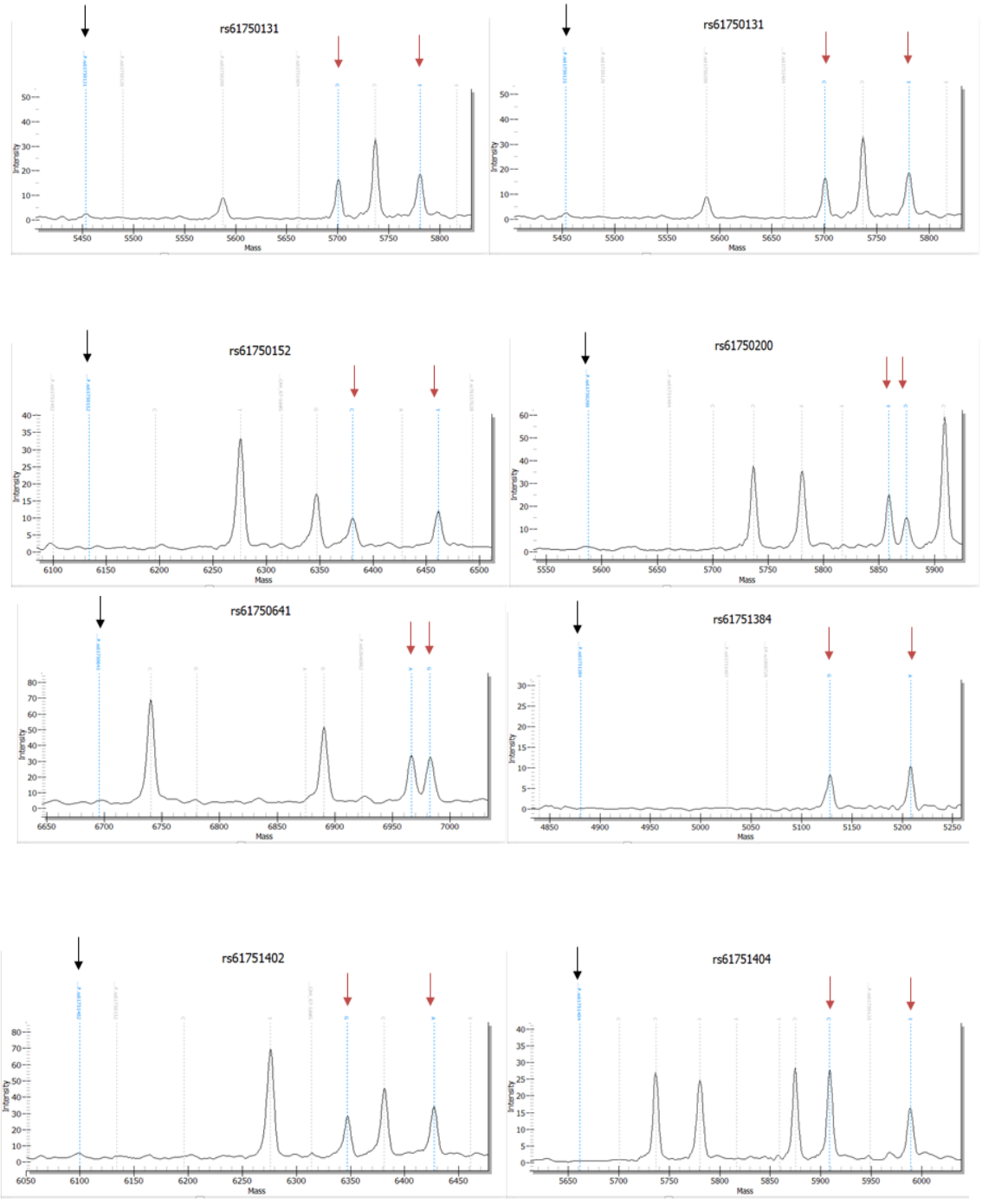
rs61750131
rs61750131
rs61750152
rs61750200
rs61750641
rs61751384
rs61751402
rs61751404
Intensity
Mass

C

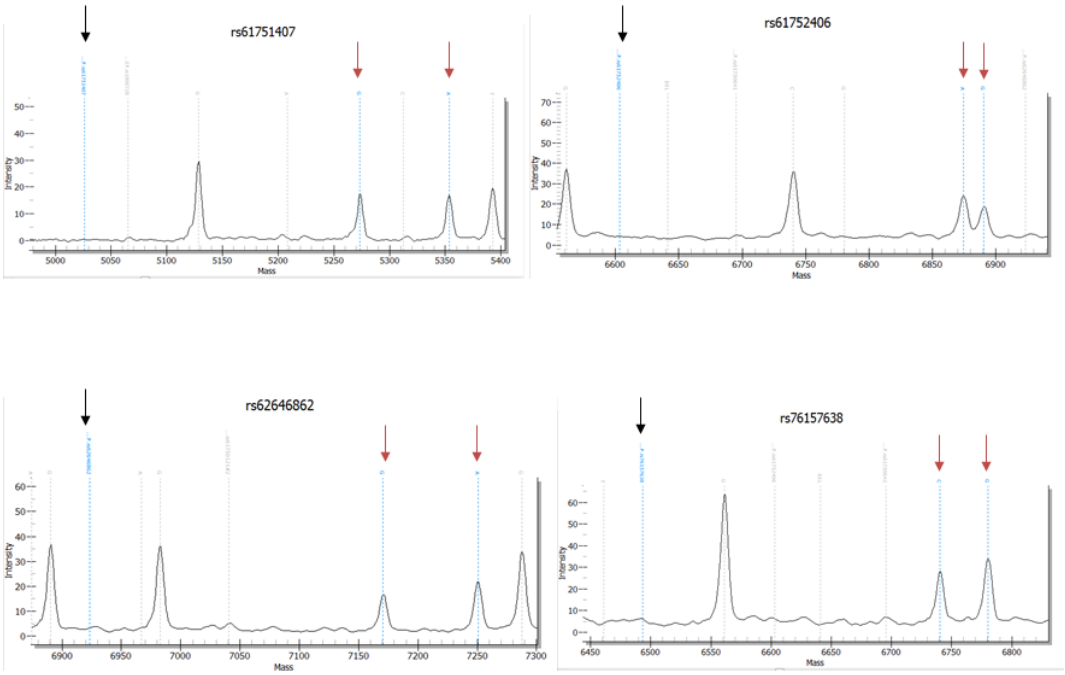

D

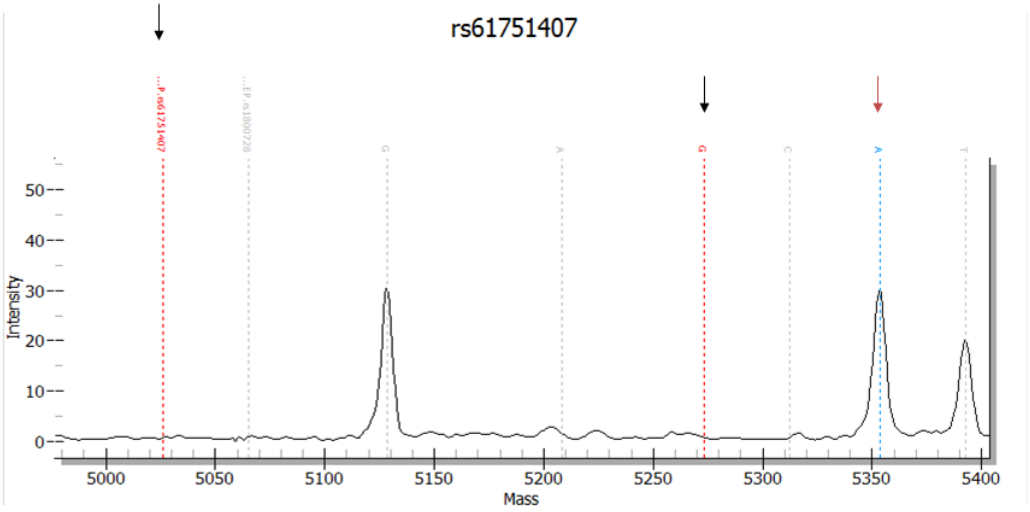

Figure 3.5. Representative mass spectrometry pictures of all the SNVs included in the 1x20-plex LDT panel after optimization (**A-C**). The coloured dotted lines indicate the mentioned SNV and the grey dotted lines indicate other SNVs with different masses. The first red dotted line with black arrow on top on the right side of each plot represents the unexpended primer. Having no peak (or just small peak) under that line indicates that most of the primer has been used. The other two (2) coloured dotted lines on the left side of each plot indicate the alternative alleles that can be called. Called alleles have a peak the line and a red arrow on the top verifies that call. Panels A, B and C represent all SNVs in the 1x20-plex LDT panel in heterozygous status with an acceptable allele

height and SNR. Panel D represents the only mutated homozygous call in the optimization cohort.

3.7.3 – Final calling algorithm parameters

Based on our investigations, four important factors that need to be considered in order to accept an automated genotype call were: 1) yield; 2) allele height(s); 3) percentage of used primer; and 4) signal to noise ratio. **Figure 3.6** represents the homozygous and heterozygous calling algorithms.

Yield of greater than 50% and AH of greater than 10 intensity units for homozygous calls and greater than 5 intensity units for heterozygous calls are required. If the yield was greater than 50% but AH was between the range of 7 and 10 intensity unit, and 4 and 5 intensity unit for homozygous and heterozygous calls respectively, then the UP% of greater than 80% and SNR of 20 and 12 are required for homozygous and heterozygous calls, respectively. In case the mentioned criteria were not met, that genotype is failed and unacceptable.

The requirements for a run to be acceptable with regards to the NTC were as below: 1) at least one NTC without any automated genotype call; and 2) random calls for less than 2.5% of SNVs with an automated genotype call.

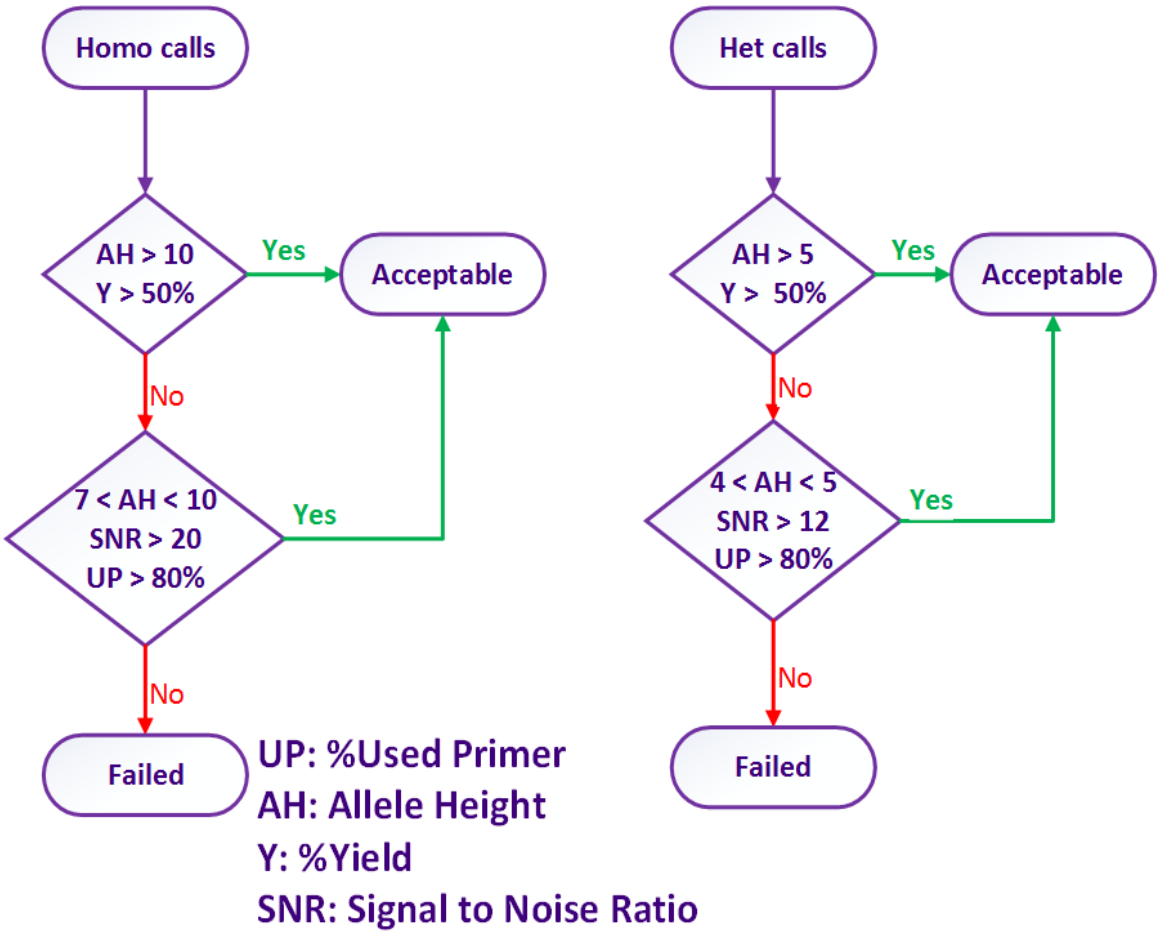

Figure 3.6. Calling algorithm for homozygous and heterozygous calls. This algorithm represents the primary and secondary parameters with their respective thresholds to accept automated genotype calls after visual inspection.

3.8 – ANALYTICAL VALIDATION

The validation cohort was comprised of 78 samples that were previously tested in a molecular laboratory. The phenotype and genotype of each individual comprising the validation cohort is indicted in **Table 3.13**.

Table 3.13. Validation cohort details of clinical and genotyping status.

DNA #	Status	Clinical Data	Pathogenic Variant detected by optimized 1x20-plex LDT
	Patient/parent/sibling	Indicate whether they have any clinical examinations done	
1	Relative	No	WT
2	Patient	Yes	c.[4139C>T];[4139C>T]
3	Parent	No	c.[5461-10T>C]
4	Sibling	No	c.[5714+5G>A]
5	Patient	Yes	c.[5714+5G>A];[5714+5G>A]
6	Sibling	Yes	WT
7	Sibling	No	c.[5714+5G>A]
8	Patient	Yes	c.[5714+5G>A];[5714+5G>A]
9	Patient	Yes	c.[5461-10T>C(;)5714+5G>A]
10	Patient	Yes	WT
11	Niece	Yes	WT
12	Sibling	No	WT
13	Patient	Yes	c.[67-1delG(;)5714+5G>A]
14	Cousin	No	WT
15	Patient	Yes	c.[5461-10T>C];[5461-10T>C]
16	Sibling	No	WT
17	Relative	No	c.[3322C>T]
18	Patient	Yes	c.[5461-10T>C];[5461-10T>C]
19	Sibling	No	WT
20	Patient	Yes	c.[455G>A;4163T>C];[455G>A;4163T>C] *rs61750200 (failed to generate a call)
21	Patient	Yes	c.[5714+5G>A];[5714+5G>A]
22	Patient	Yes	c.[5714+5G>A];[5714+5G>A]
23	Sibling	No	WT
24	Sibling	No	c.[4469G>A]
25	Parent	No	c.[5714+5G>A]
26	Parent	No	c.[1522C>T]
27	Parent	No	WT
28	Patient	Yes	c.[5714+5G>A];[5714+5G>A]
29	Patient	Yes	c.[4577C>T]

30	Sibling	No	WT
31	Parent	No	c.[5714+5G>A]
32	Sibling	No	c.[5714+5G>A]
33	Parent	No	c.[4537delC]
34	Parent	No	c.[5714+5G>A]
35	Parent	Yes	WT
36	Patient	Yes	c.[5461-10T>C(;)5714+5G>A]
37	Parent	No	c.[5461-10T>C]
38	Patient	Yes	WT
39	Patient	Yes	c.[67-1delG(;)5714+5G>A]
40	Sibling	No	c.[2588G>C(;)5714+5G>A]
41	Patient	Yes	c.[4139C>T(;)5714+5G>A]
42	Patient	Yes	c.[4577C>T(;)5714+5G>A]
43	Parent	No	c.[5461-10T>C]
44	Relative	No	c.[2564G>A]
45	Patient	Yes	c.[455G>A(;)4163T>C(;)5714+5G>A]
46	Patient	Yes	c.[5714+5G>A];[5714+5G>A]
47	Relative	No	c.[3322C>T]
48	Patient	Yes	c.[3322C>T(;)5714+5G>A]
49	Patient	Yes	c.[455G>A;4163T>C];[455G>A;4163T>C] *rs61750200 (failed to generate a call)
50	Sibling	No	c.[2588G>C(;)5714+5G>A]
51	Patient	Yes	c.[455G>A(;)4163T>C(;)4469G>A]
52	Patient	Yes	c.[455G>A(;)4163T>C(;)5714+5G>A]
53	Parent	No	c. [2588G>C(;)5714+5G>A]
54	Relative	No	c.[455G>A]
55	Parent	No	c.[5461-10T>C]
56	Patient	Yes	c.[5461-10T>C];[5461-10T>C]
57	Patient	Yes	WT
58	Patient	Yes	c.[3322C>T(;)5714+5G>A]
59	Patient	Yes	c.[5714+5G>A];[5714+5G>A]
60	Parent	No	c.[2588G>C]
61	Patient	Yes	WT
62	Parent	No	c.[5714+5G>A]
63	Patient	Yes	c.[1522C>T(;)2564G>A]

64	Parent	No	c.[2564G>A]
65	Sibling	No	c.[2588G>C(;)5714+5G>A]
66	Patient	Yes	c. [2564G>A(;)5714+5G>A]
67	Patient	Yes	WT
68	Patient	Yes	WT
69	Parent	No	c.[2588G>C(;)5714+5G>A]
70	Parent	No	c.[2588G>C]
71	Patient	Yes	c.[2564G>A];[5461-10T>C]
72	Sibling	No	c.[2588G>C]
73	Parent	No	c.[5714+5G>A]
74	Parent	No	c.[3322C>T]
75	Patient	Yes	WT
76	Patient	Yes	c.[455G>A(;)5461-10T>C]
77	Patient	Yes	c.[455G>A(;)5461-10T>C]
78	Relative	No	c.[5461-10T>C]

*No genotype call was generated for the c.634C>T in sample 20 and 49.

As shown in the **Table 3.13,** sample #20 and #49 in the validation cohort failed to produce any genotype call for rs61750200. Also, these two individuals were homozygous for the same pathogenic variants (i.e., c.4163T>C and c.455G>A) Sanger sequencing analysis on these individuals showed that at the genotype location where the EXT primer binds on the R strand, there was a polymorphism (i.e., c.635G>A). Sample #20 and #49 in the validation cohort were determined to be homozygous for the c. 635G>A SNP (**Figure 3.7**).

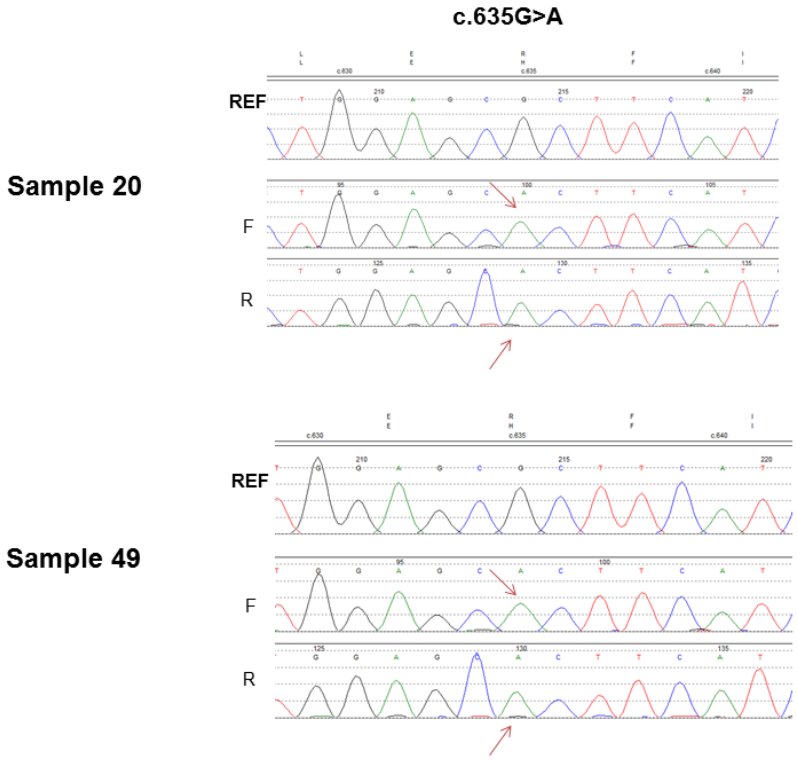

Figure 3.7. Sanger sequencing results for sample #20 and #49 in the validation cohort that were homozygous for the c.635G>A SNV**.**

All genotypes produced in the validation cohort passed the calling algorithm threshold criteria. The analytical validity results of the optimized 1x20-plex LDT are displayed in **Table 3.14**. The validation cohort using the optimized 1x20-plex LDT panel had an analytical sensitivity and specificity of 100%. The optimized 1x20-plex LDT panel displayed 100% accuracy (i.e., concordance) with the results from previous testing in an external reference facility. The optimization cohort produced the same results when assessed using the 1x20-

plex LDT panel in triplicate (i.e., 100% precision). The reference and reportable ranges are indicated in **Table 3.15**.

Table 3.14. Analytical validity of the optimized 1x20-plex LDT for the 78 samples in the validation cohort.

True-positive rate (%)	True-negative rate (%)	Analytical sensitivity (%)	Analytical specificity (%)	Accuracy (%)	Precision (%)
78/78 (100%)	(100%)	(100%)	(100%)	78/78 (100%)	*42/42 (100%)

*To determine the precision the optimization cohort was assessed 3 times.

Table 3.15. Reference and reportable range for all 20 SNVs included in the 1x20-plex LDT panel, and the precision determined for each SNV.

Pathogenic variant	Reference range	Reportable range
c.67-1delG	G	G, del
c.455G>A	G	G, A
c.634C>T	C	C, T
c.1522C>T	C	C, T
c.2564G>A	G	G, A
c.2588G>C	G	G, C
c.3064G>A	G	G, A
c.3322C>T	C	C, T
c.3323G>A	G	G, A
c.4139C>T	C	C, T
c.4163T>C	T	T, C
c.4222T>C	T	T, C
c.4469G>A	G	G, A
c.4537delC	C	C, del
c.4577C>T	C	C , T
c.4918C>T	C	C, T
c.5461-10T>C (IVS38)	T	T, C

c.5714+5G>A (IVS40)	G	G, A
c.6089G>A	G	G, A
c.6449G>A	G	G, A

3.9 – CLINICAL VALIDITY OF THE 1X20-PLEX LDT PANEL

Assessing 15 individuals using the optimized 1x20-plex LDT panel resulted in identifying 1 patient with 3 pathogenic variants (i.e., c.455G>A; c.4163T>C; c.4469G>A), and 4 carriers (**Table 3.16**). Sample #1 was a carrier for the most common mutation in NL (i.e., c.5714+5G>A); sample #4 was a carrier for the c.5461-10T>C SNV and samples #11 and #12 were both carriers for c.455G>A SNV (**Table 3.16**). The individuals who were heterozygous for any SNV included in the panel were confirmed using Sanger sequencing.

Table 3.16. Clinical and genotyping information for the unknown genotype validation cohort.

DNA #	Status	Clinical Data available?	Symptomatic	Pathogenic Variant by 1x20-plex LDT
	Family History of STGD1			
1	Yes	No	No	c.[5714+5G>A]
2	No	No	No	WT
3	No	Yes	Yes	WT
4	Yes	Yes	Yes	c.[5461-10T>C]
5	No	No	Unknown	WT
6	No	Yes	Yes	WT
7	No	Yes	Yes	WT
8	No	Yes	Yes	WT
9	No	Yes	Yes	WT
10	No	Yes	Yes	WT
11	No	Yes	Yes	c.[455G>A]

12	No	Yes	Yes	c.[455G>A]
13	No	No	Yes	WT
14	No	Yes	Yes	WT
15	Yes	No	Yes	c.[455G>A(;)4163T>C(;)4469G>A]

If it is not stated as (homo) variants were in heterozygous status

Chapter 4

4.0 – DISCUSSION

4.1 – STUDY APPROACHES

This custom LDT panel will be the preliminary test to identify the underlying genetic causes in individuals newly diagnosed with Stargardt or Stargardt-like disease, and in individuals at-risk of being a carrier in the NL population. Also, the panel assisted in calculating the carrier frequency for the 20 pathogenic variants.

4.2 – BENEFITS OF CLINICAL GENETIC TESTING FOR STARGARDT DISEASE

Stargardt disease (STDG1) is a recessive disorder, which causes progressive loss of central vision. Clinical features of STGD1 mostly appear in the second decade of life (Zernant et al. 2014b). The hallmark feature of disease is the appearance of yellow flecks surrounding the macular area (Burke, Tsang 2011). Pathogenic variants in the ABCA4 gene are the only genetic contributions associated with STGD1. However, the ABCA4 gene is large comprised of 50 exons. Approximately one thousand pathogenic variants have been detected in the ABCA4 gene that not only cause STGD1 but are also associated with disorders such as CRD or RP (Sangermano et al. 2016).

The development of a successful genetic test for a condition in which a clinical diagnosis is often difficult to make or often happens in later stages will lead to immediate improvements for those individuals. Although there is no

specific therapy available for STGD1 yet (Auricchio, Trapani & Allikmets 2015), there are a number of benefits in knowing a patient's genotype status: 1) earlier diagnosis including in the absence of any clinical features (i.e., asymptomatic); 2) preparation or planning for future use of vision-assisting tools; 3) affected individuals can be identified for interventional trials, such as gene therapy (Sangermano et al. 2016); and 4) identifying carriers can be useful for family planning. In addition, methods such as in vitro fertilization can assist affected and carrier parents to have healthy offspring. To this end, the first successful study to achieve an unaffected child from an STGD1 patient father and a carrier mother using IVF and preimplantation genetic diagnosis was performed by Sohrab et al in 2010 (Sohrab et al. 2010). During this project intracytoplasmic sperm injection produced embryos which were either affected or carriers as detected by single cell DNA testing. Implantation of an embryo with a single ABCA4 pathogenic allele resulted in delivering a healthy live born female (Sohrab et al. 2010).

4.3 – APPROACHES TO GENETIC TESTING FOR STARGARDT DISEASE

According to the literature, using a targeted SNP-based microarray chip is one of the most common methods utilized for genetic testing of STGD1 (Burke, Tsang 2011). However, there is a debate on the outcome of using the ABCA4 microarray testing in routine clinical practice because there may be false positive or false negative results (Ernest et al. 2009). Some studies have used other methods (i.e., denaturing gradient gel electrophoresis, denaturing high-performance liquid chromatography and multiplex ligation-dependent probe

amplification) to assist SNP-based microarray in detection of STGD1 pathogenic variants (Ernest et al. 2009, Aguirre-Lamban et al. 2009). Also, since some variants in ABCA4 causing STGD1 are ethnic-specific, general SNP-based microarray may not detect some of these variants. The other useful but expensive way of detecting pathogenic variants is using traditional Sanger sequencing (Aguirre-Lamban et al. 2009). Sanger sequencing has a higher and more successful detection rate compared with SNP-based microarray but it is more time-consuming and not cost-efficient (Burke, Tsang 2011, Aguirre-Lamban et al. 2009) (the cost for 1 sample screening 20 amplicon is ~630$ Canadian). The other efficient way of genotyping utilized in recent years is next generation sequencing (NGS) technologies, which is also beneficial in detecting novel mutations but remains costly to perform clinically (Chiang et al. 2015).

This project was the first translational study at Memorial University to develop a clinically useful diagnostic test. Previously, research on 29 NL families diagnosed with STGD1 resulted in the identification of 20 common pathogenic variants (T.L. Young and J. Green, 2013, personal communication). Eleven out of these 20 pathogenic variants were recurrent pathogenic variants.

The iPLEX chemistry with the Sequenom MassARRAY technology was selected as the genotyping platform for the LDT panel due to the following: 1) it enables multiplexing of various pathogenic variants; 2) it is a cheap (the cost for 1 sample screening 20 amplicon is ~20$ Canadian) and a less time-consuming technology compared with other genotyping techniques (because fluorescent

dyes are not required); 3) it is a highly automated technique; 4) it uses a small reaction volume; 5) it has accurate genotyping calls (Blumenstiel et al. 2016, Farkas et al. 2010); 6) it has a more streamlined process minimizing contamination; and 7) it has a customizable open platform permitting custom panels to be designed and adding additional variants (i.e., newly discovered pathogenic variants) is a relatively easy process.

A summary of the steps for genotyping with the Sequenom MassARRAY iPLEX chemistry is as follows: 1) amplification using PCR (required to amplify areas of interest); 2) cleanup step using SAP reaction; 3) primer extension; and 4) conditioning the iPLEX reaction using resin. The last step is crucial in order to optimize the mass spectrometry analysis of the iPLEX reaction products because it deionizes the reaction products to ensure an optimal result. Matrix-assisted laser desorption ionization time-of-flight (MALDI-TOF) mass spectrometry was used to identify pathogenic variants. MALDI-TOF mass spectrometric detection coupled with iPLEX chemistry resulted in allele-discrimination of various DNA samples in the multiplex LDT panel (Meyer, Ueland 2011). This technology represents the lowest cost-per-variant technology currently available for genotyping as it uses the mass of specific nucleotides to make genotype calls.

4.4 – CHALLENGES WITH DESIGNING A CUSTOM MULTIPLEX LDT PANEL

The first challenge encountered when developing the custom LDT panel was with respect to the in-silico design of the multiplex reaction. Initially, specific SNVs

were rejected in the Assay Design Suite software and excluded from subsequent design due to having high dimer or hairpin potentials. Once the rejected SNVs were incorporated into the design by changing the stringency, the incompatibility of the designed primers resulted in spreading the SNVs across multiple wells. Given that the ultimate goal for any LDT panel for clinical testing is to be cheap, fast, accurate and reliable, we tried to reduce the number of wells, which would lower the cost and time per test.

Two LDT panel designs were tested, a 2x10-plex and a 1x20-plex design. The 2x10-plex LDT panel was achieved using a trial-and-error approach with the Assay Design Suite software. However, due to the issues encountered designing the 1x20-plex LDT panel (i.e., testing all 20 pathogenic variants in one well) with Assay Design Suite software, the manufacturer (i.e., Agena BioSciences) suggested to use a desktop version of the design software called Typer4, which is similar to Assay Design Suite but more robust and flexible with respect to assay design. For example, this off-line software doesn't produce as many rejects because it does not process data the same way as the Assay Design Suite software, thus it was better for multiplexing more SNVs in fewer wells. The 1x20-plex LDT panel was created using the Typer4 software. The strategy of designing two different multiplex LDT panels enabled us to compare and contrast the quality performance of the 20 SNVs. The performance of any custom LDT panel regardless of whether it is a uniplex or multiplex assay must be analyzed in the laboratory in order to assess the quality of the in-silico design.

Before assessing a single sample on the custom designed LDT panel, it was critical to adjust the extension (EXT) primers for both LDT panels. This step was critical because different EXT products having distinct molecular weights result in the detection of different alleles and the mass of extension products has an inverse relationship with the SNR (Farkas et al. 2010). Primers for each SNV were designed within a window of 4,000 to 95,000Da and every SNV allele had to differ by at least 5Da in mass in order for successful genotyping. Although having equal amounts of the EXT primers in the mix was impossible, it was necessary to adjust the mix in a way that the SNR for all primers was above an acceptable value (>15%) and almost equal to each other (using a trial-and-error approach) as suggested by the manufacturer in order for optimum EXT reaction to proceed.

4.5 – ASSESSMENT AND SELECTION OF THE BEST PERFORMING LDT PANEL

To check the performance of each LDT panel a cohort of 14 samples that contained at least one heterozygous allele for each of the 20 pathogenic variants was assessed on both LDT panels. This allowed us to assess each SNV within a single run, shortening the optimization time resulting in a time-efficient and cost-effective approach to panel development.

The initial assessment of performance of both the 1x20-plex and 2x10-plex LDT panels used iPLEX Gold chemistry. No false positive or false negative results in the tested samples were observed for either LDT panel. To determine

whether the obtained result was reproducible, the same samples were assessed again and 100% precision was achieved for both LDT panels. The yield for all SNVs was greater than 50% for all runs indicating that the reaction was efficient. However, the allele heights of the automated genotype calls were too low and unreliable for clinical testing. Some of the calls were as low as background noise (i.e., AH of 2 and 1.5 intensity units for homozygous and heterozygous calls, respectively). Also, in the NTC wells, multiple automated genotype calls were observed that were either random or were repeated in different wells.

The quality performance metrics for both LDT panels (i.e., 1x20-plex and 2x10-plex) was unsatisfactory attributed to: 1) the presence of genotype “calls” in the NTC wells for multiple assays; and 2) lower allele heights (AH) than expected. With respect to the observed poor quality metrics (i.e., multiple automated genotype calls in NTC and low AH), the manufacturer suggested that switching genotyping chemistry from iPLEX Gold to iPLEX Pro, as the latter has a higher fidelity enzyme likely to improve quality and overall performance of the LDT panels. Also, automated genotype calls in the NTC wells might be attributed to a possible negative interaction between the PCR and EXT primers. In the latter theory, the hybridization of various primers in the iPLEX reaction results in a targeted sequence of DNA for EXT primers to bind, which could explain the observed automated calls. However, if a call for the same SNV is observed in different NTC wells within a run and across runs, it strongly suggests a poor design of those primers in the multiplex reaction. The experiment to test for an

interaction between PCR and EXT primers led to a conclusion that the EXT primers alone were not causing SNVs to have genotype calls in the NTC wells. Rather, the automated genotype calls were caused by a random interaction between the PCR and EXT primers.

Next, the optimization cohort was assessed using the two chemistries on both LDT panels. Both the 1x20-plex and 2x10-plex LDT panels performed better using the iPLEX Pro chemistry compared with iPLEX Gold chemistry. In order to compare the AH for the 1x20-plex and the 2x10-plex LDT panel using iPLEX Gold versus Pro chemistry, the AH were averaged regardless of the SNV. However, the SNVs in the 2x10-plex LDT panel displayed more complexity compared with the 1x20-plex LDT panel. There were always more SNVs that were called in the NTC wells of the 2x10-plex LDT panel compared with the 1x20-plex LDT panel. Importantly, greater than or equal to 50% of these calls were non-random SNVs in the NTC wells of the 2x10-plex LDT panel. This finding is consistent with a design error for one or more SNVs in the 2x10-plex LDT panel, which were run-dependent. Given that the 1x20-plex LDT panel yielded better initial results for all SNVs, had significantly fewer automated genotype calls in the NTC wells and the automated genotype calls that appeared in the NTC wells were random, provided the first indication that the 1x20-plex LDT panel would be selected for subsequent optimization and validation. Although statistical analysis was performed comparing the homozygous calls across each SNV, a comparison across the heterozygous SNVs was not possible

for the initial assessment because of the small number of heterozygous alleles in the optimization cohort. A possible explanation for the lack of a significant difference in AH between the iPLEX Gold and Pro chemistry for the rs61751404 SNV suggests that either the primer design/location or the amplicon generated worked sufficiently well regardless of enzyme fidelity.

Results obtained from assessing the optimization cohort comparing the 1x20-plex and 2x10-plex LDT panel using only the iPLEX Pro chemistry indicated that although a greater number of SNVs performed better in the 2x10-plex LDT panel (i.e., higher allele heights) compared with the 1x20-plex LDT panel, the quality performance of each SNV varied. Even though the 2x10-plex LDT panel appeared to perform better than the 1x20-plex LDT panel based on AH of most SNVs (i.e., 55% had a higher average allele height for homozygous calls in the 2x10-plex LDT panel compared with the 1x20-plex LDT panel) the 1x20-plex LDT panel was still selected for subsequent optimization and validation as the 1x20-plex LDT panel did not produce automated SNV calls in the NTC wells, unlike the 2x10-plex LDT panel. Based on multiplex design, one would expect the well containing a lower multiplex (i.e., 2x10-plex) to out perform a well containing a higher multiplex (i.e., 1x20-plex). One possible explanation for this finding is that the parameters used to select primers for the 1x20-plex LDT panel using the Typer4 software were different than parameters used to select primers for the 2x10-plex LDT panel using the Assay Design Suite software, which would produce different primers for the same SNV across the two panels.

Sanger sequencing was performed and confirmed the results obtained by the STGD1 LDT panels. Such confirmation is required for novel genomic discoveries and clinical validation to rule out technological artifacts (i.e., false positives). However, a reverse sequence was not obtained for sample #7 in the optimization cohort, which could be attributed to the PCR template to be used for the reverse sequencing was not present in sufficient amount or the possibility of a SNP located in the primer binding site for the reverse sequencing primer.

4.6 – OPTIMIZATION OF THE 1X20-PLEX LDT PANEL

It was important to optimize the selected LDT panel since the highest sensitivity, specificity, accuracy and precision, a requirement for a clinical LDT panel, could not be achieved unless the processes and reagents used in the study were optimized. In order to optimize the 1x20-plex LDT panel, multiple runs were performed to adjust different variables. If an improvement was achieved based on adjustments performed in the experiment, that modification was applied to subsequent runs to optimize the LDT panel.

4.6.1 – Adjustments to eliminate automated genotype calls in NTC wells

In an attempt to eliminate the automated genotype calls in the NTC wells, the annealing temperature of 57 instead of 56 was used to reduce the amount of non-specific activity during the PCR phase. However, due to still having automated genotype calls in the NTC wells and the observed decrease in the AH for all samples (as expected), we decided to switch back to the normal annealing temperature. The experiment to test for an interaction between PCR and EXT

primers led to a conclusion that the EXT primers alone were not causing SNVs to have genotype calls in the NTC wells. Rather, the automated genotype calls were caused by an interaction between the PCR and EXT primers. In another attempt to eliminate the automated genotype calls in the NTC wells, Uracil N-Glycosylase (UNG) enzyme was utilized. Using the UNG enzyme in the PCR is a useful way of eliminating carryover contaminations. Unfortunately, the percentage of SNVs that were called in the NTC wells was not reduced in subsequent runs. These results suggest that the automated calls in the NTC wells were not attributed to carryover contamination in the PCR step.

4.6.2 – Adjustments to increase allele height

In an attempt to increase allele heights, several experiments with the instruments used to spot the extended product and detect alleles were performed to determine the effect of: 1) auto-tuning; 2) viscosity; and 3) the relationship between the volume spotted and AH. From experience in order to spot the optimal amount of iPLEX reaction on the chip, we knew if the spotted volumes were below 4nl and above 40nl, the MassARRAY system was unable to detect any spectrum and thus could not discriminate allelic calls. Due to the unpredictable nature of the Nanodispenser machine to spot volumes on the chip, a range of 8nl to 18nl and the target volume of 14nl were selected. With this setup we were hoping to achieve a consistent volume spotted not below 10 or above 20 units. To determine if auto-tuning results in consistently higher volumes compared with manual spotting, 64 samples were spotted with and without the

auto-tuning function enabled. Given that there was no significant difference with the auto-tune function enabled compared with it being disabled but with the auto-tune function enabled resulted in higher spotting volumes closer to the target volume (i.e., 14nl), we decided to enable this function for the optimization and validation in our study.

To determine if the viscosity of the multiplex LDT panel affects the volume spotted, 64 samples were spotted with and without the detergent Tween 20. Tween-20 is a polysorbate surfactant with a fatty acid ester moiety and a long polyoxyethylene chain, and the decrease in viscosity caused by Tween-20 is due to decreasing the surface tension, which would allow a greater spotted volume (Vinardell, Infante 1999). That Tween 20 did not result in significantly higher spotting volumes suggests that the viscosity of the iPLEX reaction products was not a factor with respect to spotted volume. That finding coupled with adding another variable that could increase the chance of contamination, we decided to not use this detergent in the optimization and validation study.

To determine if a correlation existed between the spotted volume and AH, a subset of samples used for allele frequency determination were selected. Based on the results of that experiment, no direct relationship or correlation was observed between the targeted volume (i.e., 14nl) spotted and AH. This was an unexpected finding as having more iPLEX reaction products spotted onto the chip and ionized by the MassArray system logically would be expected to produce higher AHs. Although lower spotted volumes produced a greater number

of acceptable allele heights (i.e., AH>7), higher spotted volumes yielded unacceptable allele heights (i.e., AH<7) in three samples for the rs61750152 SNV, which was responsible for the statistically significant finding. A possible explanation for the significant difference in spotted volume and AH for the rs61750152 SNV suggests that either the primer design/location or the amplicon generated worked relatively poorly regardless of spotted volume.

Primer (i.e., both PCR and EXT) adjustments were also made to optimize the 1x20-plex LDT panel. For the SNVs that performed poorly (possibly be due to having insufficient amount of amplification or extension products), the amount of primers in the mix was adjusted. Unlike adjusting the PCR cocktail (which resulted in no beneficial effect), doubling the amount of EXT primers in the extension cocktail improved the performance of the LDT panel with respect to AH.

The odd finding for the rs1800728 SNV (i.e., the average and minimum AH values for homozygous calls decreased, but the average and minimum AH for heterozygous calls increased) that was observed after the amount of 3 PCR primers were adjusted in the PCR pool can be possibly explained by having a non-homogenous reaction in the plate at the time of spotting. Thus, the reaction non-homogeneity resulted in an overall lower AH for homozygous calls for the rs1800728 SNV.

4.6.3 – Allele frequency determination

The initially optimized 1x20-plex LDT panel was ready to be assessed using a higher number of samples. Up to this point, regardless of the numerous runs that were performed using the 1x20-plex LDT panel, the only cohort of samples assessed on the LDT panel was the optimization cohort. However, to assist finalizing the optimization step, results from a larger cohort (i.e., 1039 alleles) determined the quality performance of each SNV, and assisted in improving the problematic SNVs. Estimating the minor allele frequency (MAF) for each pathogenic variant causing STGD1 was important to approximate the carrier frequency of the 20 pathogenic variants in the general population and to determine if the frequencies differ between NL and non-NL populations. As expected, the allele frequencies for the majority of SNVs were similar for the combined European descent dataset (i.e., NL and non-NL population) compared with the European non-Finnish dataset (ExAC browser). The finding that the MAF for the c.5714+5G>A SNV was significantly increased in the NL population compared with the non-NL population was not surprising and consistent with a previous study (T.L. Young and J. Green, 2013, personal communication). That the rs61750120 (i.e., c.3322C>T) SNV was homozygous in a single non-NL individual, not reported in the EXAC browser, and not detected in the NL population indicates a possible novel genotype. This likelihood was strengthened by ruling out the presence of a SNP under the primer-binding site by Sanger sequencing. Unfortunately, although the genotype was consistent with Stargardt

disease, given that the control samples used in this study were de-identified, it was impossible to correlate genotype findings with clinical information. Interestingly, a non-NL sample was heterozygous for the c.67-1delG pathogenic variant, which was previously discovered as a novel or family-specific pathogenic variant in the NL population (T.L. Young and J. Green, 2013, personal communication), suggesting that the individual might have NL ancestry.

As previously mentioned, instead of visually inspecting and accepting the automated genotype calls, an algorithm was developed to systematically confirm the automated genotype calls. The large cohort of samples assessed using the LDT panel to determine the MAF also assisted to better understand the parameters and thresholds to be considered and included in the calling algorithm. Initially, yield and AH were selected as important factors to be considered. A greater than 50% yield demonstrated that the reaction was highly efficient. Although the AH threshold was set at 7 and 4.5 intensity units for homozygous and heterozygous calls respectively, with further optimization these numbers increased to 10 and 5 intensity units respectively. Subsequently, secondary parameters were selected to more stringently accept the automated genotype calls for homozygous and heterozygous calls, and thresholds were set for each parameter. The secondary parameters are applied if the primary parameters (i.e., yield and allele height) were below threshold but within a specific range (i.e., AH for homozygous between the range of 7 and 10 intensity unites, and for heterozygous calls between the range of 4 and 5 intensity units).

The secondary parameters included: 1) SNR, which determines the level of acquired signal to the background noise, set to be greater than 20 for homozygous calls and greater than 12 for heterozygous calls; and 2) the amount of EXT primer that was used in the reaction, was set to be greater than 80%, meaning that more than 80 percent of unexpended primer must be used in the reaction to produce the genotype call in order to be acceptable when the secondary parameters are applied.

4.7 – ANALYTICAL VALIDATION

Prior to starting the analytical validation study, the final optimization of the selected 1x20-plex LDT panel was based on the data collected using the allele frequency cohort. A second adjustment of the EXT primer cocktail was performed for the SNVs that were selected as “lower quality performers”. The result was satisfactory as adjustment of the EXT primer cocktail for the lower quality SNVs improved the AH.

It is necessary that a test is validated (even if it has been optimized) and the accuracy of results proven before utilized in a clinical setting (Mattocks et al. 2010). Results from genotyping the validation cohort were concordant with their previously known genotypes (i.e., accuracy of 100%) with no false-negative or false-positive calls. Based on Burd 2010 accuracy, precision, reportable range, reference interval, analytical sensitivity, and analytical specificity are the performance characteristics that must be established before implementation of a LDT. All these characteristics have to be acceptable for the test to pass, for

example analytical sensitivity of greater than 95% is noted (Burd 2010). Also, American College of Medical Genetics and the College of American Pathologists Molecular Genetics Laboratory Survey requires analytical sensitivity, and analytical specificity of 95 percent CI 93.0 to 100% and 95 percent CI 96.0 to 100% respectively (https://www.cdc.gov/genomics/gtesting/file/print/fbr/bcanaval.pdf). The 1x20-plex LDT panel had an analytical accuracy, sensitivity, specificity and precision of 100%, indicating that our STGD1 LDT panel passed the requirements for a molecular diagnostic test and it can be utilized in a clinical setting (Grosse, Khoury 2006, Burd 2010).

Interestingly, two (2) samples from the validation cohort failed to produce a genotype call for a specific SNV (i.e., c.634C>T) after multiple assessments using the 1x20-plex LDT panel. Two (2) possibilities to explain this finding were investigated: 1) the potential of having a SNP at the PCR primer binding site that prevent the amplification of the target sequence; and 2) the potential of having a SNP at the EXT primer binding site that prevented the amplicon from extending. Sanger sequencing failed to identify a SNP under the PCR primer binding site thus excluding this as a possibility for the observed results. Sanger sequencing data from a previous study (T.L. Young and J. Green, 2013, personal communication) revealed a SNP at the genomic location c.635G>A which is the primer binding site for the EXT primers. Interestingly, follow-up investigation revealed that the two individuals (one from this study and one from a previous

study) were related and possibly inherited the same genotype. Sanger sequencing analysis on both individuals revealed that there was a homozygous polymorphism at the genotype location that the EXT primer binds (i.e., c.635G>A) preventing the extension reaction, thus creating a null allele.

4.8 – CLINICAL VALIDITY

According to Grosse et al., a diagnostic test can have a clinical utility if it has effective access to appropriate interventions (Grosse, Khoury 2006). In other words, clinical utility of a test is based on the information that a test generates and any outcomes produced by the test considered important to individuals and families (Grosse, Khoury 2006). The results from assessing a cohort of 15 unknown patients on the optimized and validated 1x20-plex LDT panel revealed a patient who was carrier for multiple SNVs (i.e., heterozygous status for 3 SNVs) tested in the panel; and 4 individuals who were carriers (i.e., each person detected with one heterozygous SNV that was tested in the panel). That this custom LDT panel identified individuals with one or more pathogenic ABCA4 variants support the utility of this panel for individuals with Stargardt or Stargardt-like disease.

4.9 – STRENGTHS AND LIMITATIONS OF STUDY

This study represents the first KT genomics project conducted at Memorial. The 1x20-plex LDT panel could not have been achieved without all the clinical data on a large cohort of samples from affected and unaffected samples that were

collected over several years by Dr. Jane Green. Also, her specialty in the area of inherited eye disorders, specifically Stargardt disease, was the biggest component of and motivation for starting this translational project. This study also complimented previous research performed by Drs. Young and Green by translating their findings into a clinical diagnostic. Having access to such a large cohort of samples (i.e., 1,039 individuals) from the general population or individuals that participated in other studies from Drs. Young, Rahman and O'Rielly enabled the estimation of allele frequencies of the 20 pathogenic variants and optimization of the 1x20-plex LDT panel.

Perhaps the most important strength of this study were the lessons learned with respect to the issues associated with using a new technology for this first time, the valuable experience in assay troubleshooting and the stringent requirements for a clinical diagnostic. Furthermore, this study resulted in the introduction of a new technology to the molecular diagnostic laboratory of Eastern Health. This project has also paved the way for developing other diagnostic LDT panels using MassArray MALDI-TOF spectrophotometry.

This study has several weaknesses or limitations. First, there are approximately 1000 variants associated with STGD1 all over the world, but the custom 1x20-plex LDT panel can only detect the 20 SNVs currently known to be pathogenic in the NL population causing STGD1 that were included in the panel. Second, samples with a SNP under primer binding sites of either PCR or EXT primers for any of the SNVs in the multiplex, MassARRAY system will fail to

generate a genotype call for that specific SNV. This occurred in this study with two (2) samples (#22 and #49) in the validation cohort that had a SNP at the genomic binding location of the EXT primers and thus failed to generate a genotype call. Third, there was no access to the clinical vision information on population control samples to investigate the genotype-phenotype correlation. Fourth, the 1x20-plex LDT panel was developed, optimized, and validated using the Sequenom MassArray technology. The assay design may not be transferrable to other similar technologies with respect to multiplexing and cost. Finally, the assessment of the clinical validity of the 1x20-plex LDT panel was limited given the relatively small sample cohort.

4.10 – FUTURE DIRECTIONS

Determining the practicality of this LDT panel in the clinical laboratory remains to be addressed. Calculating the statistical detection rate of the optimized LDT panel on a cohort of randomly selected participants from the NL population would be beneficial as a future project. A project such as this can help to determine the genetically unsolved cases of NL STGD1.

4.11 – SUMMARY AND CONCLUSION

This was the first translational study developed at Memorial University to be used clinically as a diagnostic test. The primary outcome will be a comprehensive (20 pathogenic variants), time-efficient (<24 hours) and cost-effective (~$20) preliminary test to identify the underlying genetic cause in individuals newly

diagnosed with Stargardt or Stargardt-like disease, and individuals at-risk of developing this condition in the NL population. Importantly, the 20-plex LDT panel can easily incorporate additional pathogenic variants as they become identified. Clinically, knowing the mutational status for this recessive disorder will help affected individuals or those at-risk to better plan their future (because the phenotype varies based on the pathogenic variants an affected individual carries). A genetic counselor can assist patients by educating them about the severity of their condition, the different stages of their disease and what tools are available to help them in each stage (they can be more prepared to use the helpful tools if they know their disease in advance). Also, the STGD1 LDT panel assisted in calculating the carrier frequency for the 20 pathogenic variants. Given the low-cost associated with this 20-plex panel and that several common mutations in Caucasians are included, this panel might also be utilized on individuals outside of the NL population with or without NL ancestry.

REFERENCES

Abràmoff, M.D., Garvin, M.K. & Sonka, M. 2010, "Retinal imaging and image analysis", Biomedical Engineering, IEEE Reviews in, vol. 3, pp. 169-208.

Aguirre-Lamban, J., Riveiro-Alvarez, R., Maia-Lopes, S., Cantalapiedra, D., Vallespin, E., Avila-Fernandez, A., Villaverde-Montero, C., Trujillo-Tiebas, M.J., Ramos, C. & Ayuso, C. 2009, "Molecular analysis of the ABCA4 gene for reliable detection of allelic variations in Spanish patients: identification of 21 novel variants", The British journal of ophthalmology, vol. 93, no. 5, pp. 614-621.

Allikmets, R., Singh, N., Sun, H., Shroyer, N.F., Hutchinson, A., Chidambaram, A., Gerrard, B., Baird, L., Stauffer, D., Peiffer, A., Rattner, A., Smallwood, P., Li, Y., Anderson, K.L., Lewis, R.A., Nathans, J., Leppert, M., Dean, M. & Lupski, J.R. 1997, "A photoreceptor cell-specific ATP-binding transporter gene (ABCR) is mutated in recessive Stargardt macular dystrophy", Nature genetics, vol. 15, no. 3, pp. 236-246.

Anderson, K.L., Baird, L., Lewis, R.A., Chinault, A.C., Otterud, B., Leppert, M. & Lupski, J.R. 1995, "A YAC contig encompassing the recessive Stargardt disease gene (STGD) on chromosome 1p", American Journal of Human Genetics, vol. 57, no. 6, pp. 1351-1363.

Annilo, T., Shulenin, S., Chen, Z.Q., Arnould, I., Prades, C., Lemoine, C., Maintoux-Larois, C., Devaud, C., Dean, M., Denefle, P. & Rosier, M. 2002, "Identification and characterization of a novel ABCA subfamily member, ABCA12, located in the lamellar ichthyosis region on 2q34", Cytogenetic and genome research, vol. 98, no. 2-3, pp. 169-176.

Arcos-Burgos, M. & Muenke, M. 2002, "Genetics of population isolates", Clinical genetics, vol. 61, no. 4, pp. 233-247.

Argote, L. & Ingram, P. 2000, "Knowledge transfer: A basis for competitive advantage in firms", Organizational behavior and human decision processes, vol. 82, no. 1, pp. 150-169.

Armstrong, J.D., Meyer, D., Xu, S. & Elfervig, J.L. 1998, "Long-term follow-up of Stargardt's disease and fundus flavimaculatus", Ophthalmology, vol. 105, no. 3, pp. 448-57; discussion 457-8.

Auricchio, A., Trapani, I. & Allikmets, R. 2015, "Gene Therapy of ABCA4-Associated Diseases", Cold Spring Harbor perspectives in medicine, vol. 5, no. 5, pp. 10.1101/cshperspect.a017301.

Azarian, S.M., Megarity, C.F., Weng, J., Horvath, D.H. & Travis, G.H. 1998, "The human photoreceptor rim protein gene (ABCR): genomic structure and primer set information for mutation analysis", Human genetics, vol. 102, no. 6, pp. 699-705.

Bear, J.C., Nemec, T.F., Kennedy, J.C., Marshall, W.H., Power, A.A., Kolonel, V.M. & Burke, G.B. 1988, "Inbreeding in outport Newfoundland", American Journal of Medical Genetics, vol. 29, no. 3, pp. 649-660.

Birnbach, C.D., Jarvelainen, M., Possin, D.E. & Milam, A.H. 1994, "Histopathology and immunocytochemistry of the neurosensory retina in fundus flavimaculatus", Ophthalmology, vol. 101, no. 7, pp. 1211-1219.

Blumenstiel, B., DeFelice, M., Birsoy, O., Bleyer, A.J., Kmoch, S., Carter, T.A., Gnirke, A., Kidd, K., Rehm, H.L., Ronco, L., Lander, E.S., Gabriel, S. & Lennon, N.J. 2016, "Development and Validation of a Mass Spectrometry-Based Assay for the Molecular Diagnosis of Mucin-1 Kidney Disease", The Journal of molecular diagnostics : JMD, .

Boon, C.J., Jeroen Klevering, B., Keunen, J.E., Hoyng, C.B. & Theelen, T. 2008, "Fundus autofluorescence imaging of retinal dystrophies", Vision research, vol. 48, no. 26, pp. 2569-2577.

Borst, P. & Elferink, R.O. 2002, "Mammalian ABC transporters in health and disease", Annual Review of Biochemistry, vol. 71, pp. 537-592.

Burd, E.M. 2010, "Validation of laboratory-developed molecular assays for infectious diseases", Clinical microbiology reviews, vol. 23, no. 3, pp. 550-576.

Burke, T.R., Fishman, G.A., Zernant, J., Schubert, C., Tsang, S.H., Smith, R.T., Ayyagari, R., Koenekoop, R.K., Umfress, A., Ciccarelli, M.L., Baldi, A., Iannaccone, A., Cremers, F.P., Klaver, C.C. & Allikmets, R. 2012, "Retinal phenotypes in patients homozygous for the G1961E mutation in the ABCA4 gene", Investigative ophthalmology & visual science, vol. 53, no. 8, pp. 4458-4467.

Burke, T.R. & Tsang, S.H. 2011, "Allelic and phenotypic heterogeneity in ABCA4 mutations", Ophthalmic genetics, vol. 32, no. 3, pp. 165-174.

CARR, R.E. 1965, "Fundus Flavimaculatus", Archives of ophthalmology (Chicago, Ill.: 1960), vol. 74, pp. 163-168.

Chacon-Camacho, O.F., Granillo-Alvarez, M., Ayala-Ramirez, R. & Zenteno, J.C. 2013, "ABCA4 mutational spectrum in Mexican patients with Stargardt disease: Identification of 12 novel mutations and evidence of a founder effect for the common p.A1773V mutation", Experimental eye research, vol. 109, pp. 77-82.

Chiang, J.P., Lamey, T., McLaren, T., Thompson, J.A., Montgomery, H. & De Roach, J. 2015, "Progress and prospects of next-generation sequencing testing for inherited retinal dystrophy", Expert review of molecular diagnostics, vol. 15, no. 10, pp. 1269-1275.

Colella, P., Trapani, I., Cesi, G., Sommella, A., Manfredi, A., Puppo, A., Iodice, C., Rossi, S., Simonelli, F. & Giunti, M. 2014, "Efficient gene delivery to the cone-enriched pig retina by dual AAV vectors", Gene therapy, vol. 21, no. 4, pp. 450-456.

Cremers, F.P., van de Pol, D.J., van Driel, M., den Hollander, A.I., van Haren, F.J., Knoers, N.V., Tijmes, N., Bergen, A.A., Rohrschneider, K., Blankenagel, A., Pinckers, A.J., Deutman, A.F. & Hoyng, C.B. 1998, "Autosomal recessive retinitis pigmentosa and cone-rod dystrophy caused by splice site mutations in the Stargardt's disease gene ABCR", Human molecular genetics, vol. 7, no. 3, pp. 355-362.

Cuevas, P., Outeirino, L.A., Angulo, J. & Gimenez-Gallego, G. 2012, "Treatment of Stargardt disease with dobesilate", BMJ case reports, vol. 2012, pp. 10.1136/bcr-2012-007128.

de Magalhaes, J.P., Finch, C.E. & Janssens, G. 2010, "Next-generation sequencing in aging research: emerging applications, problems, pitfalls and possible solutions", Ageing research reviews, vol. 9, no. 3, pp. 315-323.

Dean, M. & Annilo, T. 2005, "Evolution of the ATP-binding cassette (ABC) transporter superfamily in vertebrates", Annual review of genomics and human genetics, vol. 6, pp. 123-142.

Dorey, C.K., Wu, G., Ebenstein, D., Garsd, A. & Weiter, J.J. 1989, "Cell loss in the aging retina. Relationship to lipofuscin accumulation and macular degeneration", Investigative ophthalmology & visual science, vol. 30, no. 8, pp. 1691-1699.

Doucette, L., Green, J., Black, C., Schwartzentruber, J., Johnson, G.J., Galutira, D. & Young, T. 2013, "Molecular genetics of achromatopsia in Newfoundland reveal genetic heterogeneity, founder effects and the first cases of Jalili syndrome in North America", Ophthalmic genetics, vol. 34, no. 3, pp. 119-129.

Ernest, P.J., Boon, C.J., Klevering, B.J., Hoefsloot, L.H. & Hoyng, C.B. 2009, "Outcome of ABCA4 microarray screening in routine clinical practice", .

Farkas, D.H., Miltgen, N.E., Stoerker, J., van den Boom, D., Highsmith, W.E., Cagasan, L., McCullough, R., Mueller, R., Tang, L. & Tynan, J. 2010, "The suitability of matrix assisted laser desorption/ionization time of flight mass spectrometry in a laboratory developed test using cystic fibrosis carrier screening as a model", The Journal of molecular diagnostics, vol. 12, no. 5, pp. 611-619.

Fishman, G.A. 2010, "Historical evolution in the understanding of Stargardt macular dystrophy", Ophthalmic genetics, vol. 31, no. 4, pp. 183-189.

Fishman, G.A. & Sokol, S. 2001, Electrophysiologic testing in disorders of the retina, optic nerve, and visual pathway, Foundation of the American academy of Ophthalmology San Francisco, Calif, USA.

Fishman, G.A., Farber, M., Patel, B.S. & Derlacki, D.J. 1987, "Visual acuity loss in patients with Stargardt's macular dystrophy", Ophthalmology, vol. 94, no. 7, pp. 809-814.

Fishman, G.A., Farbman, J.S. & Alexander, K.R. 1991, "Delayed rod dark adaptation in patients with Stargardt's disease", Ophthalmology, vol. 98, no. 6, pp. 957-962.

Gabriel, S., Ziaugra, L. & Tabbaa, D. 2009, "SNP genotyping using the Sequenom MassARRAY iPLEX platform", Current protocols in human genetics, , pp. 2.12. 1-2.12. 16.

Green, J.S., Bear, J.C. & Johnson, G.J. 1986, "The burden of genetically determined eye disease", The British journal of ophthalmology, vol. 70, no. 9, pp. 696-699.

Green, J.S. & Johnson, G.J. 1983, "Hereditary diseases as causes of blindness in Newfoundland: preliminary report", Canadian journal of ophthalmology.Journal canadien d'ophtalmologie, vol. 18, no. 6, pp. 281-284.

Green, J.S., Parfrey, P.S., Harnett, J.D., Farid, N.R., Cramer, B.C., Johnson, G., Heath, O., McManamon, P.J., O'Leary, E. & Pryse-Phillips, W. 1989, "The cardinal manifestations of Bardet-Biedl syndrome, a form of Laurence-Moon-Biedl syndrome", The New England journal of medicine, vol. 321, no. 15, pp. 1002-1009.

Grosse, S.D. & Khoury, M.J. 2006, "What is the clinical utility of genetic testing", .

Haji Abdollahi, S. & Hirose, T. 2013, "Stargardt-Fundus flavimaculatus: recent advancements and treatment", Seminars in ophthalmology, vol. 28, no. 5-6, pp. 372-376.

Han, Z., Conley, S.M., Makkia, R.S., Cooper, M.J. & Naash, M.I. 2012, "DNA nanoparticle-mediated ABCA4 delivery rescues Stargardt dystrophy in mice", The Journal of clinical investigation, vol. 122, no. 9, pp. 3221-3226.

Han, Z., Conley, S.M. & Naash, M.I. 2014, "Gene therapy for Stargardt disease associated with ABCA4 gene", Advances in Experimental Medicine and Biology, vol. 801, pp. 719-724.

Handcock, G. 2000, , Heritage Newfoundland and Labrador. Available: http://www.heritage.nf.ca/articles/society/settlement.php [2016, .

Heathfield, L., Lacerda, M., Nossek, C., Roberts, L. & Ramesar, R.S. 2013, "Stargardt disease: towards developing a model to predict phenotype", European journal of human genetics : EJHG, vol. 21, no. 10, pp. 1173-1176.

Itabashi, R., Katsumi, O., Mehta, M.C., Wajima, R., Tamai, M. & Hirose, T. 1993, "Stargardt's disease/fundus flavimaculatus: psychophysical and electrophysiologic results", Graefe's archive for clinical and experimental ophthalmology = Albrecht

von Graefes Archiv fur klinische und experimentelle Ophthalmologie, vol. 231, no. 10, pp. 555-562.

Jaakson, K., Zernant, J., Külm, M., Hutchinson, A., Tonisson, N., Glavač, D., Ravnik-Glavač, M., Hawlina, M., Meltzer, M. & Caruso, R. 2003, "Genotyping microarray (gene chip) for the ABCR (ABCA4) gene", Human mutation, vol. 22, no. 5, pp. 395-403.

Jager, R.D., Mieler, W.F. & Miller, J.W. 2008, "Age-related macular degeneration", The New England journal of medicine, vol. 358, no. 24, pp. 2606-2617.

Jansen, P.L., Strautnieks, S.S., Jacquemin, E., Hadchouel, M., Sokal, E.M., Hooiveld, G.J., Koning, J.H., De Jager-Krikken, A., Kuipers, F., Stellaard, F., Bijleveld, C.M., Gouw, A., Van Goor, H., Thompson, R.J. & Muller, M. 1999, "Hepatocanalicular bile salt export pump deficiency in patients with progressive familial intrahepatic cholestasis", Gastroenterology, vol. 117, no. 6, pp. 1370-1379.

Kaminski, W.E., Piehler, A. & Wenzel, J.J. 2006, "ABC A-subfamily transporters: structure, function and disease", Biochimica et biophysica acta, vol. 1762, no. 5, pp. 510-524.

Kaplan, J., Gerber, S., Larget-Piet, D., Rozet, J.M., Dollfus, H., Dufier, J.L., Odent, S., Postel-Vinay, A., Janin, N. & Briard, M.L. 1993, "A gene for Stargardt's disease (fundus flavimaculatus) maps to the short arm of chromosome 1", Nature genetics, vol. 5, no. 3, pp. 308-311.

Karvonen, M., Viik-Kajander, M., Moltchanova, E., Libman, I., LaPorte, R. & Tuomilehto, J. 2000, "Incidence of childhood type 1 diabetes worldwide. Diabetes Mondiale (DiaMond) Project Group", Diabetes care, vol. 23, no. 10, pp. 1516-1526.

Klevering, B.J., Deutman, A.F., Maugeri, A., Cremers, F.P. & Hoyng, C.B. 2005, "The spectrum of retinal phenotypes caused by mutations in the ABCA4 gene", Graefe's archive for clinical and experimental ophthalmology = Albrecht von Graefes Archiv fur klinische und experimentelle Ophthalmologie, vol. 243, no. 2, pp. 90-100.

Klien, B.A. & Krill, A.E. 1967, "Fundus flavimaculatus. Clinical, functional and histopathologic observations", American Journal of Ophthalmology, vol. 64, no. 1, pp. 3-23.

Klugbauer, N. & Hofmann, F. 1996, "Primary structure of a novel ABC transporter with a chromosomal localization on the band encoding the multidrug resistance-associated protein", FEBS letters, vol. 391, no. 1-2, pp. 61-65.

Kristoffersson, U., Schmidtke, J. & Cassiman, J. 2010, Quality issues in clinical genetic services, Springer.

Lambertus, S., van Huet, R.A., Bax, N.M., Hoefsloot, L.H., Cremers, F.P., Boon, C.J., Klevering, B.J. & Hoyng, C.B. 2015, "Early-onset stargardt disease: phenotypic and genotypic characteristics", Ophthalmology, vol. 122, no. 2, pp. 335-344.

Lois, N., Holder, G.E., Bunce, C., Fitzke, F.W. & Bird, A.C. 2001, "Phenotypic subtypes of Stargardt macular dystrophy-fundus flavimaculatus", Archives of ophthalmology (Chicago, Ill.: 1960), vol. 119, no. 3, pp. 359-369.

Luciani, M.F., Denizot, F., Savary, S., Mattei, M.G. & Chimini, G. 1994, "Cloning of two novel ABC transporters mapping on human chromosome 9", Genomics, vol. 21, no. 1, pp. 150-159.

Maeda, A., Golczak, M., Chen, Y., Okano, K., Kohno, H., Shiose, S., Ishikawa, K., Harte, W., Palczewska, G., Maeda, T. & Palczewski, K. 2011, "Primary amines protect against retinal degeneration in mouse models of retinopathies", Nature chemical biology, vol. 8, no. 2, pp. 170-178.

Mannion, J.J. 1977, "The Peopling of Newfoundland: essays in historical geography", .

Mantyjarvi, M. & Tuppurainen, K. 1992, "Color vision in Stargardt's disease", International ophthalmology, vol. 16, no. 6, pp. 423-428.

Mardis, E.R. 2008, "Next-generation DNA sequencing methods", Annu.Rev.Genomics Hum.Genet., vol. 9, pp. 387-402.

Martin, L.J., Crawford, M.H., Koertvelyessy, T., Keeping, D., Collins, M. & Huntsman, R. 2000, "The population structure of ten Newfoundland outports", Human biology, vol. 72, no. 6, pp. 997-1016.

Mattocks, C.J., Morris, M.A., Matthijs, G., Swinnen, E., Corveleyn, A., Dequeker, E., Muller, C.R., Pratt, V., Wallace, A. & EuroGentest Validation Group 2010, "A standardized framework for the validation and verification of clinical molecular genetic tests", European journal of human genetics : EJHG, vol. 18, no. 12, pp. 1276-1288.

Maugeri, A., Klevering, B.J., Rohrschneider, K., Blankenagel, A., Brunner, H.G., Deutman, A.F., Hoyng, C.B. & Cremers, F.P. 2000, "Mutations in the ABCA4 (ABCR) gene are the major cause of autosomal recessive cone-rod dystrophy", American Journal of Human Genetics, vol. 67, no. 4, pp. 960-966.

Maugeri, A., van Driel, M.A., van de Pol, D.J., Klevering, B.J., van Haren, F.J., Tijmes, N., Bergen, A.A., Rohrschneider, K., Blankenagel, A., Pinckers, A.J., Dahl, N., Brunner, H.G., Deutman, A.F., Hoyng, C.B. & Cremers, F.P. 1999, "The 2588G-->C mutation in the ABCR gene is a mild frequent founder mutation in the Western European population and allows the classification of ABCR mutations in patients with Stargardt disease", American Journal of Human Genetics, vol. 64, no. 4, pp. 1024-1035.

Meyer, K. & Ueland, P.M. 2011, "Use of matrix-assisted laser desorption/ionization time-of-flight mass spectrometry for multiplex genotyping", Advances in Clinical Chemistry, vol. 53, pp. 1-29.

Miller, S.A., Dykes, D.D. & Polesky, H.F. 1988, "A simple salting out procedure for extracting DNA from human nucleated cells", Nucleic acids research, vol. 16, no. 3, pp. 1215.

Miraglia, S., Godfrey, W., Yin, A.H., Atkins, K., Warnke, R., Holden, J.T., Bray, R.A., Waller, E.K. & Buck, D.W. 1997, "A novel five-transmembrane hematopoietic stem cell antigen: isolation, characterization, and molecular cloning", Blood, vol. 90, no. 12, pp. 5013-5021.

Molday, R.S. & Zhang, K. 2010, "Defective lipid transport and biosynthesis in recessive and dominant Stargardt macular degeneration", Progress in lipid research, vol. 49, no. 4, pp. 476-492.

Molday, R.S. & Moritz, O.L. 2015, "Photoreceptors at a glance", Journal of cell science, vol. 128, no. 22, pp. 4039-4045.

Montezuma, S.R., Sobrin, L. & Seddon, J.M. 2007, "Review of genetics in age related macular degeneration", Seminars in ophthalmology, vol. 22, no. 4, pp. 229-240.

Mosser, J., Douar, A.M., Sarde, C.O., Kioschis, P., Feil, R., Moser, H., Poustka, A.M., Mandel, J.L. & Aubourg, P. 1993, "Putative X-linked adrenoleukodystrophy gene shares unexpected homology with ABC transporters", Nature, vol. 361, no. 6414, pp. 726-730.

National Human Genome Research Insititue 03/2012, , **Task Force Makes Final Recommendations on U.S. Genetic Testing**. Available: https://www.genome.gov/10000667/1997-release-task-force-makes-final-recommendations-on-us-genetic-testing/#top07/2016].

Nentwich, M.M. & Rudolph, G. 2013, "Hereditary retinal eye diseases in childhood and youth affecting the central retina", Oman journal of ophthalmology, vol. 6, no. Suppl 1, pp. S18-25.

Noble, K.G. & Carr, R.E. 1979, "Stargardt's disease and fundus flavimaculatus", Archives of ophthalmology (Chicago, Ill.: 1960), vol. 97, no. 7, pp. 1281-1285.

Oldani, M., Marchi, S., Giani, A., Cecchin, S., Rigoni, E., Persi, A., Podavini, D., Guerrini, A., Nervegna, A., Staurenghi, G. & Bertelli, M. 2012, "Clinical and molecular genetic study of 12 Italian families with autosomal recessive Stargardt disease", Genetics and molecular research : GMR, vol. 11, no. 4, pp. 4342-4350.

Papermaster, D.S., Reilly, P. & Schneider, B.G. 1982, "Cone lamellae and red and green rod outer segment disks contain a large intrinsic membrane protein on their

margins: an ultrastructural immunocytochemical study of frog retinas", Vision research, vol. 22, no. 12, pp. 1417-1428.

Pope, A.M., Carr, S.M., Smith, K.N. & Marshall, H.D. 2011, "Mitogenomic and microsatellite variation in descendants of the founder population of Newfoundland: high genetic diversity in an historically isolated population", Genome / National Research Council Canada = Genome / Conseil national de recherches Canada, vol. 54, no. 2, pp. 110-119.

Quellec, G., Russell, S.R., Scheetz, T.E., Stone, E.M. & Abramoff, M.D. 2011, "Computational quantification of complex fundus phenotypes in age-related macular degeneration and Stargardt disease", Investigative ophthalmology & visual science, vol. 52, no. 6, pp. 2976-2981.

Radu, R.A., Mata, N.L., Nusinowitz, S., Liu, X., Sieving, P.A. & Travis, G.H. 2003, "Treatment with isotretinoin inhibits lipofuscin accumulation in a mouse model of recessive Stargardt's macular degeneration", Proceedings of the National Academy of Sciences of the United States of America, vol. 100, no. 8, pp. 4742-4747.

Rahman, P., Jones, A., Curtis, J., Bartlett, S., Peddle, L., Fernandez, B.A. & Freimer, N.B. 2003, "The Newfoundland population: a unique resource for genetic investigation of complex diseases", Human molecular genetics, vol. 12 Spec No 2, pp. R167-72.

Rattner, A. & Nathans, J. 2006, "Macular degeneration: recent advances and therapeutic opportunities", Nature reviews.Neuroscience, vol. 7, no. 11, pp. 860-872.

Rekik, R. & Charfeddine, R. 2012, "Priminary observations of the effects of ACE inhibitor ramipril in patients with Stargardt's disease", Acta Ophthalmologica, vol. 90, no. s249, pp. 0-0.

Riordan, J.R., Rommens, J.M., Kerem, B., Alon, N., Rozmahel, R., Grzelczak, Z., Zielenski, J., Lok, S., Plavsic, N. & Chou, J.L. 1989, "Identification of the cystic fibrosis gene: cloning and characterization of complementary DNA", Science (New York, N.Y.), vol. 245, no. 4922, pp. 1066-1073.

Rivolta, C., Sharon, D., DeAngelis, M.M. & Dryja, T.P. 2002, "Retinitis pigmentosa and allied diseases: numerous diseases, genes, and inheritance patterns", Human molecular genetics, vol. 11, no. 10, pp. 1219-1227.

Roberts, L.J., Nossek, C.A., Greenberg, L.J. & Ramesar, R.S. 2012, "Stargardt macular dystrophy: common ABCA4 mutations in South Africa--establishment of a rapid genetic test and relating risk to patients", Molecular vision, vol. 18, pp. 280-289.

Rosenberg, T., Klie, F., Garred, P. & Schwartz, M. 2007, "N965S is a common ABCA4 variant in Stargardt-related retinopathies in the Danish population", Molecular vision, vol. 13, pp. 1962-1969.

Ryan, S.J., Schachat, A.P., Wilkinson, C.P., Hinton, D.R., Sadda, S.R. & Wiedemann, P. 2013, Retina, 5th edn, Elsevier, Toronto.

Sanger, F., Nicklen, S. & Coulson, A.R. 1977, "DNA sequencing with chain-terminating inhibitors", Proceedings of the National Academy of Sciences of the United States of America, vol. 74, no. 12, pp. 5463-5467.

Sangermano, R., Bax, N.M., Bauwens, M., van den Born, L.I., De Baere, E., Garanto, A., Collin, R.W., Goercharn-Ramlal, A.S., den Engelsman-van Dijk, A.H., Rohrschneider, K., Hoyng, C.B., Cremers, F.P. & Albert, S. 2016, "Photoreceptor Progenitor mRNA Analysis Reveals Exon Skipping Resulting from the ABCA4 c.5461-10T-->C Mutation in Stargardt Disease", Ophthalmology, vol. 123, no. 6, pp. 1375-1385.

Schwartz, S.D., Hubschman, J., Heilwell, G., Franco-Cardenas, V., Pan, C.K., Ostrick, R.M., Mickunas, E., Gay, R., Klimanskaya, I. & Lanza, R. 2012, "Embryonic stem cell trials for macular degeneration: a preliminary report", The Lancet, vol. 379, no. 9817, pp. 713-720.

Schwartz, S.D., Tan, G., Hosseini, H. & Nagiel, A. 2016, "Subretinal Transplantation of Embryonic Stem Cell-Derived Retinal Pigment Epithelium for the Treatment of Macular Degeneration: An Assessment at 4 Years", Investigative ophthalmology & visual science, vol. 57, no. 5, pp. ORSFc1-9.

Shroyer, N.F., Lewis, R.A., Yatsenko, A.N. & Lupski, J.R. 2001, "Null missense ABCR (ABCA4) mutations in a family with stargardt disease and retinitis pigmentosa", Investigative ophthalmology & visual science, vol. 42, no. 12, pp. 2757-2761.

Sohrab, M.A., Allikmets, R., Guarnaccia, M.M. & Smith, R.T. 2010, "Preimplantation genetic diagnosis for stargardt disease", American Journal of Ophthalmology, vol. 149, no. 4, pp. 651-655.e2.

Stargardt, K. 1909, "Über familiäre, progressive Degeneration in der Maculagegend des Auges", Graefe's Archive for Clinical and Experimental Ophthalmology, vol. 71, no. 3, pp. 534-550.

Sun, H. & Nathans, J. 1997, "Stargardt's ABCR is localized to the disc membrane of retinal rod outer segments", Nature genetics, vol. 17, no. 1, pp. 15-16.

Sundaram, V. 2014, Gene therapy for inherited retinal diseases, Ph.D. thesis, UCL (University College London).

Thomas, C.E., Ehrhardt, A. & Kay, M.A. 2003, "Progress and problems with the use of viral vectors for gene therapy", Nature Reviews Genetics, vol. 4, no. 5, pp. 346-358.

Trapani, I., Colella, P., Sommella, A., Iodice, C., Cesi, G., de Simone, S., Marrocco, E., Rossi, S., Giunti, M., Palfi, A., Farrar, G.J., Polishchuk, R. & Auricchio, A. 2014,

"Effective delivery of large genes to the retina by dual AAV vectors", EMBO molecular medicine, vol. 6, no. 2, pp. 194-211.

Valverde, D., Riveiro-Alvarez, R., Bernal, S., Jaakson, K., Baiget, M., Navarro, R. & Ayuso, C. 2006, "Microarray-based mutation analysis of the ABCA4 gene in Spanish patients with Stargardt disease: evidence of a prevalent mutated allele", Mol Vis, vol. 12, pp. 902-908.

Vinardell, M.P. & Infante, M.R. 1999, "The relationship between the chain length of non-ionic surfactants and their hemolytic action on human erythrocytes", Comparative biochemistry and physiology.Part C, Pharmacology, toxicology & endocrinology, vol. 124, no. 2, pp. 117-120.

Weleber, R.G. 1994, "Stargardt's macular dystrophy", Archives of ophthalmology (Chicago, Ill.: 1960), vol. 112, no. 6, pp. 752-754.

Weng, J., Mata, N.L., Azarian, S.M., Tzekov, R.T., Birch, D.G. & Travis, G.H. 1999, "Insights into the function of Rim protein in photoreceptors and etiology of Stargardt's disease from the phenotype in abcr knockout mice", Cell, vol. 98, no. 1, pp. 13-23.

Westerfeld, C. & Mukai, S. 2008, "Stargardt's disease and the ABCR gene", Seminars in ophthalmology, vol. 23, no. 1, pp. 59-65.

Woods, M.O., Hyde, A.J., Curtis, F.K., Stuckless, S., Green, J.S., Pollett, A.F., Robb, J.D., Green, R.C., Croitoru, M.E., Careen, A., Chaulk, J.A., Jegathesan, J., McLaughlin, J.R., Gallinger, S.S., Younghusband, H.B., Bapat, B.V. & Parfrey, P.S. 2005, "High frequency of hereditary colorectal cancer in Newfoundland likely involves novel susceptibility genes", Clinical cancer research : an official journal of the American Association for Cancer Research, vol. 11, no. 19 Pt 1, pp. 6853-6861.

Yu, D., Yu, P., Balaratnasingam, C., Cringle, S., Su, E., Méndez-Vilas, A. & Díaz, J. 2010, "Microscopic structure of the retina and vasculature in the human eye", Microscopy: Science, Technology, Applications and Education, , pp. 867-875.

Zernant, J., Collison, F.T., Lee, W., Fishman, G.A., Noupuu, K., Yuan, B., Cai, C., Lupski, J.R., Yannuzzi, L.A. & Tsang, S.H. 2014a, "Genetic and Clinical Analysis of ABCA4-Associated Disease in African American Patients", Human mutation, vol. 35, no. 10, pp. 1187-1194.

Zernant, J., Schubert, C., Im, K.M., Burke, T., Brown, C.M., Fishman, G.A., Tsang, S.H., Gouras, P., Dean, M. & Allikmets, R. 2011, "Analysis of the ABCA4 gene by next-generation sequencing", Investigative ophthalmology & visual science, vol. 52, no. 11, pp. 8479-8487.

Zernant, J., Xie, Y.A., Ayuso, C., Riveiro-Alvarez, R., Lopez-Martinez, M.A., Simonelli, F., Testa, F., Gorin, M.B., Strom, S.P., Bertelsen, M., Rosenberg, T., Boone, P.M.,

Yuan, B., Ayyagari, R., Nagy, P.L., Tsang, S.H., Gouras, P., Collison, F.T., Lupski, J.R., Fishman, G.A. & Allikmets, R. 2014b, "Analysis of the ABCA4 genomic locus in Stargardt disease", Human molecular genetics, vol. 23, no. 25, pp. 6797-6806.

Zhang, K., Kniazeva, M., Han, M., Li, W., Yu, Z., Yang, Z., Li, Y., Metzker, M.L., Allikmets, R., Zack, D.J., Kakuk, L.E., Lagali, P.S., Wong, P.W., MacDonald, I.M., Sieving, P.A., Figueroa, D.J., Austin, C.P., Gould, R.J., Ayyagari, R. & Petrukhin, K. 2001, "A 5-bp deletion in ELOVL4 is associated with two related forms of autosomal dominant macular dystrophy", Nature genetics, vol. 27, no. 1, pp. 89-93.

APPENDIX A.

Table 0.1. Genomic location of pathogenic variants included in the custom LDT panel with coding sequences and corresponding FASTA format and SNV "rs" identification numbers

Genomic location	rs number
NM_000350.2(ABCA4):c.5714+5G>A	rs61751407
NM_000350.2(ABCA4):c.5461-10T>C	rs1800728
NM_000350.2(ABCA4):c.4163T>C	rs61750131
NM_000350.2(ABCA4):c.2564G>A	rs61752406
NM_000350.2(ABCA4):c.4139C>T	rs61750130
NM_000350.2(ABCA4):c.3322C>T	rs61750120
NM_000350.2(ABCA4):c.4577C>T	rs61750152
NM_000350.2(ABCA4):c.1522C>T	rs138157885
NM_000350.2(ABCA4):c.4469G>A	rs61751402
NM_000350.2(ABCA4):c.3323G>A	rs61750121
NM_000350.2(ABCA4):c.634C>T	rs61750200
NM_000350.2(ABCA4):c.6449G>A	rs61751384
NM_000350.2(ABCA4):c.6089G>A	rs61750641
NM_000350.2(ABCA4):c.3064G>A	rs61749459
NM_000350.2(ABCA4):c.4222T>C	rs61750135
NM_000350.2(ABCA4):c.4918C>T	rs61751404
NM_000350.2(ABCA4):c.455G>A	rs62646862
NM_000350.2(ABCA4):c.2588G>C	rs76157638
NM_000350.2(ABCA4):c.67-1delG	FASTA sequence
NM_000350.2(ABCA4):c.4537delC	FASTA sequence

Table 0.2. Spotting settings under Method section selected for the Nanodispenser.

	Aspirate	Dispense
Time	5 (sec)	0.2(sec)
Offset	6.75(mm)	1(mm)
Speed	60(mm/sec)	100(sec/mm)

	Calibrant
Dipense/aspirate	1
Dispense speed	150

Table 0.3. Forward and reverse primer sequences for Sanger sequencing the 16 exons in the LDT panels.

Exon	Forward primer sequence	Reverse primer sequence	Annealing Temperature (°C)
2	GTCTGCTCTGGTTACGTTTTC	TCTAGACAAAAGGCCCAGAC	55
5	GCTGTTTTCCTTTTTTTGACCC	ATATTTCTTGCCTTTCTCAGG	54
5*	ACTGGCAAGAGCCTCACCT	TCTGAATGTGAACACAAGGAAGA	54
6	TTAGGACGTGGGTGTCTTTC	TCGTGAGGCTCTGCTACC	55
11	GGCTGAAGAACAAGACCAAAG	CTTGCTAAGGGAGCTCTGG	56
16	CTGGGTGCTGTTGCATTG	ATGAATGGAGAGGGCTGG	55
21	TCTGTAAGATCAGCTGCTGG	CTGGGTGCACTGGGGAG	60
22	TCCTCACCCTCCACAGCC	CTAGGGCTGCAGTGAGAGC	62
22*	CTAAGAGGCAGCACCAAACC	TTGGGAAGTAGGTTGCATCA	60
28	CGCACGTGTGACATCT	GTGCCCCAAACCCACAG	58

	CC		
30	CCTAGGGATTTGTCAGCAAC	CTCCCCTAGTCCCTCTGTG	55
31	AAGACAACAAGCAGTTTCAC	TTATCTTCTGTCCCTAGTTAATATC	54
35	TTCCTTCACTGATTTCTGCTTT	CTCAGGATGTTCAAAGAGTGG	55
39	GTTTGCCCCGTTTCCAAC	CCCTCCCAGCTTTGGAC	54
39*	ATGCTCTGCTGGACAAATCC	GAGGCACCCTAATCCTCTCC	54
40	TAGTGGGCCCTGTGCTGT	GCTCCTGAGGAAAGAAATGACC	60
44	GCCCTAGCTCTATGGTCATC	GCACTCTCATGAAACAGGC	55
47	AGAGATTCCCAGGGCTGG	TCAATGGAGAACACAGGATCC	60

*The redesigned primers for exon 5, 22 and 39 are indicated with an asterisk.

Table 0.4. SNVs rejected and the reason for the rejection.

rs61749459	Rejected [244] - High dimer potential (29.09) for reverse extend primer. High hairpin potential (32.60) for forward extend primer.
ABCA4_4537delC	Rejected [242] - High hairpin potential (51.36) for forward extend primer. GGGGGG sequence blocks reverse extend primer design.
rs138157885	Rejected [244] - High dimer potential (4.52) for reverse extend primer. High hairpin potential (3.60) for forward extend primer

Table 0.5. Details of design settings with 3 rejects for rs61749459, ABCA4_delC and rs138157885.

Allow INDEL/MNP strand design	Yes	**Minimum EP binding Tm**	45
Allow multiSnp strand design	Yes	**Mplex Amp.Len.Var.**	ScrWt = 1
Allowed Spacer Masses	138.1(#)	**Mplex Ave.Amp.**	ScrWt = 1
Amp. Length	ScrWt = 1	**Mplex B.Score Dev.**	Max = 40

Amplicon design score cutoffs (u/m-plex)	0.3, 0.4	**Mplex FP**	ScrWt = 2
Amplicon length control	80, 100, 120	**Mplex PCRP Tm.Var.**	ScrWt = 1
Analyte/probe peak separation	30, 0	**Mplex PDimer**	ScrWt = 2
Annotation type	Scan and Restrict	**Mplex Repass Base**	Max = 60
Assay Type	SBE	**Multiplexing**	12, 1
By-product mass offsets	none	**Mutant allele occlusion control**	Optimize
Contaminant peaks	none	**PCRP FPrime**	ScrWt = 100
EP FPrime	ScrWt = 100	**PCRP Hp/D**	ScrWt = 10, w/Tags = No
EP GC Content	ScrWt = 1	**PCRP Hyb.Tm**	Min = 50, Opt = 60, Max = 80, ScrWt = 1
EP Hp/D	ScrWt = 10	**PCRP LCase**	ScrWt = 1
EP Seq.Gs	Max = 6, ScrWt = 1	**PCRP Length**	Min = 18, Opt = 20, Max = 24, ScrWt = 1
EP/1stByprod. Sep.	ScrWt = 1	**PCRP PDimer**	ScrWt = 1
Extend pausing code	-1	**PCRP Pc GC**	Min = 0, Opt = 50, Max = 100, ScrWt = 1
Extend primer score cutoff (uniplex)	0.4	**PCRP Seq.Gs**	Max = 6, ScrWt = 1
Ignore dimers during exchange PDC	No	**Primer Tags**	ACGTTGGATG (1), ACGTTGGATG (2)
MBE EP Extend	Max = 3, ScrWt = 1	**Primer-dimer control**	Min Exc Dist = 10, Min Tm Exceed = 0
MSNP Forced EP Length	Min = 15, ScrWt = 1	**Report verbosity**	Detailed
Mass window	4300.0 - 9000.0	**SNP Set Representation**	Once per Run
Max alleles/SNP	4	**Stop Mix**	iPLEX
Max. EP length	30	**Tm Calculation method**	Nearest Neighbor (NN.)
Maximum EP binding Tm	100	**Use exchange replexing**	Yes, 0, No

Maximum Non-templated extend primer	5, 0, 15, 1	**numOfIter**	1
Min. EP length	15	**selectionCriteria**	0

Table 0.6. Details of settings required to remove rejects in the assay design.

Allow INDEL/MNP strand design	Yes	**Minimum EP binding Tm**	45
Allow multiSnp strand design	Yes	**Mplex Amp.Len.Var.**	ScrWt = 1
Allowed Spacer Masses	138.1(#)	**Mplex Ave.Amp.**	ScrWt = 1
Amp. Length	ScrWt = 1	**Mplex B.Score Dev.**	Max = 40
Amplicon design score cutoffs (u/m-plex)	0.3, 0.0	**Mplex FP**	ScrWt = 2
Amplicon length control	80, 100, 700	**Mplex PCRP Tm.Var.**	ScrWt = 1
Analyte/probe peak separation	30, 0	**Mplex PDimer**	ScrWt = 2
Annotation type	Scan and Restrict	**Mplex Repass Base**	Max = 60
Assay Type	SBE	**Multiplexing**	20, 1
By-product mass offsets	none	**Mutant allele occlusion control**	Optimize
Contaminant peaks	none	**PCRP FPrime**	ScrWt = 100
EP FPrime	ScrWt = 0.5	**PCRP Hp/D**	ScrWt = 10, w/Tags = No
EP GC Content	ScrWt = 1	**PCRP Hyb.Tm**	Min = 50, Opt = 60, Max = 80, ScrWt = 1
EP Hp/D	ScrWt = 0.6	**PCRP LCase**	ScrWt = 1
EP Seq.Gs	Max = 10, ScrWt = 0	**PCRP Length**	Min = 18, Opt = 20, Max = 24, ScrWt = 1
EP/1stByprod. Sep.	ScrWt = 1	**PCRP PDimer**	ScrWt = 1
Extend pausing code	-1	**PCRP Pc GC**	Min = 0, Opt = 50, Max = 100, ScrWt = 1
Extend primer score cutoff (uniplex)	0.4	**PCRP Seq.Gs**	Max = 9, ScrWt = 0
Ignore dimers during exchange PDC	No	**Primer Tags**	ACGTTGGATG(1), ACGTTGGATG(2)
MBE EP Extend	Max = 3, ScrWt = 1	**Primer-dimer control**	Min Exc Dist = 10, Min Tm Exceed = 0
MSNP Forced EP Length	Min = 15,	**Report verbosity**	Detailed

	ScrWt = 1		
Mass window	4300.0 - 9000.0	**SNP Set Representation**	Once per Run
Max alleles/SNP	4	**Stop Mix**	iPLEX
Max. EP length	30	**Tm Calculation method**	Nearest Neighbor (NN.)
Maximum EP binding Tm	100	**Use exchange replexing**	Yes, 0, No
Maximum Non-templated extend primer	5, 0, 15, 1	**numOfIter**	1
Min. EP length	15	**selectionCriteria**	0

The main attributes that were changed in the settings are as follow: 1) the amplicon length control; 2) the stringency of the false priming, dimer potential, hair pin potential, number of sequential G's and overall cut-off for extension primers; and 3) the number of sequential G's for PCR primers were changed.

Table 0.7. Details of the 2x10-plex LDT panel design.

Multiplexing	10, 1	**Primer-dimer control**	Min Exc Dist = 10, Min Tm Exceed = 0
Max alleles/SNP	4	**PCRP Length**	Min = 18, Opt = 20, Max = 24, ScrWt = 1
Allow multiSnp strand design	Yes	**PCRP Hyb.Tm**	Min = 50, Opt = 60, Max = 80, ScrWt = 1
Allow INDEL/MNP strand design	Yes	**PCRP Pc GC**	Min = 0, Opt = 50, Max = 100, ScrWt = 1
Mutant allele occulsion control	Optimize	**PCRP Seq.Gs**	Max = 6, ScrWt = 1
Annotation type	Scan and Restrict	**PCRP LCase**	ScrWt = 1
SNP Set Representation	Once per Run	**PCRP FPrime**	ScrWt = 100
Use exchange replexing	Yes, 0, No	**PCRP Hp/D**	ScrWt = 100, w/Tags = No
Report verbosity	Detailed	**PCRP PDimer**	ScrWt = 1
Amplicon length control	50, 100, 1000	**Amp. Length**	ScrWt = 1

Amplicon design score cutoffs (u/m-plex)	0.3, 0.4	**MBE EP Extend**	Max = 3, ScrWt = 1
Primer Tags	ACGTTGGATG(1), ACGTTGGATG(2)	**MSNP Forced EP Length**	Min = 15, ScrWt = 1
Min. EP length = 17	Max. EP length = 30	**EP Seq.Gs**	Max = 8, ScrWt = 0
Analyte/probe peak separation	30, 10	**EP/1stByprod. Sep.**	ScrWt = 1
Peak mass shifts	-78.0(termination), -62.0(pausing)	**EP GC Content**	ScrWt = 0
Tm Calculation method	Nearest Neighbor (NN.)	**EP FPrime**	ScrWt = 1
Minimum EP binding Tm	45	**EP Hp/D**	ScrWt = 0.5
Maximum EP binding Tm	100	**Mplex FP**	ScrWt = 0
Maximum Non-templated extend primer	0, 0, 15, 0	**Mplex PDimer**	ScrWt = 0
Extend primer score cutoff (uniplex)	0.4	**Mplex Amp.Len.Var.**	ScrWt = 1
Contaminant peaks	none	**Mplex PCRP Tm.Var.**	ScrWt = 1
Mass window	4500.0 - 8500.0	**Mplex Ave.Amp.**	ScrWt = 1
Extend pausing code	-1	**Mplex Repass Base**	Max = 60
By-product mass offsets	none	**Mplex B.Score Dev.**	Max = 40

The main attributes that were changed in the settings are as follows: 1) change the multiplex level to 10; 2) change the amplicon length control; 3) change the stringency of the number of sequential G's , GC content and hairpin dimer for extension primers; and 4)change the stringency of multiplex primer dimer.

Table 0.8. PCR primer pairs for well#1 of the 2x10-plex LDT panel.

SNP ID	Forward PCR	Reverse PCR	Uniplex confidence score

rs61751404	TGGCTAATGACG GTGATTCC	TTCTCAATGTGGC CCACAAC	86.20%
rs76157638	ATAGGGAGACTC CTTCGACT	GAAAGTACCAAGG AAGTGGG	100.00%
ABCA4_67-1delG	CTTAGCACCACT GAACTTTC	GATAAAGGCCACA CGAGTTC	86.20%
rs61750120	AGACTGAGCAGC AGCTGTTA	CTTACTCGAGACG CTCAATC	93.80%
rs1800728	GAAGACAATGAG CAGCTTCC	TTGCCCCGTTTCC AACAGTC	88.10%
rs61751407	CAGCGCCACTTC TTCCTCT	GTGGGTATAAGGT CCAGTTC	86.20%
rs138157885	AGGTATTGATTG ACCAGGCG	CTGACGACATGGC CAACTTC	99.70%
rs61751402	CAGGTCAACCCT TCACCATC	CCCGTTGTTTGGA GGTCAG	97.90%
rs62646862	ATTTCCCCTTCAA CACCCTG	AGTGTCAGTGTTT CTTCATC	99.90%
rs61751384	AATGTGAGGCAC TGTGTACC	CACCATCTGCTTA CTTGGAC	97.00%

Table 0.9. PCR primer pairs for well#2 of the 2x10-plex LDT panel.

SNP ID	Forward PCR	Reverse PCR	Uniplex confidence score
rs61750135	AAGAAGGTGTAC TGCTGCCC	GTCTATTCTCCCA CAGATCG	86.20%
rs61749459	CTAAGCCACTGC TTTTCTCG	CTTTCAGCTGGGC ATAGAAC	100.00%
rs61750130	AAGAAGGTGTAC TGCTGCCC	GTCTATTCTCCCA CAGATCG	86.20%
rs61750200	TGCAGTTCGCTC ATGGAGTC	GCGTCTCTGGCTG AAGATGA	93.80%
ABCA4_4537delC	CCCGTTGTTTGG AGGTCAG	CAGGTCAACCCTT CACCATC	88.10%
rs61750131	AAGAAGGTGTAC TGCTGCCC	GTCTATTCTCCCA CAGATCG	86.20%
rs61750152	CCAAGAAGTCGG AGATGTTC	TAACGTGGGTGTC TCATTGC	99.70%
rs61750641	TACTGTCCTCAG TTTGATGC	TTCTTCTGCTGGT ACACCTC	97.90%
rs61752406	TACCCTATAGAG	TGCTGCTGTCTAT	99.90%

	GAGGATGC	GGCTTAC	
rs61750121	CTTACTCGAGAC GCTCAATC	AGACTGAGCAGCA GCTGTTA	97.00%

Table 0.10. Extension primers for well#1 of the 2x10-plex panel.

SNP ID	UEP Direction	UEP Sequence	Alternative Alleles		Uniplex confidence Score
rs61751404	F17	CCCACAACGC CATCTTA	C(C)	T(T)	100.00%
rs76157638	F17	GTGGGGTTCC ATAGTCT	C(C)	G(G)	97.50%
ABCA4_67-1delG	R18	TTCCACCACA AAGCGAAT	C(G)	T(DEL)	99.40%
rs61750120	F19	GGATCTGCTC CTGAAGTAT	C(C)	T(T)	99.50%
rs1800728	F20	GTTTCCAACA GTCCTACTTC	C(C)	T(T)	98.50%
rs61751407	R21	TGGCCCAGGG TGTGGCATGG A	C(G)	T(A)	96.00%
rs138157885	R22	GGACATATTTA ACATCACTGA T	C(G)	T(A)	95.00%
rs61751402	R22	GGTGAGCTTC TCCCTGGTGC TG	C(G)	T(A)	90.80%
rs62646862	R23	CATCTTTCAAG ATATCCCTTAT T	C(G)	T(A)	100.00%
rs61751384	R24	TTGAGATGCT GAATGGTGCC CATA	C(G)	T(A)	97.10%

Table 0.11. Extension primers for well#2 of the 2x10-plex LDT panel.

SNP ID	UEP Direction	UEP Sequence	Alternative Alleles	Uniplex confidence Score

rs61750135	F17	CTTTGACCC TTCACCCC	C(C)	T(T)		90.30%
rs61749459	R17	ATAGAACAG CATGTGCT	C(G)	T(A)		86.90%
rs61750130	F18	TCCCACAGA TCGTGCTCC	C(C)	T(T)		99.40%
rs61750200	R18	GGCTGAAGA TGATGAAGC	A(T)	G(C)		84.20%
ABCA4_453 7delC	F19	CGGGGGCCT CCCGCCCCC C	C(C)	A(DEL)		54.40%
rs61750131	F19	ACCTTTGTGT TTTTGGCTC	C(C)	T(T)		99.50%
rs61750152	F20	GGAAATTCT ACAAGACCT GA	C(C)	T(T)		100.00%
rs61750641	R21	GCATAAAGG TAAAGATGTT CT	C(G)	T(A)		66.70%
rs61752406	F22	GCTGTCTAT GGCTTACTC GCTT	A(A)	G(G)		82.70%
rs61750121	R22	TGAGCAGCA GCTGTTACC TGAG	C(G)	A(T)	T(A)	76.40%

Table 0.12. Details of warnings in both well#1 and well#2 of 2x10-plex LDT panel

SNP ID	Warning description
*Well#1	
rs76157638	(g) extend primer contains a GGGG sequence
*Well#2	
rs61749459	(h) extend primer has weak extend self-dimer potential
ABCA4_4537del C	(s) extend primer has weak false priming potential (0.261) with it's own amplicon
	(G) extend primer contains a GGGGG sequence
	(h) extend primer has weak extend hairpin potential (0.390)
rs61750641	(s) extend primer has weak false priming potential (0.289) with it's own amplicon

*letters in the parenthesis are the software codes for each warning

Table 0.13. Summary of validation hits for both well#1 and well#2 of the 2x10-plex LDT panel.

WELL	SNP ID	H.TRUE	H.FALSE	H.NULL	H.PCR2	H.PCR1
W1	rs76157638	1	0	0	108	14
W1	rs61751404	1	0	0	35	18
W1	rs62646862	1	0	0	210	87
W1	ABCA4_67-1delG	1	0	0	20	68
W1	rs61751407	1	0	0	28	117
W1	rs138157885	1	0	0	23	12
W1	rs1800728	1	0	0	31	97
W1	rs61751384	1	0	0	34	44
W1	rs61750120	1	0	0	2	77
W1	rs61751402	1	0	0	61	58
W2	rs61749459	1	0	0	43	15
W2	rs61750641	1	0	0	38	41
W2	rs61752406	1	0	0	29	46
W2	rs61750152	1	0	0	49	18
W2	rs61750200	1	0	0	122	5
W2	rs61750130	1	0	0	15	39
W2	ABCA4_4537delC	1	0	0	58	61
W2	rs61750131	1	0	0	15	39
W2	rs61750135	1	0	0	15	39
W2	rs61750121	1	0	0	77	2

Table 0.14. Details of design settings with Typer4 for the 1x20-plex LDT panel.

Multiplexing:	50, 1	Primer-dimer control:	Min Exc Dist = 10, Min Tm Exceed = 0
Max alleles/SNP:	4	PCRP Length:	Min = 18, Opt = 20, Max = 24, ScrWt = 1
Allow multiSnp strand design:	Yes	PCRP Hyb.Tm:	Min = 50, Opt = 60, Max = 80, ScrWt = 1
Allow INDEL/MNP	Yes	PCRP Pc GC:	Min = 0, Opt =

strand design:			50, Max = 100, ScrWt = 1
Mutant allele occulsion control:	Optimize	PCRP Seq.Gs:	Max = 6, ScrWt = 1
Annotation type:	Scan and Restrict	PCRP LCase:	ScrWt = 1
SNP Set Representation:	Once per Run	PCRP FPrime:	ScrWt = 100
Use exchange replexing:	Yes, 0, No	PCRP Hp/D:	ScrWt = 100, w/Tags = No
Report verbosity:	Detailed	PCRP PDimer:	ScrWt = 1
Amplicon length control:	50, 100, 1000	Amp. Length:	ScrWt = 1
Amplicon design score cutoffs (u/m-plex):	0.3, 0.4	MBE EP Extend:	Max = 3, ScrWt = 1
Primer Tags:	ACGTTGGATG(1), ACGTTGGATG(2)	MSNP Forced EP Length:	Min = 15, ScrWt = 1
Min. EP length =	15, Max. EP length = 30	EP Seq.Gs:	Max = 8, ScrWt = 0
Analyte/probe peak separation:	30, 0	EP/1stByprod. Sep.:	ScrWt = 1
Peak mass shifts:	-78.0(termination), -62.0(pausing)	EP GC Content:	ScrWt = 0
Tm Calculation method:	Nearest Neighbor (NN.)	EP FPrime	ScrWt = 1
Minimum EP binding Tm:	45	EP Hp/D	ScrWt = 1
Maximum EP binding Tm:	100	Mplex FP	ScrWt = 0
Maximum Non-templated extend primer:	5, 0, 15, 1	Mplex PDimer	ScrWt = 0
Extend primer score cutoff (uniplex):	0.4	Mplex Amp.Len.Var.	ScrWt = 1
Contaminant peaks:	none	Mplex PCRP Tm.Var.	ScrWt = 1
Mass window:	4300.0 - 9000.0	Mplex Ave.Amp.	ScrWt = 1
Extend pausing code:	-1	Mplex Repass Base	Max = 60
By-product mass offsets:	none	Mplex B.Score Dev.	Max = 40

The main attributes that were changed in the settings are as follow: 1) change the multiplex level to 50; and 2) change the stringency of the primer hairpin for extension primers.

Table 0.15. PCR primer pairs for the design with Typer4 for the 1x20-plex LDT panel.

SNP ID	Forward PCR	Reverse PCR	Uniplex confidence score
ABCA4_4537 delC	CCCGTTGTTTGG AGGTCAG	CAGGTCAACCCTTC ACCATC	88.10%
rs61750130	AAGAAGGTGTAC TGCTGCCC	GTCTATTCTCCCAC AGATCG	86.20%
rs61751384	AATGTGAGGCA CTGTGTACC	CACCATCTGCTTAC TTGGAC	98.60%
rs61751407	CAGCGCCACTT CTTCCTCT	GTGGGTATAAGGTC CAGTTC	94.00%
rs1800728	GAAGACAATGA GCAGCTTCC	TTGCCCCGTTTCCA ACAGTC	98.50%
rs61750131	AAGAAGGTGTAC TGCTGCCC	GTCTATTCTCCCAC AGATCG	86.20%
rs61750120	AGACTGAGCAG CAGCTGTTA	CTTACTCGAGACGC TCAATC	97.00%
rs61750200	TGCAGTTCGCTC ATGGAGTC	GCGTCTCTGGCTGA AGATGA	93.80%
rs61751404	TGGCTAATGACG GTGATTCC	TTCTCAATGTGGCC CACAAC	99.70%
rs61750135	AAGAAGGTGTAC TGCTGCCC	GTCTATTCTCCCAC AGATCG	86.20%
rs61751402	CAGGTCAACCCT TCACCATC	CCCGTTGTTTGGAG GTCAG	88.10%
rs61750152	CCAAGAAGTCG GAGATGTTC	TAACGTGGGTGTCT CATTGC	99.70%
ABCA4_67-1delG	CTTAGCACCACT GAACTTTC	GATAAAGGCCACAC GAGTTC	98.60%
rs76157638	ATAGGGAGACT CCTTCGACT	GAAAGTACCAAGGA AGTGGG	98.70%
rs61752406	TACCCTATAGAG GAGGATGC	TGCTGCTGTCTATG GCTTAC	99.90%
rs61750641	TTCTTCTGCTGG TACACCTC	TACTGTCCTCAGTTT GATGC	97.90%
rs62646862	ATTTCCCCTTCA ACACCCTG	AGTGTCAGTGTTTC TTCATC	93.50%
rs61750121	CTTACTCGAGAC GCTCAATC	AGACTGAGCAGCAG CTGTTA	97.00%
rs138157885	AGGTATTGATTG ACCAGGCG	CTGACGACATGGCC AACTTC	98.60%

rs61749459*	CTTTCAGCTGGG CATAGAAC	CTAAGCCACTGCTT TTCTCG	100.00%

*rs61749459 separately designed and manually forced into the 19-plex well creating a 20-plex well design.

Table 0.16. Details of warnings for the design with Typer4 for the 1x20-plex LDT panel.

SNP ID	Warning description
rs61750200	(H) extend primer has moderate extend hairpin potential
rs76157638	(g) extend primer contains a GGGG sequence
rs138157885	(H) extend primer has moderate extend self-dimer potential

Table 0.17. UEP for the design with Typer4 for the 1x20-plex LDT panel.

SNP ID	UEP Direction	UEP Sequence	Alternative Alleles			Uniplex confidence Score
ABCA4_4537delC	F15	GGCCTCCCGCCCCCC	C(C)	A(DEL)		58.80%
rs61750130	F15	CACAGATCGTGCTCC	C(C)	T(T)		100.00%
rs61751384	R16	CTGAATGGTGCCCATA	C(G)	T(A)		100.00%
rs61751407	R15	aAGGGTGTGGCATGGA	C(G)	T(A)		97.80%
rs1800728	F17	TCCAACAGTCCTACTTC	C(C)	T(T)		100.00%
rs61750131	F18	CCTTTGTGTTTTTGGCTC	C(C)	T(T)		100.00%
rs61750120	F18	GATCTGCTCCTGAAGTAT	C(C)	T(T)		100.00%
rs61750200	R17	tGCTGAAGATGATGAAGC	A(T)	G(C)		84.60%
rs61751404	F16	ccaCCACAACGCCATCTTA	C(C)	T(T)		100.00%
rs61750135	F16	ccgaTTTGACCCTTCACCCC	C(C)	T(T)		89.80%

rs61751402	R15	cgagaTTCTCCCTGGTGCTG	C(G)	T(A)		92.90%
rs61750152	F20	GGAAATTCTACAAGACCTGA	C(C)	T(T)		100.00%
ABCA4_67-1delG	R16	ccccgCCACCACAAAGCGAAT	C(G)	T(DEL)		100.00%
rs76157638	F17	ggacGTGGGGTTCCATAGTCT	C(C)	G(G)		96.90%
rs61752406	F17	ccttcCTATGGCTTACTCGCTT	A(A)	G(G)		84.60%
rs61750641	F18	ccttATGAGCTGCTCACAGGAC	A(A)	G(G)		83.20%
rs62646862	R23	CATCTTTCAAGATATCCCTTATT	C(G)	T(A)		100.00%
rs61750121	R19	ctgcGCAGCAGCTGTTACCTGAG	C(G)	A(T)	T(A)	77.00%
rs138157885	R25	GAGGGACATATTTAACATCACTGAT	C(G)	T(A)		80.50%
rs61749459*	F15	AGCCTCACGGTGGCT	A(A)	G(G)		70.80%

*Assay separately designed and manually forced into the 19-plex well creating a 1x20-plex LDT design.

Table 0.18. Comparison of spotting volumes with and without auto-tuning enabled.

	Autotuning enabled	**Autotuning disabled**
Minimum	7nl	4.3nl
Maximum	34.12nl	29.2nl
Mean	14.18781nl	14.67344nl
SD	5.056737	5.538645
SD Error	0.632092	0.692331
Lower 95% CI	12.92468	13.28993
Upper 95% CI	15.45095	16.05695

Table 0.19. Comparison of spotting volumes with and without Tween 20.

	With Tween 20	**Without Tween 20**
Minimum	6.5nl	4.3nl
Maximum	34.12nl	29.9nl
Mean	14.70813nl	14.15313nl

SD	5.605669	4.978652
SD Error	0.700709	0.622331
Lower 95% CI	13.30787	12.90949
Upper 95% CI	16.10838	15.39675

Table 0.20. Correlation of spotted volumes with the peak heights for homozygous alleles.

SNV id	Allele height	Volume		P-value
		<14 nl	>14 nl	
ABCA4_4537delC	>7	241	119	1
	<7	1	0	
ABCA4_67-1delG	>7	244	119	1
	<7	0	0	
rs138157885	>7	230	111	1
	<7	16	8	
rs1800728	>7	234	115	1
	<7	7	3	
rs61749459	>7	232	113	1
	<7	12	6	
rs61750120	>7	244	119	1
	<7	2	0	
rs61750121	>7	244	115	0.0913
	<7	2	4	
rs61750130	>7	241	117	0.60006
	<7	2	2	
rs61750131	>7	237	117	1
	<7	6	2	
rs61750135	>7	242	119	1
	<7	1	0	
rs61750152	>7	244	116	0.034
	<7	0	3	

rs61750200	>7	242	118	0.3296
	<7	0	1	
rs61750641	>7	243	119	1
	<7	0	0	
rs61751384	>7	242	119	0.2501
	<7	1	0	
rs61751402	>7	243	118	0.3287
	<7	0	1	
rs61751404	>7	244	119	1
	<7	0	0	
rs61751407	>7	241	116	0.1074
	<7	0	2	
rs61752406	>7	243	117	0.5996
	<7	2	2	
rs62646862	>7	243	116	0.325
	<7	0	1	
rs76157638	>7	238	116	1
	<7	1	0	

Table 0.21. Comparison of homozygous and heterozygous allele heights using the old and new EXT primers for the ABCA4_4537delC, rs61750131 and rs61751407 SNVs.

		Homozygous Allele Height		**Heterozygous Allele Heights**			
		Old extension primer mix	**New extension primer mix**	**Old extension primer mix**		**New extension primer mix**	
ABCA4_4537delC	MIN	1.1	5.0	2.1	1.7	6.5	5.2
	AVG	4.5	13.4				
rs61750131	MIN	1.5	3.3	0.7*	0.5*	2.2	2.2
	AVG	5.2	8.5			3.4	3.8
rs61751407	MIN	2.7	6.3	2.1	1.7	0.9	0.9
	AVG	8.7	8.5	2.3	2.4	2.1	2.0

In the optimization cohort for ABCA4_4537delC there is just one heterozygous call.
* Just one sample produced a genotype call with the old extension primer.

Table 0.22. Comparison of Homozygous and Heterozygous allele heights using old and new PCR primers for rs138157885, rs1800728 and rs61749459.

		Homozygous Allele Height		Heterozygous Allele Heights			
		Old PCR primer mix	New PCR primer mix	Old PCR primer mix		New PCR primer mix	
rs138157885	MIN	6.9	5.7	3.3	3.7	4.1	5.3
	AVG	10.3	11.3				
rs1800728	MIN	10.0	7.8	4.6	4.3	9.0	9.1
	AVG	16.1	13.8				
rs61749459	MIN	6.2	5.4	4.2	3.3	6.5	5.3
	AVG	10.9	11.1				

In the optimization cohort, there was just one heterozygous call for rs138157885, rs1800728 and rs61749459.

Table 0.23. Homozygous and heterozygous AHs for 3 SNVs with new and old extension primers**.**

		Homozygous Allele Height		Heterozygous Allele Heights			
		Old EXT primer mix	New EXT primer mix	Old EXT primer mix		New EXT primer mix	
rs138157885	MIN	5.5	13.5	4.8	6.5	12.0	15.3
	AVG	10.3	22.7				
rs1800728	MIN	5.7	18.5	2.2	2.6	30.6	32.3
	AVG	13.7	34.0				
rs61749459	MIN	5.0	13.6	5.2	4.6	7.8	6.6
	AVG	10.1	25.7				